Pyro-gasification of municipal solid waste for hydrogen production: A Sustainable Efficiency Analysis (SEA) from Norwegian perspective

Md. Yasir Bhuiyan

SUPERVISOR
Souman Rudra
Abu Shadat Muhammad Sayem
Antonio Oliveira

University of Agder, [2024]
Faculty of Engineering and Science
Department of Engineering Sciences

Copyright Declaration

I hereby declare that I am the sole author of the thesis titled "**Pyro-gasification of municipal solid waste for hydrogen production: A Sustainable Efficiency Analysis (SEA) from Norwegian perspective**". Along with this, submitted a softcopy is true copy of my final hardcopy thesis including any required final revisions, as accepted by the board of examination.

I hereby release my copyright to **Chittagong University of Engineering and Technology (CUET)** for uploading the electronic version of the same to the '**Digital Repository(Institutional Repository)**' of CUET after one year from the day of submission. Apart from this, the existing or to be approved **Open Education Resources (OER)** policies and procedures of **Chittagong University of Engineering and Technology (CUET)** shall be applicable to this research work.

I also acknowledge my sincere delivering of copyright to Chittagong University of Engineering and Technology (CUET) to reproduce this thesis by reprography or by other means, in total or by part at the necessity of individuals for the purpose of scholarly research.

……

Signature of the Author

Abstract

The sustainable management of Municipal solid waste (MSW) or Industrial Solid Waste (ISW) is a critical challenge, particularly in regions with surplus energy potential, such as Norway. The emissions from waste incineration plants and lack of energy efficiency drive the exploration of more efficient waste conversion technology. Chemical Looping Technology (CLT) is a new thermochemical technology gaining attraction due to its efficient waste-to-hydrogen conversion with combined heating and power. The study explores the potential hydrogen, and heat production with efficient carbon capture from ISW and MSW using Sorption Enhanced Chemical Looping Gasification (SE-CLG), and Sorption Enhanced Chemical Looping Gasification with Pyrolysis (Pyro-CLG). To achieve this, the ISW was characterized as it is a critical step for effective plant design.

Three models were developed for model development and training using Aspen plus V11 software focusing on key parameters such as gasifier temperature and Oxygen Carrier (OC) selection. Out of three OCs, Ca2Fe2O5 was selected with 92.41% hydrogen production efficiency. However, the problem associated with using directly Ca2Fe2O5 in the gasifier was the formation of CaSiO3 with the interaction of ash formed in gasification which reduces its reproducibility for the looping. To solve this problem, a new model was developed combining Pyrolysis and Chemical Looping Gasification (Pyro-CLG) with acid leaching for the pretreatment of char and ash separation before char gasification with OC as the heavy metal trace presence was mentioned in ISW obtained from previous studies. 3-E (Energy, Exergy, and Environment) analysis was performed on the two models: SE-CLG2, and Pyro-CLG using OC: Ca2Fe2O5 and waste: ISW & MSW. The energy efficiency obtained for SE-CLG2 was 69.11% (ISW), 67.51%(MSW), and for Pyro-CLG 62.38%(ISW), and 59.143%(MSW). The exergy efficiency obtained for SE-CLG2 was 57.29% (ISW), and 55.16%(MSW), and for Pyro-CLG 52.59%(ISW), and 47.84%(MSW). The GWP and AP values obtained for SE-CLG2 were 2.74kgCO2-equiv. 19.031kgSO2-eqiv. (MSW), 13.94kgCO2-equiv. 57.32kgSO2-eqiv. (ISW), and for Pyro-CLG 33.62kgCO2-equiv. 19.017kgSO2-eqiv. (MSW), and 81.34kgCO2-equiv. 57.28kgSO2-eqiv. (ISW).

170 kg hydrogen with 4300litre 100^{O}C hot water, and 142.8kg with 4000litre 100^{O}C hot water were produced per ton MSW and ISW in SE-CLG2. Hydrogen production drops 16% and 20.17% when the Pyro-CLG model is used for MSW and ISW. For the Pyro-CLG model, the net product decreases by a moderate margin than SE-CLG2 for both MSW and ISW.

So, if the production of more hydrogen and hot water can overtake the manufacturing cost of Ca2Fe2O5, then the SE-CLG2 model is recommended. Otherwise, the Pyro-CLG model is suitable for implications. The MSW was found more prone to hydrogen production ISW was more toward energy and exergy efficiency.

Abstrakt

Bærekraftig håndtering av kommunalt fast avfall (MSW) eller Industrial Solid Waste (ISW) er en kritisk utfordring, spesielt i regioner med overskuddsenergipotensial, som Norge. Utslippene fra avfallsforbrenningsanlegg og mangel på energieffektivitet driver til leting etter mer effektiv avfallskonverteringsteknologi. Chemical Looping Technology (CLT) er en ny termokjemisk teknologi som får tiltrekning på grunn av sin effektive avfall-til-hydrogen-konvertering med kombinert oppvarming og kraft. Studien utforsker potensiell hydrogen- og varmeproduksjon med effektiv karbonfangst fra ISW og MSW ved bruk av Sorption Enhanced Chemical Looping Gasification (SE-CLG), og Sorption Enhanced Chemical Looping Gasification with Pyrolysis (Pyro-CLG). For å oppnå dette ble ISW karakterisert som det er et kritisk skritt for effektiv anleggsdesign.Tre modeller ble utviklet for modellutvikling og trening ved bruk av Aspen plus V11-programvare med fokus på nøkkelparametere som forgassertemperatur og valg av oksygenbærer (OC). Av tre OC ble Ca2Fe2O5 valgt med 92,41 % hydrogenproduksjonseffektivitet. Problemet knyttet til direkte bruk av Ca2Fe2O5 i forgasseren var imidlertid dannelsen av CaSiO3 med interaksjonen av aske dannet ved forgassing som reduserer reproduserbarheten for sløyfen. For å løse dette problemet ble det utviklet en ny modell som kombinerer pyrolyse og kjemisk sløyfegassifisering (Pyro-CLG) med syreutlekking for forbehandling av forkulling og askeseparasjon før forgassing med OC ettersom tungmetallsporenes tilstedeværelse ble nevnt i ISW hentet fra tidligere studier. 3-E (Energy, Exergy, and Environment) analyse ble utført på de to modellene: SE-CLG2 og Pyro-CLG ved bruk av OC: Ca2Fe2O5 og avfall: ISW & MSW. Energieffektiviteten oppnådd for SE-CLG2 var 69,11 % (ISW), 67,51 % (MSW) og for Pyro-CLG 62,38 % (ISW) og 59,143 % (MSW). Eksergieffektiviteten oppnådd for SE-CLG2 var 57,29 % (ISW) og 55,16 % (MSW), og for Pyro-CLG 52,59 % (ISW) og 47,84 % (MSW). GWP- og AP-verdiene oppnådd for SE-CLG2 var 2,74 kg CO2-ekvivalenter. 19,031 kgSO2-ekv. (MSW), 13,94 kg CO2-ekvivalent. 57,32 kgSO2-ekv. (ISW), og for Pyro-CLG 33,62 kgCO2-ekvivalenter. 19,017 kgSO2-ekv. (MSW), og 81,34 kg CO2-ekvivalenter. 57,28 kgSO2-ekv. (ISW).170 kg hydrogen med 4300 liter 100OC varmtvann, og 142,8 kg med 4000liter 100OC varmtvann ble produsert per tonn MSW og ISW i SE-CLG2. Hydrogenproduksjonen faller 16 % og 20,17 % når Pyro-CLG-modellen brukes for MSW og ISW. For Pyro-CLG-modellen reduseres nettoproduktet med en moderat margin enn SE-CLG2 for både MSW og ISW.

Så hvis produksjonen av mer hydrogen og varmt vann kan overgå produksjonskostnadene for Ca2Fe2O5, anbefales SE-CLG2-modellen. Ellers er Pyro-CLG-modellen egnet for implikasjoner. MSW ble funnet mer utsatt for hydrogenproduksjon ISW var mer mot energi- og eksergieffektivitet.

বিমূর্ত

মিউনিসিপ্যাল সলিড ওয়েস্ট বা ইন্ডাস্ট্রিয়াল সলিড ওয়েস্ট এর টেকসই ব্যবস্থাপনা একটি গুরুত্বপূর্ণ চ্যালেঞ্জ, বিশেষ করে নরওয়ের মতো উদ্বৃত্ত শক্তির সম্ভাবনা রয়েছে এমন অঞ্চলে। বর্জ্য পোড়ানো উদ্ভিদ থেকে নির্গমন এবং শক্তি দক্ষতার অভাব আরও দক্ষ বর্জ্য রূপান্তর প্রযুক্তির অনুসন্ধান চালায়। রাসায়নিক লুপিং টেকনোলজি (সিএলটি) হল একটি নতুন থার্মোকেমিক্যাল প্রযুক্তি যা এর দক্ষ বর্জ্য থেকে হাইড্রোজেন রূপান্তরের সাথে মিলিত উত্তাপ এবং শক্তির কারণে আকর্ষণ লাভ করে। অধ্যয়নটি সম্ভাব্য হাইড্রোজেন,ইন্ডাস্ট্রিয়াল সলিড ওয়েস্ট এবং মিউনিসিপ্যাল সলিড ওয়েস্ট থেকে কার্যকর কার্বন ক্যাপচারের সাথে তাপ উৎপাদনের অনুসন্ধান করে শোষণ উন্নত কেমিক্যাল লুপিং গ্যাসিফিকেশন, এবং শোষণ উন্নত কেমিক্যাল লুপিং গ্যাসিফিকেশন সঙ্গে পাইরোলাইসিস। এটি অর্জনের জন্য,ইন্ডাস্ট্রিয়াল সলিড ওয়েস্ট কে চিহ্নিত করা হয়েছিল কারণ এটি কার্যকর উদ্ভিদ নকশার জন্য একটি গুরুত্বপূর্ণ পদক্ষেপ।

এসপেন প্লাস V11 সফ্টওয়্যার ব্যবহার করে মডেল ডেভেলপমেন্ট এবং প্রশিক্ষণের জন্য তিনটি মডেল তৈরি করা হয়েছিল যা গ্যাসিফায়ার তাপমাত্রা এবং অক্সিজেন ক্যারিয়ার (OC) নির্বাচনের মতো মূল প্যারামিটারগুলিতে ফোকাস করে। তিনটি OC-এর মধ্যে, Ca2Fe2O5 92.41% হাইড্রোজেন উত্পাদন দক্ষতার সাথে নির্বাচিত হয়েছিল। যাইহোক, গ্যাসিফায়ারে সরাসরি Ca2Fe2O5 ব্যবহার করার সাথে সম্পর্কিত সমস্যাটি ছিল গ্যাসিফিকেশনে গঠিত ছাই এর মিথস্ক্রিয়া দ্বারা CaSiO3 গঠন যা লুপিংয়ের জন্য এর প্রজননযোগ্যতা হ্রাস করে। এই সমস্যা সমাধানের জন্য, OC এর সাথে চার গ্যাসীকরণের আগে চর এবং ছাই পৃথকীকরণের প্রিট্রিটমেন্টের জন্য পাইরোলাইসিস এবং কেমিক্যাল লুপিং গ্যাসিফিকেশন (পাইরো-সিএলজি) এর সমন্বয়ে একটি নতুন মডেল তৈরি করা হয়েছিল কারণ পূর্ববর্তী গবেষণা থেকে প্রাপ্ত ISW-তে ভারী ধাতুর ট্রেস উপস্থিতি উল্লেখ করা হয়েছিল। 3-E (শক্তি, অনুশীলন এবং পরিবেশ) বিশ্লেষণ দুটি মডেলের উপর সঞ্চালিত হয়েছিল: SE-CLG2, এবং Pyro-CLG OC: Ca2Fe2O5 এবং বর্জ্য: ISW এবং MSW ব্যবহার করে। SE-CLG2 এর জন্য প্রাপ্ত শক্তি দক্ষতা ছিল 69.11% (ISW), 67.51% (MSW), এবং Pyro-CLG 62.38% (ISW), এবং 59.143% (MSW)। SE-CLG2 এর জন্য প্রাপ্ত ব্যায়াম দক্ষতা ছিল 57.29% (ISW), এবং 55.16% (MSW), এবং Pyro-CLG 52.59% (ISW), এবং 47.84% (MSW)। SE-CLG2 এর জন্য প্রাপ্ত GWP এবং AP মানগুলি ছিল 2.74kgCO2-equiv। 19.031kgSO2-eqiv. (MSW), 13.94kgCO2-সমমান। 57.32kgSO2-eqiv. (ISW), এবং Pyro-CLG 33.62kgCO2-equiv-এর জন্য। 19.017kgSO2-eqiv. (MSW), এবং 81.34kgCO2-equiv. 57.28kgSO2-eqiv. (ISW)।
SE-CLG2-তে 4300 লিটার 100^{0}C গরম জলের সাথে 170 কেজি হাইড্রোজেন এবং 4000 লিটার 100OC গরম জলের সাথে 142.8 কেজি প্রতি টন MSW এবং ISW উত্পাদিত হয়েছিল। যখন MSW এবং ISW এর জন্য Pyro-CLG মডেল ব্যবহার করা হয় তখন হাইড্রোজেন উৎপাদন 16% এবং 20.17% কমে যায়। Pyro-CLG মডেলের জন্য, MSW এবং ISW উভয়ের জন্য SE-CLG2-এর তুলনায় নেট পণ্য একটি মাঝারি মার্জিন দ্বারা হ্রাস পায়।
তাই, যদি বেশি হাইড্রোজেন এবং গরম জলের উৎপাদন Ca2Fe2O5 এর উৎপাদন খরচকে ছাড়িয়ে যেতে পারে, তাহলে SE-CLG2 মডেলের সুপারিশ করা হয়। অন্যথায়, Pyro-CLG মডেল প্রভাবের জন্য উপযুক্ত। MSW হাইড্রোজেন উৎপাদনের জন্য বেশি প্রবণ পাওয়া গেছে ISW শক্তি এবং এক্সারজি দক্ষতার দিকে বেশি ছিল।

Preface

The study aims to investigate the hydrogen generation potential of industrial solid waste and municipal solid waste in Norway by integrating chemical looping gasification for district heating and power with lower emissions. The thesis has been written to fulfill graduation requirements for the degree of Masters of Science in Renewable Energy at the Faculty of Engineering and Science, University of Agder in Grimstad, Norway. I am a former research assistant and lecturer and came from Bangladesh to do thesis under the scholarship of CARE project. The waste generation in Bangladesh is really high and becoming a major issue for its growth towards development. This highly motivated me for this thesis so I can learn and implement it for the problem solving in Bangladesh.

The thesis was based on the industrial solid waste which was supplied by Geo4Dynamics. Researching and writing of this thesis were performed from August to December 2024 and the thesis was conducted under the supervision of Professor Souman Rudra.

All praise belongs to almighty Allah for the blessings and successful completion of the thesis. First, I like to thank my supervisor Professor Souman Rudra for his valuable support and guidance. Thanks to Geo4Dynamics Antonio Oliveira for sending the waste samples and helping throughout the work. Thanks to Diani Ph.D. research fellow and Odin lab engineer for the guidance during waste characterization.

Finally, thanks to my wife, my mother, and the family members for supporting and motivating me throughout the work.

Md. Yasir Bhuiyan

University of Agder

Grimstad, December 2024

Individual/group Mandatory Declaration

The individual student or group of students is responsible for the use of legal tools, guidelines for using these and rules on source usage. The statement will make the students aware of their responsibilities and the consequences of cheating. Missing statement does not release students from their responsibility.

1.	I/We hereby declare that my/our report is my/our own work and that I/We have not used any other sources or have received any other help than mentioned in the thesis.	☒
2.	I/we further declare that this thesis: - has not been used for another exam at another department/university/university college in Norway or abroad; - does not refer to the work of others without it being stated; - does not refer to own previous work without it being stated; - have all the references given in the literature list; - is not a copy, duplicate or copy of another's work or manuscript.	☒
3.	I/we am/are aware that violation of the above is regarded as cheating and may result in cancellation of exams and exclusion from universities and colleges in Norway, see Universitets- og høgskoleloven §§4-7 og 4-8 og Forskrift om eksamen §§ 31.	☒
4.	I/we am/are aware that all submitted theses may be checked for plagiarism.	☒
5.	I/we am/are aware that the University of Agder will deal with all cases where there is suspicion of cheating according to the university's guidelines for dealing with cases of cheating.	☒
6.	I/we have incorporated the rules and guidelines in the use of sources and references on the library's web pages.	☒

Publishing Agreement

Authorization for electronic publishing of the thesis.

Author(s) have copyrights of the thesis. This means, among other things, the exclusive right to make the work available to the general public (Åndsverkloven. §2).

All theses that fulfill the criteria will be registered and published in Brage Aura and on UiA's web pages with author's approval.

Theses that are not public or are confidential will not be published.

I hereby give the University of Agder a free right to

make the task available for electronic publishing: ☒JA ☐NEI

Is the thesis confidential? ☐JA ☒NEI

(confidential agreement must be completed and signed by the Head of the Department)

- If yes:

Can the thesis be published when the confidentiality period is over? ☐JA ☐NEI

Is the task except for public disclosure? ☐JA ☒NEI

(contains confidential information. see Offl. §13/Fvl. §13)

Table of Contents

List of Figures

List of Tables

Notation

$Ca_2Fe_2O_5$	Dicalcium-Diiron pentaoxide
CaO	Calcium Oxide
EN	Energy
EX	Exergy
HHV	Higher Heating Value
LHV	Lower Heating Value
MC	Moisture Content
VM	Volatile matter
η	Efficiency
s	Entropy
h	Enthalpy

Abbreviations

ASR	Automotive shredded Residue
ASTM	American Society for the Testing of Materials
AR	Air Reactor
AP	Acidifying Potential
CLT	Chemical Looping Technology
CF	Car Fluff
FC	Fixed Carbon
FR	Fuel Reactor
GHG	Green House Gas
GWP	Global Warming Potential
ISO	International Organization for Standardization
ISW	Industrial Solid Waste
MC	Moisture Content
MSW	Municipal Solid Waste
OC	Oxygen carrier
Pyro-CLG	Sorption Enhanced Chemical Looping Gasification with Pyrolysis
SE-CLG	Sorption Enhanced Chemical Looping Gasification
UiA	Universitetet i Agder
VM	Volatile Matter
WTE	Waste to Energy

1 Introduction

The amount of energy we use for daily living is growing every day. Global energy demand is predicted to rise by 56% over the three decades between 2010 and 2040, mostly as a result of increasing populations [10]. Investigating and using innovative, renewable, and environmentally benign energy sources is now a top priority. To match up the energy demand, fuel like hydrogen which is known for its high energy density and clean combustion, not only improves the combustion efficiency but also has less impact on the environment [11] . Recently, there has been a lot of interest in hydrogen as a fuel because of its promise as a sustainable and clean energy source. Its high gravimetric energy density, which permits effective energy conversion and storage, is one of its special qualities. Water is the main consequence of using hydrogen fuel in fuel cells or combustion processes, which has little effect on the environment and almost no greenhouse gas (GHG) emissions [12]. Fossil fuels still make up 96% of the feedstock used to produce hydrogen [13]. Instead of using energy-intensive water gas shift or general fossil coal/methane, the creation of hydrogen and syngas from renewable biomass feedstock has been seen as a possible solution to the enormous demands in the industry. The creation of new production techniques that take into consideration the significant variations in the chemical composition of the two types of feedstocks (specifically, the oxygen content, which is 0.05–1.5 weight percent in fossil hydrocarbons vs. 30–50 weight percent in biomass feedstocks) and the ensuing contrasts in physicochemical properties like thermal stability and polarity is necessary to replace polluting fossil carbons with renewable biomass-based raw materials [14]. The production of hydrogen from biomass like wheat, sugar cane, and algae is becoming an alternative way rather than fully depending on fossil fuels. However, there are some adverse effects while producing hydrogen from biomass wastes like severe food shortage, etc [15].

Municipal solid waste (MSW) has increased significantly in recent years due to the rapid urbanization of places, making it more difficult to handle MSW effectively and find sustainable disposal solutions [16]. The reported hazardous wastes like waste containing heavy metals increased by 10.4% from 2021-2022 and around 1.88 million tons of hazardous wastes were sent for treatment [17]. The dumping of MSW in landfills is a severe problem around the world as it can be a reason for harmful toxic emissions like CO2 and CH4 from incineration plants of MSW and occupation of landfills and leachate contaminants [18]. This pilling of waste in landfills can cause many other problems from country to country. In countries like Bangladesh during heavy rainfall, surface water contamination and water clogging are noteworthy problems that the government is struggling to solve [19].

To overcome the problems associated with MSW and make use of it due to its significant hydrocarbon proportion, it can be used as a potential source to produce sustainable energy and by-products by using Waste-to-energy (WtE) conversion techniques [15].

Incineration is the most widely used technique for generating electricity and heat as a product of MSW [20]. The problem associated with incineration can be termed as the release of pollutants like dioxins, furans, heavy metals, and fly ash [21] and low thermal efficiency reported [22]. The pollutant treatment cost from MSW incineration is one of the disadvantages of the process. Hydrogen can be produced using biological or thermochemical processes but due to faster process kinetics, the thermochemical process provides higher hydrogen production [23]. The thermal conversion processes available for the thermal treatment of solid wastes like MSW are pyrolysis, combustion, and gasification. Among the different, WtE conversion technologies, gasification is one of the promising methods of producing sustainable products like hydrogen-rich syngas in the form of energy from MSW

[24]. So, as a renewable H2 production source, MSW is considered in many studies [25],[22]. In recent years, pyrolysis and gasification have emerged as the most affordable and useful methods for treating Automotive Shredded Residue (ASR). High heating values of 19 MJ/kg to 23 MJ/kg found in foam, textiles, rubber, and polymers found in ASR offer significant possibilities for thermal energy recovery [26]. The problem with conventional gasification is the process energy balance and the poor gas quality due to the dilution of CO2, N2, and tar components. Chemical Looping Gasification (CLG) is now gaining interest in the field of scientific research, and industrial-level application to overcome the problems [27]. Chemical looping technology for hydrogen production has been significantly advanced in Norway thanks to several important initiatives and partnerships setting the standard. Calcium-copper looping is one of the well-known technologies under investigation. In Norway, mayenite-based calcium-copper material was utilized and a 92-93 vol% hydrogen production was achieved with a CO_2 capture of 14.6-15.0 g per 100g of methane as primary feedstock [28]. It is a method intended to effectively create hydrogen and absorb CO2 in a single integrated step. Using copper to supply the required heat for regenerating the sorbent and calcium oxide as a sorbent to absorb CO2 makes this process energy-efficient. The "6C" initiative seeks to advance this technology to an industrial scale (SINTEF)(Climit), partnering with Norwegian research institutes such as the Institute for Energy Technology (IFE) in Europe. Furthermore, one of Norway's top research organizations, SINTEF, has been focusing on chemical looping combustion (CLC). Their 150 kW pilot plant aids in refinement.[29].

The integration of MSW gasification technology with CHP/DH plants in the context of hydrogen production can be aided by researching and identifying the possible hydrogen output of MSW by gasification in the Norwegian waste environment. The production of hydrogen from these increasing MSW wastes and hot water can contribute to the growing demand for hydrogen around the world and hot water supply for district heating applications and also power generation using different technologies with MSW gasification plants. To find out the hydrogen generation potential of solid wastes like MSW and Industrial Solid Waste (ISW) which concludes car fluff, FAB incinerator waste, and FAB cement kiln waste, the solid wastes need to be characterized physically and thermochemically to study the physical and thermochemical characteristics of wastes. In this work, four types of wastes namely Car fluff (finely shredded), Car fluff (coarsely shredded), FAB incinerator waste, and FAB cement kiln combined named ISW were characterized experimentally in the laboratory of the University of Agder (UiA). The wastes were collected from an organization. In a previous study of characteristics of Norwegian MSW, using the characteristics data several case studies were performed using different chemical looping gasification and combined pyro-gasification models for model development and comparison. The ISW characteristics data were used for similar models to obtain the performance of different oxygen carriers (OCs) to evaluate their hydrogen production potential, and energy, exergy efficiency, and environmental analysis using Aspen plus commercial thermochemical simulation software. The study aims to solve the problem associated with the cyclic reproducibility of the OCs, increasing the production of hydrogen and simulation model performance according to 3E analysis, based on all step-by-step model development performed.

1.1 Background

The world population is growing, and the UN reports that by 2050, the world's population will reach a figure of 9 billion from 7 billion [30]. With the increase of the global population net power consumption, GHG emission, and waste generation is increasing at an alarming rate. The government of Norway has an aim to reduce greenhouse gas emissions by 90-95% by 2050 in comparison to 1990 [31]. Norway is one of the Nordic nations that has committed to becoming carbon neutral by 2050. Focusing on lowering GHG emissions from the energy, transportation, and industrial sectors, these nations are leaders in the fight against climate change [32]. But as stated earlier with the increasing number in population so will the increase in solid waste. Municipal solid waste (MSW) incineration facilities are an essential part of energy recovery and trash management in Norway. Currently, the nation has 17 of these plants, which treat over 1.7 million tons of MSW a year. About 333.334 GWh of electricity and 3694.45 GWh of heat for district heating are produced by these plants, which run at about 90% of their capacity [33],[34]. GHG emissions from Norwegian waste-to-energy (WtE) facilities, which burn municipal solid waste (MSW), are substantial. Depending on the waste's composition and the percentage of fossil-based items, such as plastics, these plants produce between 700kg and 1000 kg of CO_2 for every ton of burned waste. For example, the combined emissions of Norwegian WtE plants from fossil fuels in 2019 were around 450 kilotons of CO_2 [34], [35]. Due to the varying demand on customer's energy consumption, and heat energy variation depending upon the season, energy loss occurs in MSW fired-CHP or DH plants [36] and due to the characteristics of waste, it cannot be stored for a long time which leads to continuous operation of waste incineration plants throughout the year.

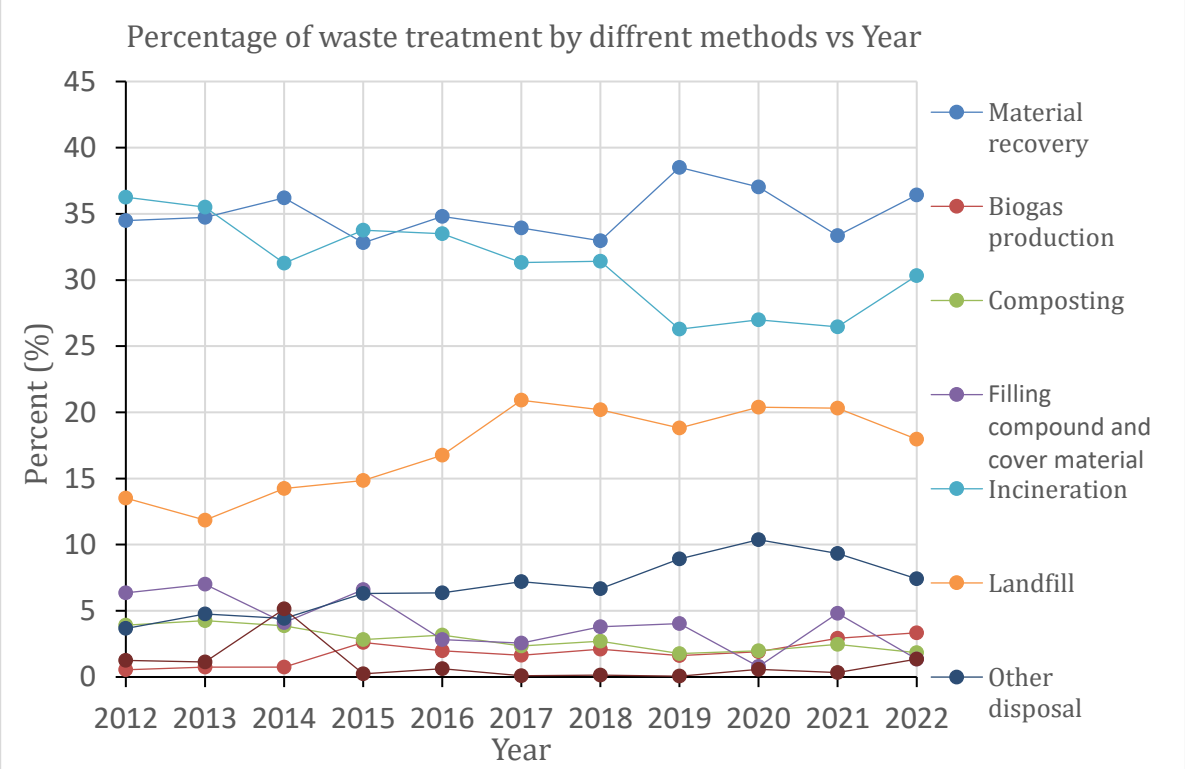

Figure 1: Non-hazardous waste percentage in terms of treatment methods in Norway [1].

The total waste generated in 2022 reported was 12.072 million tons and the waste increased from the previous year by 4 percent [37]. There are several advantages of gasification plants over fossil fuel-

based ones like feedstock flexibility which can convert municipal solid waste (MSW), forest, and agriculture residue into energy [38]. Cleaner emissions include reduced CO2 emissions compared to fossil fuel-based plants and lower sulfur and nitrogen oxide emissions and particulate matter. This emission can be further minimized using advanced filtration systems to reduce pollutants like harmful mercury, dioxins, and hydrogen chloride as it is utilized in Norwegian gasification plants like ENERGOS [39]. Klemetsrud Incineration plant which is located in Oslo is the largest in Norway processing around 350 kilotons of waste in a year and emitting approximately 300 kilotons of CO2 which is responsible for 17% of Oslo's total emission[40].

From the statistics, it is promising that the CO2 emission rate is declining, and from 1990 to 2023 the CO2 emission shows a gradual up and down trend. In 2022, it was reported that the CO2 emissions were 40808 kilotons and gradually decreased up to 4.67% in 2023, and the CO2 emissions reported 38901 kilotons. The other greenhouse gases like methane and nitrous oxide emission rates in Norway also show a promising decline from 2022 to 2023 up to 3.70% and 7.19%.

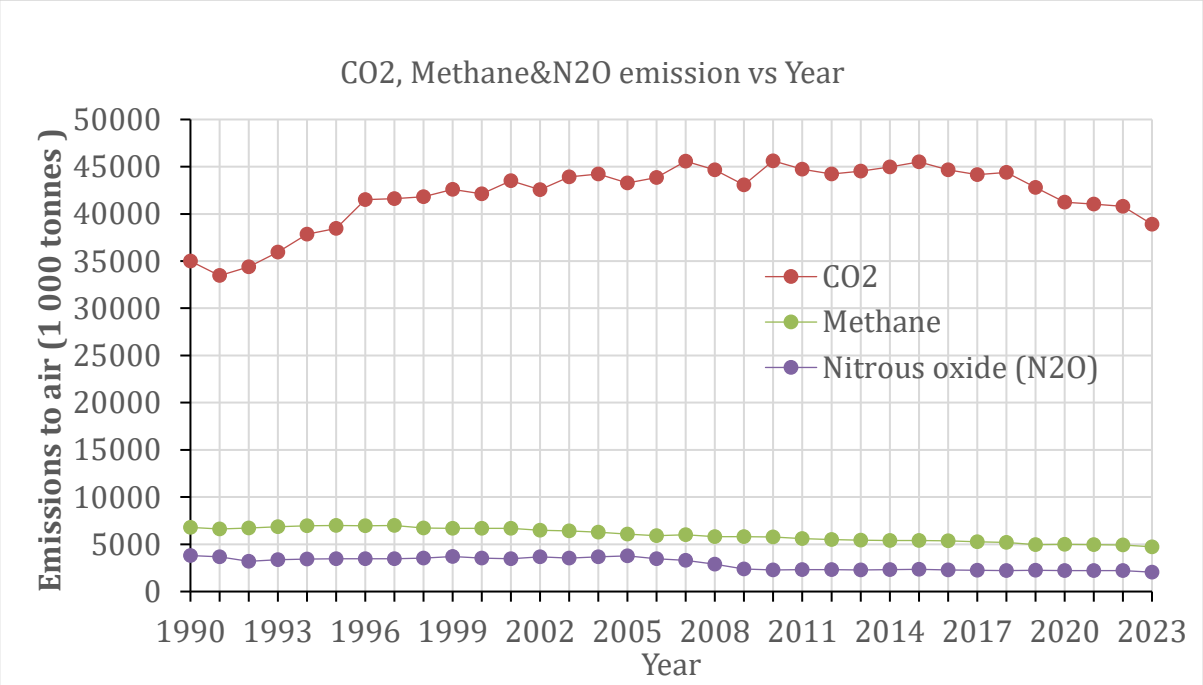

Figure 2:GHG emission over the years in Norway from all sectors [2].

The obstacles of pyrolysis-gasification technologies can be addressed as per kg of H2 production the production of CO2 is 12 kg and reaching the temperature range from 450-1000℃ requires higher energy consumption [41].

Hydrogen production through biomass gasification is an emerging technology, and Norway is actively exploring it as part of its commitment to reducing carbon emissions and transitioning to renewable energy sources. Two prominent Norwegian institutions working on the development of hydrogen generation technologies, including those based on biomass gasification, are SINTEF and Greenstat. They both aim to integrate cutting-edge technologies for effective and sustainable hydrogen production, notwithstanding the differences in their particular strategies. Here's an overview in Table 1 of the technologies for hydrogen production in Norway's current market size and the sector-wise demand for hydrogen [42]:

These initiatives by SINTEF and Greenstat are part of broader efforts to develop large-scale hydrogen production from biomass and renewable resources in Norway. By 2035, the development of low-

carbon hydrogen production and a 10% market share are expected in Europe [43]. The current market size of hydrogen in Norway is still limited but by the year 2050, the anticipated hydrogen generation is expected to grow sharply and a sizable amount will go toward export [44] and 96% of generated hydrogen will be exported and 4% will be used for transportation of particularly heavy duty and maritime transport [45].

Table 1: Technology & Use of Hydrogen in Norway.

Technologies for Hydrogen Production in Norway		
Company's name	Technology in use+Project	Process
SINTEFF	Plasma Gasification	Uses high-temperature plasma to produce hydrogen from biomass.
SINTEFF+Reinertsen	Palladium Membrane	Extracts high-purity hydrogen from syngas. Removes CO2.
Greenstat+Glomfjord	Electrolysis	Uses hydropower for electrolysis.
Greenstat+NEL	Electrolysis	Uses hydropower for green hydrogen production linked to regional hydropower and industrial clusters.

The waste supply for waste characterization and simulation in this thesis was supplied by Geo4 Dynamics. With an emphasis on cutting-edge material processing methods, Geo4 Dynamics seeks to convert a variety of feedstocks, including wastes, and biomass into useful chemicals and renewable energy. Their goal is to promote a circular economy and reach net-zero emissions to advance global sustainability. Their main product, the Geo4:ONE system, produces more than twice as much energy as conventional systems by effectively breaking down complicated molecules using cold plasma vortex technology. Without sorting or drying, it handles a variety of waste streams, such as hazardous, industrial, and municipal wastes. The system provides a cost-effective and environmentally friendly waste-to-energy conversion option because it is modular, scalable, and built to emit little pollutants. Geo4 Dynamics is dedicated to solving the world's emission problems and building a more environmentally friendly future [46]. The company demanded to estimate of how the acid leaching is performing for complete heavy metal removal, Cold Gas Efficiency before and after the water-gas-shift-reactor, and the maximum hydrogen production using ISW.

1.2 Motivation

The background mentioned above shows that the emission of GHG should be declining and to decrease the GHG emission, we need to focus on renewable energy. It is the best way to effectively use the increasing generation of MSW and minimize the emission from incineration plants is to generate hydrogen focusing on the hydrogen production of Norway and its high energy density and cleaner power production. The poly-generation system based on pyrolysis and Chemical Looping Gasification (CLG) has advantages over the MSW incineration plant by combinedly producing heat/electricity, as well as syngas. It has the advantage over individual processes based on lower pollution, and higher efficiency [47]. So, combining the Chemical Looping Technology (CLT) for hydrogen production with heat and power production using MSW will be the best use of waste. The motivation also includes my homeland Bangladesh which is struggling to generate power and a huge amount of waste generation. So, it will be a great move for both the countries' waste management and power generation.

The main objective of this study is to create a new pathway to process Industrial Solid Waste (ISW) simulating Chemical Looping Technology (CLT) for the Combined Production of Hydrogen, Heat, and Power while capturing CO2 to reduce GHG emissions.

- A deep observation of Industrial Solid Waste (ISW) properties with waste characterization and comparison with Municipal Solid Waste (MSW).
- Estimating the impact of different Oxygen carriers (CaO, Fe2O3, and Ca2Fe2O5) and steam on CLT models using MSW.
- Model training and development for the highest hydrogen production using MSW.
- Oxygen carrier reproducibility problem solving with integrated model, due to the ash formation in gasification MSW and ISW.
- Integrating heat and power production in selected models, and performing 3-E analysis (Energy, Exergy, and Environment) using MSW and ISW.
- Sustainable suggestion based on obtained results.

1.3 Assumptions and Limitations

The ultimate analysis for the elemental composition estimation was intended to be performed using the CHN analyzer in UiA. However, the device did not operate properly during the whole period. Due to this, we have to use correlations for ISW elemental composition estimation. Another intended experiment was the calorific value measurement of ISW using a Bomb calorimeter. Similarly, the device was not functioning, and the LHV & HHV values were obtained using correlations used in relevant literature. The simulation assumptions are discussed in the section (3.5 Aspen Simulation Assumption & Plant Design)

1.4 Research Questions

The waste-to-energy concept is gaining more and more interest as the growing rate of waste and effectively converting it into useful products without harming the environment. A lot of research is available and continuing on waste to energy, especially on chemical looping gasification for hydrogen production and carbon dioxide minimization. The questions to be answered throughout the thesis are mentioned below-

- How was the model developed according to the property of waste?
- How much will be the potential hydrogen, heat, and power production from chemical looping gasification?
- How do the gasification, pyrolysis, water-gas-shift reactor parameters, and variation of oxygen carriers and their flow rate affect the products?
- Do the processes minimize the CO2 emissions with effective CO2 capture and storage?
- What will be the possible value of global warming potential and acidifying potential of the developed process?

1.5 Outline of Thesis

The thesis focuses on Industrial Solid Waste (ISW) characterization, property analysis, and simulating Sorption Enhanced Chemical Looping Gasification (SE-CLG) and combined Sorption Enhanced Chemical Looping Gasification with Pyrolysis (Pyro-CLG). The sensitivity analysis of the processes was carried out for different reactor temperatures, and OC flow rates and used different types of OCs to find out the best hydrogen, heat, and power production with lower GWP and AP. Model development (Pyro-CLG) was done to solve the problem associated with OC reproducibility due to ash formation in gasification reactors. The impact of model development on hydrogen, heat, and power production and pollutants emission, was compared and discussed. The thesis outlines in the following way-

Chapter 1 presents an introduction and background of the aim of this work which includes associated problems, motivation to solve these problems, questions related to the study, and desired goals for the work

Chapter 2 presents the theoretical studies related to the research work and is divided into sub-chapters. The subchapters include Waste properties, Waste characterization, theory of chemical looping gasification and pyrolysis, and theory of energy, exergy, and environmental analysis.

Chapter 3 presents the methods and experimental setup employed in this work. The chapter includes a flow diagram of methodology, waste sample composition, description, and characterization with SE-CLG and Pyro-CLG plant design and simulation method.

Chapter 4 presents the results and discussion of the ISW characterization and the sensitivity, H2 efficiency, and 3-E analysis of the developed processes.

Chapter 5 presents the findings and suggestions. Some future works are also included.

2 Theory

2.1 Introduction

This chapter includes the developed theoretical background related to the upcoming materials and methods. Waste properties inspection, characterization & systematic development to minimize the challenges of preparing the waste feed for further processing are explored. Based on this, model development ways are discussed.

2.2 Feedstock Properties

An essential first step in assessing waste feedstock is characterizing MSW and ISW to choose a suitable waste treatment technique. Characterization is required for thermal conversion processes to avoid operational problems, optimizing the process, and to produce an effective design. The key characterization procedures of MSW and ISW need to be examined under the different literature [9], [48], [49] are the proximate analysis, ultimate analysis, calorific value, and thermogravimetric analysis (TGA). In ISW, debris such as automobile fluff may contain both organic and inorganic pollutants, such as heavy metals, polychlorinated biphenyls (PCBs), and total petroleum hydrocarbons (TPH). The U.S. Environmental Protection Agency (EPA) reported that lead, chromium, mercury, cadmium, polyvinyl chloride, arsenic, and PCBs are present in Automobile Shredder Residue (ASR) which are found in ISW. Some volatile and semi-volatile organic chemicals are present in trace amounts in vehicle fluff [50]. The ASR requires pollutant/ environmental analysis which requires TPH, PCB, PAHs, and BTEX (Benzene, Toluene, Ethylbenzene, and Xylene) analysis [51]. These characterization procedures, their operating conditions, and necessary equations for the determination of final properties are discussed- The proximate analysis requires conventional lab equipment like drying ovens, furnaces, crucibles, and weight balance. For thermogravimetric analysis and CHNS analysis, TGA and CHNS analyzers are required which are sophisticated. A bomb calorimeter is referred to as the experimental calorific value measurement of solid fuels. To evaluate the solid fuel properties for MSW and ISW, standard operating procedures are followed to determine and evaluate the fuel properties effectively. The standards are maintained for the determination of properties like chemical composition, density, heating value, and others for feedstock by ISO, Standard Norway, ASTM, and other organizations. The standards included in the Table are followed for the sample preparation and waste characterization.

Table 2.1: Solid biofuels sample preparation and characterization standards by Standard Norway based on national, European & International standards.

Standards	Description
ISO 14780:2017	Solid biofuels — Sample preparation
ISO 18134-1:2015	Solid biofuels — Determination of moisture content — Oven dry Method-Part 1: Total Moisture-Reference method
ISO 18134-3	Solid biofuels — Determination of moisture content — Oven dry method
NS-EN -15402:2011	Solid recovered fuels- Determination of the content of volatile matter
NS-EN ISO 18122:2015	Solid biofuels-Determination of Ash content
NS-EN 15407:2011	Solid recovered fuels —Methods for the determination of carbon (C), hydrogen (H) and nitrogen (N) content

The primary components of gasifier feedstock are moisture (MC), fixed carbon (FC), volatile organic matter (VC), and minerals or ash which can be determined using proximate analysis.

2.2.1 MSW & ISW sorting

The fact is that both wastes are heterogeneous in the case of their physical and chemical composition. Because MSW and ISW are heterogeneous, it is difficult to manage and handle trash in a way that complies with environmental regulations, particularly waste regulations. For characterization processes, some require only a few grams of samples which is also challenging to make the sample representative of the whole waste pile. From the works of literature, the ASR physical components, which are a part of ISW are foam 16.04%, plastic 24.12%, rubber 16.09%, textile 29.69%, wood 2.16%, metal 5.71%, glass 0.46%, sand 5.25%, and paper 0.47% reported by [52] on a weight basis.

2.2.3 Bases for expressing feedstock

Depending on the circumstance, a feedstock's proximal and ultimate analytical values are typically expressed as a dry basis or wet basis. More precisely, four bases can be used to express the bases of the two analyses. Air-dry, completely dry, ash-free bases, and as received. From proximate and ultimate analysis we obtain values like moisture content, volatile matter, fixed carbon, ash, carbon (C), hydrogen(H), oxygen(O), nitrogen(N), and sulfur(s). The as-received feedstock contains surface moisture and air-dry loses the surface moisture but consists of inherent moisture. The completely dry loses the inherent moisture content and ash-free bases lose ash content from the feedstock [53].

2.3 Proximate analysis

Moisture content, volatile matter, ash, and fixed carbon are the composition of solid fuel determined using the proximate analysis. It evaluates the potential of biomass or any other solid residue as a fuel. The process is simple and three compositions are measured experimentally and fixed carbon is measured by subtracting the total of three measured components from 100%. All four compositions are in weight percentage. Majumder et al. [54] reported the estimation of moisture content, volatile matter, fixed carbon, and ash by thermogravimetric analysis according to ASTM-D5142 proximate analyzer (Model TGA-601).

2.3.1 Moisture Content

The primary issue with using biomass energy resources is that biomass has a lower energy density than fossil fuels like coal, and its calorific value is strongly influenced by its moisture content, which can rise to extremely high levels, particularly when it comes to green biomass and waste materials [55]. There are a number of factors that greatly affect the moisture content of MSW, including variations in waste composition, time of year, location, and weather at the time of sample. Since the energy consumed for evaporation is not recovered, the moisture content of MSW depletes a large portion of the thermochemical conversion plant's deliverable energy. However, in a gasifier that uses steam as a gasifying agent, the evaporated moisture can either take the place of or lessen the requirement for steam to be injected into the plant as a gasifying medium [9]. For the gasifier to be properly designed and operated, moisture content is a crucial design parameter. Simple gravity-based forced convection

dryers that can keep the temperature between 104°C and 110°C are used to measure the moisture content of feedstock [56]. Ozcan et al. [57] measured the moisture content of MSW following the TS1049 standard and dried the sample for 24h at 105℃. The samples were cooled in a desiccator, cooled down to room temperature, and weighed again.
The moisture content in the feedstock can be determined using the following equation [58]

$$MC(\%) = \frac{M2 - M3}{M2 - M1} \times 100 \quad (1)$$

Where: *MC* percentage of moisture composition on the dry basis, $M1$ is the weight of the crucible, $M2$ is the combined weight of the crucible and waste of sample before drying, $M3$ is the weight of the dried sample with the crucible.

2.3.2 Volatile matter

Drake et al. [59] determined the volatile matter of MSW by following ASTM standard E-872 and used three duplicate samples. The samples that were used for moisture content measurement were further heated for 2 hours in a furnace using a crucible. The crucible was cooled in a desiccator and the weight was measured. The volatile matter was recorded as the difference in weight before heating and weight after heating.
The volatile matter can be estimated using the following equation-

$$VM(\%) = \frac{100 \times (M2 - M3)}{M2 - M1} - \mathrm{MC} \quad (2)$$

Where, VM (%)=Volatile matter M1= Mass of empty crucible with lid(gram), M2= Mass of sample with crucible with lid(gram) before heating, M3= Mass of sample with crucible with lid(gram) after heating, and MC=Moisture content of sample(%) [60].

2.3.3 Ash content

The ash content is important for fuel properties because it causes slagging and corrosion in the combustion equipment and oxygen carrier. So, it is important to the amount of ash present in a fuel as it is a by-product of combustion.
Drake et al. [59] measured the ash content in municipal solid waste by following according to ASTM D1102, 2013. After the volatile matter determination, the remaining samples were further combusted in the furnace at a temperature of 575℃ for 1hr. The samples were again weighed when there was no carbon remaining. The difference in weight from the previous value of volatile matter was recorded as ash content.

The ash content can be determined using the following equation-

$$Ash(\%) = \frac{(M3 - M1)}{M2 - M1} \times 100 \times \frac{100}{100 - MC} \quad (3)$$

Where, Ash(%)= Ash content in the sample, M1= Mass of the empty crucible, M2= Mass of the sample with empty crucible before heating, M3=Mass of the sample with empty crucible after heating [61].

2.3.4 Fixed carbon

The fixed carbon is the non-volatile organic matter which is measured by subtracting the sum of moisture content, volatile matter, and ash content from 100.

$$FC(\%) = 100 - \big(MC(\%) + VM(\%) + Ash(\%)\big) \quad (4)$$

Where FC-Fixed carbon, MC-Moisture content, VM-Volatile matter, and Ash-Ash content [59].

2.4 Ultimate analysis

The elemental or ultimate analysis is done to obtain the air-dried samples' carbon, nitrogen, hydrogen, and sulfur values. This process is done in a CHN-O Elemental Analyzer. Kalyani et al. [62] performed the elemental analysis on an air-dried biomass sample in which approximately 1 mg of the air-dry sample in homogenized powder form was weighed on a tin foil boat, formed into a pellet placed in a sample carousel, and subjected to complete combustion in a pure oxygen environment. The elemental composition of each biomass species is determined using a thermal conductivity detector. The following equation was used to determine the oxygen content in the sample-

$$C + N + H + O + S + residues = 100\% \quad (5)$$

Residues are the combination of the percentage of moisture and ash obtained from the proximate analysis.

Among the different properties of biomass, the elemental composition is an important property to find out the energy content of biomass and clean and efficient use of it. Very skilled analysts and very costly equipment are needed for the final study. On the other hand, comparatively, performing the proximate analysis with just common laboratory equipment is easy.

Shen et al. reported that the developed correlations using the proximate analysis values could be used to determine the ultimate analysis values of biomass which contains a high ash portion.

$$C = 0.460 \times VM - 0.095 \times Ash + 0.635 \times FC \quad (6)$$

$$H = 0.060 \times VM + 0.010 \times Ash + 0.059 \times FC \quad (7)$$

$$O = 0.469 \times VM - 0.023 \times Ash + 0.340 \times FC \quad (8)$$

The above-mentioned correlations were developed based on 66 data and validated with 20 related data with average bias errors reported 0.19%, -0.34%, and 0.19% [63].

There are many analyses for predicting elemental compositions from proximate values for coal and biomass but only one paper was found fully covering the C, H, N, O, and S values prediction for MSW using multiple regression analysis. From [64] reported the proximate and ultimate analysis data of the organic portion of MSW. The multiple regression analysis was performed for MSW collected from 23 locations using Anaye-it statistical software. The resulting correlations reported are presented below

$$C(\%) = 0.555 \times VM + 0.618 \times FC - 0.028 \times Ash \quad (9)$$

$$H(\%) = 0.062 \times VM + 0.056 \times FC - 0.003 \times Ash \quad (10)$$

$$O(\%) = 1.116 \times VM + 5.433 \times FC + 0.038 \times Ash \quad (11)$$

$$N(\%) = 0.022 \times VM + 0.044 \times FC + 0.002 \times Ash \quad (12)$$

$$S(\%) = 0.005 \times VM + 0.009 \times FC + 0.002 \times Ash \quad (13)$$

2.5 Calorific Value Analysis

The quantity of heat produced when a unit weight of coal is burned fully and the combustion products cool to a standard temperature of 25℃ is known as the calorific value. Typically, it is stated as a higher heating value (HHV), which is another name for a gross calorific value (GCV) [65]. A bomb calorimeter is used to quantify the HHV of a coal sample experimentally. Higher fuel heating values (HHV) are crucial for conducting energy analyses of any system. The bomb calorimeter is a sophisticated, expensive, and time-consuming method for determining the HHVs of solid and liquid fuels. Correlations have been created to estimate fuel heating values utilizing the outcomes of proximate and ultimate analysis to circumvent such challenges.

LHV is usually termed as the heating value of fuel and the practical significance of LHV is more than HHV cause the water vapor produced during the combustion, leaves the boiler at a temperature higher than its condensation temperature [66].

Hassan et al. [67] calculated the HHV and LHV of MSW using by following correlation-

$$HHV\left(\frac{MJ}{kg}\right) = 0.3491 \times C(\%) + 1.1783 \times H(\%) - 0.1043 \times O(\%) \quad (14)$$

$$LHV\left(\frac{MJ}{kg}\right) = HHV\left(\frac{kJ}{kg}\right) - 2420 \times 9 \times H(\%) \quad (15)$$

Where, C(%), H(%), and O(%) are the elemental compositions of MSW and 2420kJ/kg is the latent heat of the vaporization of water.

2.6 Automotive Shredder Residue (ASR)

Car fluff or Automotive fluff (AF) consists of plastics, textiles, foam, glass, and rubber, which can be termed a complex mixture. The concern is according to the U.S Environmental Protection Agency (EPA), certain toxic organic and inorganic compounds like Poly Chlorinated Biphenyl (PCBs), Ploy Vinyl chloride (PVC), lead, arsenic, mercury, cadmium, and chromium are present in the AF [68]. The End of Life Vehicle (ELV) directive mentions 8-9 million tons of trash generated by ELVs inside the community yearly, which estimates a figure of 2-2.5 million tons ASR/year, constituting 10% of overall hazardous waste in the EU. ASR can be subdivided into two categories: light ASR and heavy ASR. Light ASR constitutes 80% or more of the total ASR and is obtained when the non-ferrous section is subsidized using air classification processes in non-metallic and metallic sections and contains lighter components like plastic and rubber in large quantities. The heavy ASR includes less than 20% of the total ASR and contains the contaminants rejected during the processing. It also contains heavy components in high proportions, such as glass and metal fines[69].

2.6.1 Heavy metal components, halogen, and sulfur components in ASR:

As mentioned earlier, the heterogeneous nature of ASR made it complex to treat it as a feedstock for thermal conversion. Heavy metals like Chromium (Cr), Lead (Pb), Cadmium (Cd), Zinc (Zn), Mercury (Hg), and Copper (Cu) are detected. The amount of Pb, Cr, Cu, and Zn in mg/kg is stated as 412, 151, 332, and 3600 [70].

2.6.2 State of heavy metals during pyrolysis:

Lead tends to maintain its solid phase during processes like pyrolysis and is found mostly in solid components like char [71]. The reason behind this is that the vapor pressure of lead remains low at temperatures lower than its boiling point which is 1749℃. So, at 800℃, the lead tends to be in the solid phase unless chlorine is present. Studies found that the presence of chlorine and an increase in the quantity of chlorine tends to increase the volatility of lead as PbCl2, which can be volatilized at temperatures lower than 800℃ [72].

The main issues with ASR landfilling, are due to its specific weight, high porosity of large components leading to compactness issues, high calorific values causing significant fire hazards, potential chemical reactions, etc. Additionally, disposing of ASR in a landfill takes up a lot of room, wastes potentially useful materials, and contaminates the soil and air [73]. Because ASR contains metallic species and chlorine, using it as fuel in incineration can be problematic [74]. If operating conditions and gas cleaning systems are not closely monitored, toxic pollutants such as polychlorinated dioxins and furans (PCDD/Fs) and polychlorinated biphenyls (PCBs) may be produced as byproducts during the incineration [75]. Additionally, heavy metals—especially the more volatile ones—concentrate in flue gas or the smallest particles, necessitating the use of effective, albeit costly, gas cleaning equipment. Additionally, bottom ash contains a concentration of non-volatile elements, which may necessitate higher handling and disposal expenses [76]. The main problem with ASR gasification is the presence of heavy metals and a higher percentage of sulfur and chlorine. Meng et al. (2016) noted that sulfate (S^{6+}) and sulfite (S^{4+}) make up the majority of the liquid phase of sulfur, whereas hydrogen sulfide (with a smaller amount of carbonyl sulfide (COS)) makes up the majority of the gas phase following gasification. It was discovered that calcium-based adsorbents like limestone and dolomite have a good potential for removing hydrogen sulfide when they are utilized to remove materials [77].

2.7 Pretreatment of ASR

The acid leaching is performed to separate the heavy metals from the char using a solvent. After SSE the chars are required to preheat in a muffle furnace at a temperature of 350℃, for 2 hours before acid leaching. After heating the char is subjected to acid leaching with 1M hydrochloric acid (HCl) solution with an acid-to-char ratio of 100ml/g at a temperature of 60℃ and for a period of 60 minutes. The process requires continuous stirring for two successive leaching stages. When these steps are performed the mixtures are allowed to settle down and use of filtration is employed to separate the pyrolytic char, the mixed heavy metal salts, and the acid. The pyrolytic char is washed with deionized water several times to remove the solubilized salts and residual acid. The final step is to dey the char samples at 110℃ for 24 hours [78].

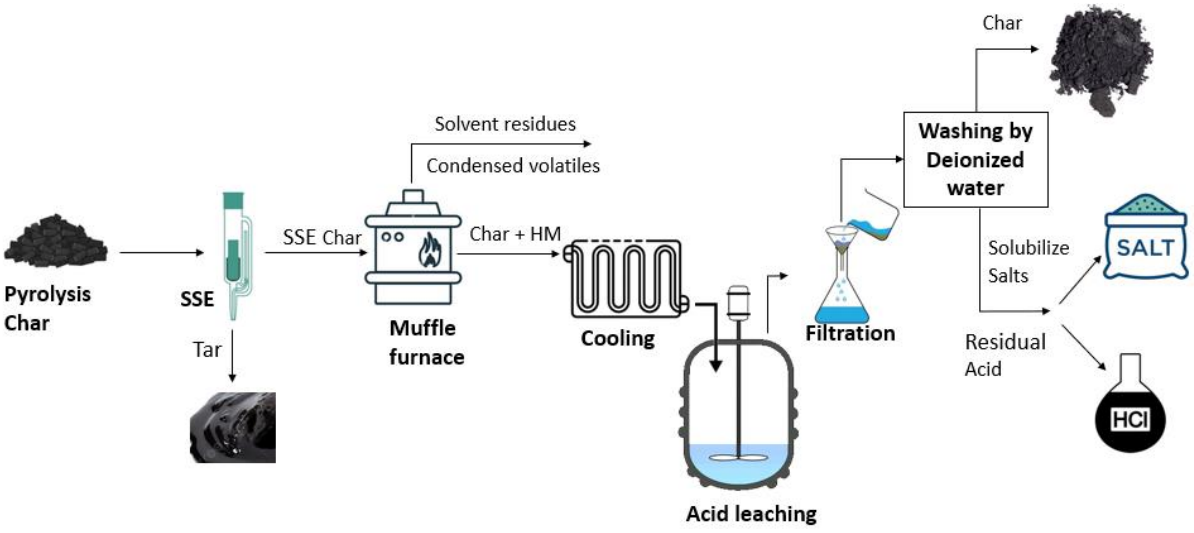

Figure 3:Acid leaching of pyrolysis char using 1M HCl.

2.8 Combined Thermochemical Processes

Poly-generation combined systems tend to have higher efficiency and fewer pollutants than individual systems and heat, electricity, and useful chemicals can be produced simultaneously. As reported, improved thermal efficiency, effective carbon utilization, reduced tar and char, and removal of wastewater treatment can be achieved [79].

2.8.1 Chemical Looping Gasification(CLG) and CLG coupled with pyrolysis

Chemical Looping Hydrogen Production (CLH) is employed for clean hydrogen production in which metal-based Oxygen Carriers (OC) break down carbon-rich fuels like biomass. Reduction and oxidation are two stages that the oxygen carriers have to go through to supply oxygen for fuel through intra-lattice migration of oxygen and electrons. Some oxygen carriers also have to go through air oxidation for their recyclability. The OC functions as both a reactant and mass separation agent which helps avoid the mixing of air with fuel. This helps reduce the use of energy-intensive air separation units and simplifies the process of reducing GHG emissions, energy loss, and cost [80]. The three and two reactors are the most commonly reported reactor configurations for Chemical Looping Technology (CLT). The three-reactor configuration consists of a Fuel Reactor (FR), an Air Reactor (AR), and a Steam Reactor (SR) whereas in the case of the two-reactor configuration an AR and FR are used [81]. Chemical looping gasification (CLG) is an innovative gasification technology that utilizes lattice oxygen for gasification via an oxygen carrier (OC) that circulates between the fuel reactor and the air reactor [82].The production of hydrogen can be achieved through the CLG process via cyclic water gas shift and re-oxidation of reduced oxygen carriers with water, which enhances the quality of syngas for potential applications in clean energy, fuel cells, or chemical precursors [83].

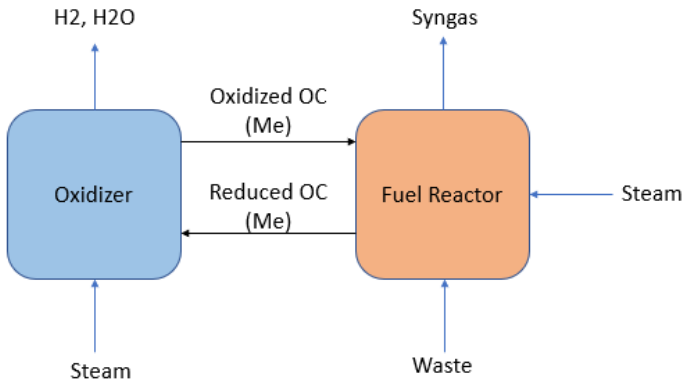

Figure 4:Chemical looping gasification schematic illustration.

Pyrolysis involves the thermal decomposition of solid fuels in an inert environment to produce char, tar, and pyrolytic gas. The pyrolysis gases from ASR primarily consist of light hydrocarbons, hydrogen, and methane, along with minor components such as CO, CO2, and H2S. For the pyrolysis process, temperature is an important factor in the final product yield. From temperatures ranging from 550°C to 800°C, the liquid yield from pyrolysis of ASR decreased from 28% to only 7%, and the drop of yield in the light hydrocarbon yield and increase of CH4 and H2. The mechanism of pyrolysis can explain this factor, as heavier hydrocarbons are broken down into lighter hydrocarbons due to the increase of

temperature. Due to high-temperature pyrolysis, gas yield increases from 42% to 65%. The solid product in the form of char has a mixed yield of reaching the highest yield up to 34% at 600℃ and from 500℃ to 800℃ the char yield varies from 30% to 28% with an HHV value of 18.99 to 17.86 MJ/kg [84]. The organic components in ASR are recovered more effectively in pyrolysis, and it is easier to separate heavy metals in pyrolysis from pyrolysis char [85]. Allothermal or Indirect gasification is one of the most effective thermochemical processes for obtaining nitrogen-free syngas as a product [3]. The gasification process involves heating and decomposing of waste, which results in the pyrolysis process that generates char, gas, and tar. The char is further gasified with the gasifying agent to produce gas which can be treated by WSG reaction to produce hydrogen. The primary reactant in ASR gasification is pyrolysis char, and the reactivity of gasification is closely related to the carbon crystal structure, surface functional groups, and pore structure of char. Other significant factors influencing gasification include temperature and gasification atmosphere [86].

Table 2: Combined Thermochemical Processes & Main Findings.

Reference	Production capacity	Technology & Reactor configurations	Main findings
Anaya et al. [87]	607tons/day of H2	Chemical Looping Partial oxidation Two reactor systems (FR&AR) (Syngas production, Hydrogen production, and carbon capture)	Hydrogen yield: 2.87mol H2/mol of natural gas. GHG emissions: 2.86CO2/kg-H2. 57% lower than SMR with CCS.
Kun et al. [88]	115.39 kg/h syngas(CO,H2) 50.17kg/h of char.	Pyrolysis unit, CLG Two reactor systems(FR&AR) with pyrolysis and drying reactor.	Combined system thermal efficiency 43.12%. Exergy utilization is 88.2% higher than individual pyrolysis and gasification.
Li et al. [89]	8.03kg/h of hydrogen. 35.51kW net electric power.	Biomass-Pyrolysis-Gasification-Hydrogen(BPGH) process. Heat Recovery Steam Generator(HRSG) and Organic Rankine Cycle(ORC) 4 reactors(Pyrolysis, Gasification, tar reforming and Hydrogen generation)	Energy Efficiency is 59.35 Exergy efficiency is 49.24% Biomass conversion efficiency is 52.49% High H2 generation efficiency is 8.03% CO2 can be captured and stored.
Santos et al. [90]	48.7% hydrogen production efficiency(SEG)	Conventional steam gasification Sorption Enhanced Gasification(SEG)	Total efficiency 53.3 in conv. Gasification is higher than SEG.

			SEG reduces CO2 from 21.7 kg/CO2 1.4kg/CO2
Zhao et al. [91]	H2 molar fraction 73.3% CO2 emission 234.7 kg MW/h Carbon Nano Tubes	Plasma Co-Gasification System Reactors types (Plasma Gasifier, Reformer, Separation units, and Pressure Swing Adsorption (PSA)	Energy utilization efficiency is 57.8% Hydrogen conversion efficiency is 75.6%
Qi et al. [92]	112kg/h purified H2 after PSA(68.59% of H2 input)	CLG with Steam Reforming Reactor types (FR, AR, Steam Reactor, and PSA)	At 700°C, H2 selectivity reaches 60.68%. Energy efficiency 47.76%. GWP: 60.02% of GWP is contributed by CO2 emission. AP: 68.25% attributed to total Acidifying emission.
Sun et al. [93]	MSW to Hydrogen (MTH) CO2 removal efficiency:99.99% H2 purity: 99.99%	Gasification Fluidized bed gasifier with oxygen and steam gasifying agent. WGSR (adiabatic): 270-450°C	MTH GWP is 897.3kgCO2-eq/h Exergy efficiency: 46.7%

2.8.2 Key Reactions

Table 3: Chemical Reactions.

Reaction	Stoichiometry	Reference
Pyrolysis reaction:	$Biomass + Heat = Prolytic\ gas + Char + Tar$ (16)	Li et al. [89]
Gasification reactions: Reforming of char(17) Methanation(18) Boudouard(19) Water Gas Shift(20) Gas-Solid intreactions(21)	$C + H_2O \rightarrow CO + H_2 \ ; \Delta H = 131\ kJ/mole$ (17) $C + 2H_2 \rightarrow CH_4 \ ; \Delta H = -75\ kJ/mole$ (18) $C + CO_2 \rightarrow CO\ ; \Delta H = 172\ kJ/mole$ (19) $CO + H_2O \rightarrow CO_2 + H_2 \ ; \Delta H = -41\ kJ/mole$ (20) $4Ca2Fe2O5 + 3CH4 \rightarrow 8CaO + 8Fe + 3CO2 + 6H2O$ (21)	Kun et al. [88] Shah et al. [94]
Reduction (22)(23) Oxidation(24)	$CO + 3Fe2O3 \rightarrow CO2 + 2Fe3O4 \ ; \Delta H - 47\ kJ/mole$ (22) $H2 + 3Fe2O3 \rightarrow H2O + 2Fe3O4 \ ; \Delta H - 6\ kJ/mole$(23) $4Fe3O4 + O2 \rightarrow 6Fe2O3$ (24)	[88] Gopaul et al. [95]
Hydrogen generation reactions	$3FeO + H2O = Fe3O4 + H2$ (25) $3Fe + 4H2O = Fe3O4 + 4H2$ (26)	[89]
Re-oxidation using steam	$2CaO + 2Fe + 3H2O \rightarrow Ca2Fe2O5 + 3H2$ (27)	Hu et al. [96]

These reactions are chemically equilibrium reactions. So, the removal of one product from the reaction will emphasize the reaction to move rightward and increase the generation of the desired product. In the endothermic reactions with the increase of temperatures, the enhancement of products can be done and for exothermic reactions, the production of products is favored by lower temperatures.

2.8.3 Oxygen carrier

Different types of oxygen carriers are discussed here based on their oxygen transport capacity, availability, cost, hydrogen enhancement ability, and cyclic ability to oxidize and reduce. The selection and design of OC should be investigated to produce better-quality syngas from CLG biomass. The properties like durability, partly oxidation reactivity for MSW, and selectivity of CO and H2 are more desired in OC's. The study up to now on OC's are of two types: Natural and Synthetic. The Binary metal OC showed better performance in the case of H2 yielding with biomass as reported in [97]. The

combination of OC+steam biomass gasification has a higher yield of hydrogen in CLG than biomass steam gasification. The preparation of OCs for CLG and the pyrolysis of rice straw in a stainless-steel tube reactor. The reported calcium-iron oxide OCs were synthesized by wet impregnation. The purity of raw CaO on a trace metal basis was 99.995%, and Fe2O3 powder was above or equal to 96% which were directly used as OCs as a comparison with the prepared OCs referred to as Fe:Ca=2:1, 1:1, and 2:1 [97]. The preparation of those binary OCs can be demonstrated below-

Firstly, Fe(NO3)3.9H20 with CAS reagent purity greater or equal to 98% was dissolved with 100ml deionized water. Then at 80℃, the solution was impregnated with a stoichiometric amount of solid CaO (99.995% trace metal basis) by continuous stirring for 4 hours. The resulting precipitate was dried in a drying oven at 105℃ for 8 hours. Then the drying sample was calcinated in a muffle furnace with a heating rate of 10℃/min from room temperature to 800℃ and kept at 800 ℃ for 4 hours in an air atmosphere. The final step reported was to ground and sieve the calcined sample into fine powders with particle sizes in the range of 0.090-0.212mm. The highest yield of hydrogen was found for Ca2Fe2O5 with comparison with its constituents CaO and Fe2O3 and also with the other combinations Fe:Ca=1:2 and Fe:Ca=2:1 was 23.07 mmol/g of biomass. However, the problem reported using these types of OC during cyclic stability was that after repeating the CLG process five times, the formation of CaSiO3 and Fe2O3 destroyed the bimetallic Fe-Ca structure, and the hydrogen yield after the fifth cycle came down to 18.09 mmol/g of biomass. The reason for that issue was reported that the Si accumulated from the ash content after gasification, which reacted with the OC after three cycles.

The comparison among OCs can be done for CLG between Fe2O3, Ca2Fe2O5. To find out these OCs' partial oxidation temperatures were obtained from the thermodynamic data for reactions with carbon and carbon mono-oxide. The data were collected from [98] where for Ca2Fe2O5 the temperature range was 780-880℃ and Fe2O3 from zone A of Ellingham diagram was also analyzed. Regarding Fe2O3, the temperature range for partial oxidation was nonexistent, as carbon could undergo oxidation to CO2 over the entire temperature range. So, this supports the statement made in [99]. The zone A metal oxides must be used as sub-stoichiometric amounts to prevent complete oxidation. Fe2O3 has the disadvantage of low oxygen carrying capacity so instead of using it in CLC, the use of it in the CLG might give a slight advantage for its low price, availability, non-toxic nature, and high-temperature stability. The consideration made out of these is that the reaction rate is lower at the boundary temperature so a slightly higher temperature is chosen. The mole ratio of the oxygen content in the oxygen carrier that can be transferred to the solid carbon to the mole content of solid carbon was established as the O/C ratio. The oxygen-carrying capacity of Fe2O3 is 0.3 and for Fe2O3 both reactions are valid due to the formation of CO and CO2 detected by MS as both reactions occurred simultaneously.

$$Fe2O3 + 3C = 2Fe + 3CO \quad (28)$$

$$Fe2O3 + 3C = 2Fe + 1.5CO2 + 1.5C \quad (29)$$

For, Ca2Fe2O5 the OTC is 0.176.

$$Ca2Fe2O5 + 3C = 2Fe + 2CaO + 3CO \quad (30)$$

For the above-mentioned OCs, the weight loss of the mixture of OCs and CO didn't vary much with theoretical value. The reduction was carried out at high temperature in a fixed bed reactor. It was

reported according to XRD patterns that after five cycles, both the OCs were very close to the fresh OCs, indicating good regeneration properties for both OCs.

Recent studies on the improvement of OC mainly focused on developing the recycling and reactivity ability by modifying and adjusting the existing mixed metal oxides. Chemical Looping Partial Oxidation (CLPO) is a process where metal oxides are partially oxidized with the fuel like hydrocarbons or methane which generates quality syngas whereas for CLC complete oxidation occurs and generation of CO2 and H2O both GHG is produced. The chemical looping solid fuel partial oxidation to produce syngas is rarely reported in the works of literature due to many challenges.

2.8.4 Sorption Enhanced Gasification(SEG)

Tar and N2 are the most difficult contaminants to remove from syngas [3]. The CaO employment in the MSW gasifier enhances the water gas shift reaction (WGS) by capturing CO2 and according to La chattelier law, the reaction shifts rightward, decreasing the amount of CO and increasing H2. The carbonation and WGS reaction in a single reactor can make both reactions simultaneously occur and proceed in the right direction [100]. The reaction is called carbonation and it is exothermic in nature and can be described as-

$$CaO_{(s)} + CO_{2(gas)} \rightarrow CaCO_{3(solid)}, \Delta H^{o}_{298} = -178.17 kJ/mol \quad (31)$$

It was reported to diminish the external supply of CaO, a calcination process can be done in a separate reactor which is endothermic nature and can be described as-

$$CaCO_{3(s)} \rightarrow CaO_{(s)} + CO_{2(gas)}, \Delta H^{o}_{298} = 178.17 kJ/mol \quad (32)$$

Where, $CaCO_{3(s)}$ =Calcium carbonate in solid phase, $CaO_{(s)}$ =Calcium oxide in solid phase, and $CO_{2(gas)}$=Carbon di oxide in gas phase [101]. The formation of tar decreases due to the addition of CaO which is 7g/Nm^3 (dry gas) as reported-

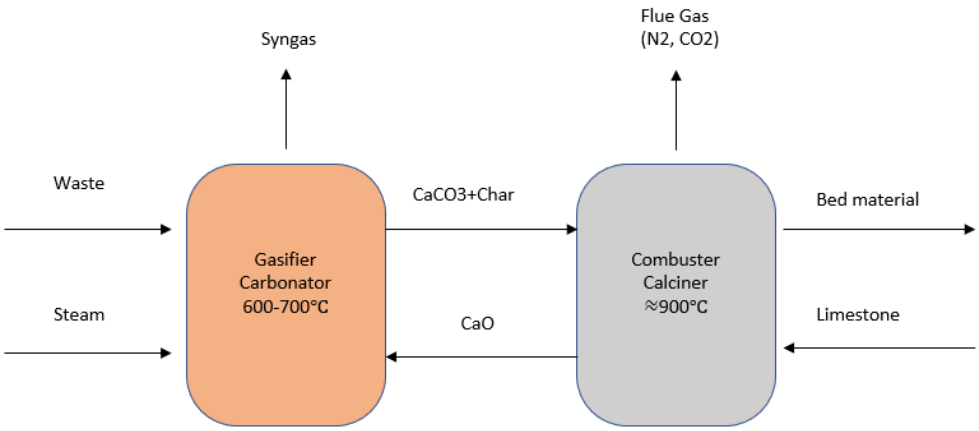

Figure 5: Sorption-Enhanced Gasification (SEG)[3]

2.9 Mass balance

The consideration made for the mass balance can be demonstrated as follows for the units that are in the system [102] . The following mass balance equation is used for the system performance-

$$\sum \dot{m}_{inlet} = \sum \dot{m}_{outlet} \tag{33}$$

Where, $\sum \dot{m}_{inlet}$= Total inlet mass flow rate, and $\sum \dot{m}_{outlet}$=Total outlet mass flow rate.

2.10 Energy balance

The energy balance equation used can be described as [103]-

$$\sum H_{in} - \sum H_{out} = \Delta \dot{E}_{system} \tag{34}$$

Where, $\sum H_{in}$= $\sum \dot{m}_{in} \times h_{in}$ and $\sum H_{out}$= $\sum \dot{m}_{out} \times h_{out}$: h_{in}= Specific enthalpy of inlet of the system and h_{out}=Specific enthalpy of outlet of the system.

2.11 Energy Analysis

Energy analysis which is based on the first law of thermodynamics is used to measure the energy quantity of the system [104]. From the conservation of energy, the total input energy is equal to total output energy. Under steady-state conditions for an open system, the energy balance equation can be described below [105]-

$$EN_{in} + Q_{supply} = EN_{out} + Q_{gen} + EN_{loss} \tag{35}$$

Where, EN_{in}=Energy of inlet streams(kW), EN_{out}=Energy of outlet streams(kW), Q_{supply}=Inlet heat supply, Q_{gen}=Output work or Heat generated, and EN_{out}=Energy loss.
The hydrogen production efficiency [106] can be determined as follows-

$$\eta_{H2}(\%) = \frac{\dot{m}_{H_2} \times LHV_{H2}}{\dot{M}_{MSW} \times LHV_{MSW}} \times 100 \tag{36}$$

Where, $\dot{m}_{H2}$=Mass flow rate H2, kg/hr, LHV_{H2}=Lower heating value of H2 which is 120 MJ/kg [107], $\dot{M}_{MSW}$= Mass flow rate of MSW, kg/hr, and LHV_{MSW}=Lower heating value of MSW.

2.12 Exergy Analysis

Material's exergy can be defined as the most work that can be accomplished between a given condition and its reference state. The quality of energy is determined through it and the areas where energy loss occurs can be identified [108]. Under steady-state conditions, the balance equation for the exergy of a system can be described as-

$$\sum Q_{in} + \sum EX_{in} = \sum Q_{out} + \sum EX_{out} + \sum EX_{loss} \quad (37)$$

Where, $\sum Q_{in}$ =Total power input(kW), $\sum EX_{in}$ = Total exergy input(kW), $\sum Q_{out}$ =Total power output(kW), $\sum EX_{out}$=Total exery output(kW), and $\sum EX_{loss}$=Total exergy loss(kW).

The ability of a material to exert energy is dependent on the system's conditions as well as its surroundings. Chemical, mechanical, and thermal reactions are considered during the calculation [109]. Based upon the 2nd law of thermodynamics, the exergy analysis helps to improve material energy, process design, and evaluation [110]. As the analysis determines the irreversibility types and values, it proves to be better than energy analysis and more efficient assessment can be presented by it [111]. The total exergy of the material is composed of four components which are physical, chemical, kinetic, and potential. The total exergy constituted after neglecting the kinetic and potential exergy as follows [112]-

$$EX = EX_{ph} + EX_{ch} \quad (38)$$

Where, EX=Total exergy, EX_{ph}=Physical exergy, and EX_{ch}=Chemical exergy.
The exergy calculation of gases is divided into physical and chemical exergy and the physical exergy is determined by using following equation [112] -

$$EX_{ph} = \sum_i n_i \times ex_i^{ph} \quad (39)$$

Where, EX_{ph}= Total physical exergy, n_i= Molar flow rate of component i, and ex_i^{ph}=Physical exergy of component i.
The physical exergy of component i can be obtained by using the following equation [112]-

$$ex_i^{ph} = (h - h_o) - T_o \times (s - s_o) \quad (40)$$

Wher, h=Enthalpy of component i at given condition, h_o=Enthalpy of component i at T_o reference temperature, s=Entropy of component i at given condition, and s_o=Entropy of component i at T_o reference temperature. The terms enthalpy and entropy are calculated using following equations-

$$h - h_o = \int_{T_o}^{T} c_p \times dT \quad (41)$$

$$s - s_o = \int_{T_o}^{T} \frac{c_p}{T} \times dT - R \times ln\frac{p}{p_o} \quad (42)$$

Where, c_p=Specific heat of gas component i, R= Universal gas constant, p= Pressure of gas component i at given condition, and p_o=Pressure of gas component i at T_o reference temperature.

The chemical exergy of the gases is determined using the following equation [113] -

$$EX_{ch} = \sum x_i \times ex_i^{ch} \quad (43)$$

Where, EX_{ch}= Total chemical exergy of gases, n_i=Molar flow rate of component i, ex_i^{ch}= Standard chemical exergy of component i, and can be obtained from

The following equation to calculate the chemical exergy of MSW[113]-

$$EX_{MSW} = (2442 \times MC + LHV_{MSW}) \times \left(0.1882 \times \frac{H}{C} + 0.0404 \times \frac{N}{C} - 0.0610 \times \frac{O}{C} + 1.0437\right) \quad (44)$$

Where, C, H, N, O, and MC are weight fractions of carbon, hydrogen, nitrogen, oxygen, and moisture conten

The standard chemical exergy for the oxygen carrier Ca2Fe2O5 is determined using the following equation equal [114]-

$$EX_{ch}^{O} = \Delta G_f^o + \sum n_i EX_{ch,i}^o \quad (45)$$

The Standard Gibbs free energy of formation ΔG_f^o of Ca2Fe2O5 is calculated using the following equation-

$$\Delta G_f^o(Ca2Fe2O5) = \Delta H_0 - T_o \Delta S_o \quad (46)$$

Where T_o=298.15K ; ΔH_0=-55kJ/mol; $\Delta S_o = 0.5755 kJ/mol$ [115]

Table 4: Standard Chemical Exergy of components [4], [5], [6].

Component	ex_i^{ch}(KJ/mol)	Component	ex_i^{ch}(KJ/mol)
H2	236.1	H2O (gas)	9.5
CO	275.5	H2O (liquid)	0.9
CO2	19.87	CaO (solid)	119.62
C (solid, graphite)	410.26		

2.13 Environmental Analysis

The environmental impact of the process can be evaluated by estimating the Global Warming Potential(GWP) and Acidification Potentital (AP) using the following two equations [116] -

$$GWP = \sum(EF_{GWP,i} \times AMT_{GG,i}) \quad (47)$$

Where, $EF_{GWP,i}$ is , GWP correlation efficient for gas , i and $AMT_{GG,i}$=Amount emitted gas i.

$$AP = \sum(EF_{AP,i} \times AMT_{AP,i}) \quad (48)$$

Where $EF_{AP,i}$ is , AP correlation efficient for gas , i and $AMT_{AP,i}$=Emission rate of gas i.
The correlation coefficients of GHP and AP are tabulated below

Table 5: Correlation co-efficients [7], [8].

Compound	GWP Coefficinet (100years)	Compound	AP Coefficient
CO2	1	SO2	1
CH4	28	NO2	0.7

2.13.1 Cold Gas Efficiency

Cold Gas Efficiency (CGE) is an effective parameter that determines how efficiently the gasification process is converting the chemical energy in waste into useful chemical components like H2, CO, and CH4. By normalizing the conversion product's heating value to the feedstock's heating value, the CGE analyzes how well the feedstock is converted into a different product [117].

$$CGE(\%) = \frac{\dot{m}_{co}LHV_{CO} + \dot{m}_{H2}LHV_{H2+}\dot{m}_{CH4}LHV_{CH_4}}{\dot{m}_{waste}LHV_{waste}} \quad (49)$$

Where, $\dot{m}_{waste}$= Mass flow rate of waste (kg/s), LHV_{waste}= Lower heating value of waste (MJ/kg), $\dot{m}_{co}$= Mass flow rate of CO(kg/s), $\dot{m}_{H2}$=Mass flow rate of H2(kg/s), $\dot{m}_{CH4}$=Mass flow rate of CH4(kg/s), LHV_{CO} =Lower heating value of CO(MJ/kg), LHV_{H2} =Lower heating value of H2(MJ/kg) and LHV_{CH4}=Lower heating value of CH4(MJ/kg).

3 Materials and Methods

In this chapter, the experimental methods implemented for waste characterization performed in the laboratory and waste processing models like Sorption Enhanced Chemical Looping Gasification (SE-CLG) developed in Aspen plus simulation software are discussed. The waste composition, waste description, and investigation, sample preparation for waste characterization, waste characterization methods, simulation model training & development, and model finalization are also discussed.

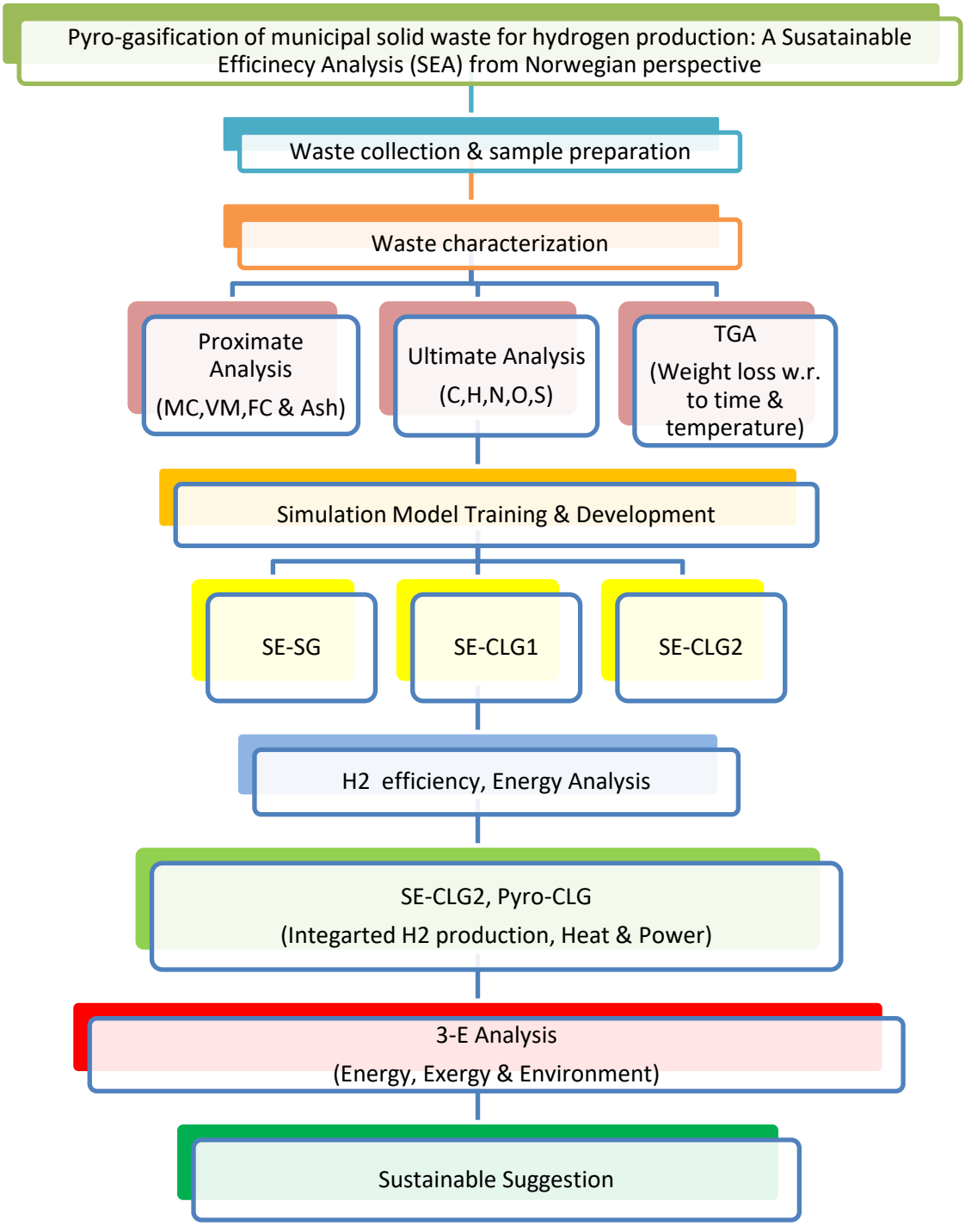

Figure 6: Flow diagram of Methodology.

3.1 ISW composition

A total of 4 samples of waste were collected from an organization named Geo4Dynamic, Asker which mainly consists of paper, wood, textiles, plastics, and shredded car parts highlighting tires. The four categories of waste are namely 1. Car-fluff (Fine and Coarse) 2.FAB incinerator waste 3.FAB cement kiln waste. The detailed waste composition is further discussed in this chapter.

3.2 Sample description

The waste samples collected from an organization included the following three categories of samples, which were further ensured by the authority which ensured namely:

1. Car fluff (fine & Coarse shredded): This comes from car demolitions, likely after the economically valuable metal parts are removed. It may also include other waste materials fed into the car shredder. Norsk Gjenvinning (NG) [118] can mix some of the finely shredded car fluff with waste sent to incinerators, while the coarsely shredded car or automotive fluff is likely sent to landfills. Finely shredded car fluff has a higher calorific value due to its rubber and plastic content and can range between 9.30 to 13.96 MJ/kg and an average of 12.56 MJ/kg [119]. Its heterogeneous composition includes polyvinyl chloride (PVC), propylene, rubber, textiles, glass, or a small amount of metals. From the waste composition, it can be said that it is combustible as well as some in-combustibles.
2. FAB incinerator waste: This is general industrial waste from various industries and offices (“næringsavfall”). It can vary significantly, due to seasonal fluctuations and day-to-day depending on the customers. While this waste theoretically should not contain food waste, samples have shown it can contain up to 5-10%.
3. FAB cement kiln waste (Norcem FAB): There are more vinyl and roofing felt in this sample. Most commonly Poly Vinyl Chloride (PVC) is a plastic polymer with the combination of ethylene and chlorine. Due to their durability and water-resistive nature, they are used for pipes, flooring, windows, and building sidings. Roofing felt is fiber or polyester saturated with asphalt or bitumen and it is used as an underlayment of building roofs. Both vinyl and roofing felt can be non-recyclable and due to their significant calorific values, they can be used as FAB [120]. The emissions from these materials can be better controlled in cement kilns because of their higher working temperatures. As part of a larger goal to enhance waste management and lessen environmental effects, Norcem's cement factories, including the one in Kjøpsvik, have been upgraded to take more alternative fuels, including Fraction of Alternative Biofuels or Fuels (FAB) waste [121].

The waste samples were analyzed visually and manual separation was employed to identify the constituent parts of the wastes. Each sample was obtained in plastic bags and each sample of waste was weighed using a digital balance. To measure the weight of the sample accurately an aluminum dish was used which had been weighted previously, and the weight was recorded as 22.24g. The measured weight of the car fluff (fine) was 451.82g, car fluff (coarse) was 1000g, FAB incinerator waste was 882.75g, and FAB cement kiln was 983.07g. Then firstly the Car fluff (fine) was taken to determine the constituents. The waste was mixed adequately by hand and a sample of weight of 103.56g was taken for further investigation. The constituents were visually inspected and manually separated using a sieve to make it dust-free. Then the organic and inorganic fractions were separated as the material used in this work which is fractional representative of ASR by separating the fines and inorganics. The separated constituents were weighted to determine the mass fraction of them in the total waste. The

same procedure was applied to the other three waste types. The car fluff was termed CF 1 for fine and CF 2 for coarse shredded. The FAB incinerator waste was termed FAB 1 and FAB 2.

CF 1: The sample was relatively homogeneous and out of a total of 429.57g mixed waste 81.32g was taken for inspection it consisted mainly of organic matter like wood splinters size of 2-30mm and it constituted around 80% of the total material in CF 1. The total weight of the wood splinters was 65.056g. The foam was 1mm-10mm and the weight was 4.8792, which was 6% of the total waste.

Figure 7:Car fluff (Fine shredded).

The plastics were found in sizes 5-15mm, and the weight was 4.0675g with a weight percentage of 5%. Stones varied in size from 1-10mm, and the weight was 0.8132g, and a weight percentage of 1%. Metal, like metal string/wire and copper flakes, was 10-50mm, and the weight was 0.832g, slightly above 1% of the total material. The glass portion of the total waste was below 1% and weighed 0.1097g.

CF 2: The sample was extremely heterogeneous and consisted mainly of large pieces of waste. The total weighed waste was around 977.76g. From visual inspection, the first thing noticed was a large shredded bicycle tire and some medium-sized shredded pieces in 100-300mm. The tire-by-weight fraction constituted 24.28% of the total waste CF 2 and it weighed 237.40g. The foam and cushion were 80-130mm in size, weighed 205.43g, and 21.01% of the total waste. Some textiles were found in the waste sample, which comprised 15.874% of the total waste and had a weight of 12.60g. Some insulated wires were found in the sample ranging in size from 150-300mm and weighed 75.60g which was 7.732% of the total sample. The presence of hard plastics was noticed from 10-15mm in size and was 20.92% of the total weight, weighing 204.547g. The remaining samples were unrecognizable which was 10.184% of the total waste.

Figure 8: Car fluff (Coarse shredded)

FAB 1: For the incinerator waste, the strategy applied was similar to the strategy applied to CF 1 as the waste was medium shredded. The total weighed sample was 860.51g, out of which 187.02g samples were taken to determine the composition. The sample was very heterogeneous and dominated by some objects. The textiles consisted of about 26.06% of the sample and weighed 48.74g. There were plastics in different sizes ranging from 100-200mm like plastic foil and hard plastics, weighing 44.42g and 23.75%. The foam portion weighed 31.67g and size ranged from 40-80mm. The foam constructed 16.93% of the total waste. The wood portion had a variety in size, from 80-130mm in size, and the weight percentage was 15.789%. The weight of the paper was 31.67g and it consisted of tissue paper, paper used in books and cardboard, and 16.934 in weight percentage. Some percentage of rope was found which included both made of plastics and textiles and added accordingly.

Figure 9: FAB incinerator waste.

FAB 2: The sample consisted of FAB cement kiln waste and the total weight obtained was 782.51g. The sample was shaken end over end and manually mixed to homogenize the sample constituents. A fraction of 197.07g was taken from the total waste for further investigation. The plastic portion consisted of some hard plastic and foil which weighed 49.62g and the weight percentage was 25.179%. The paper weighed 23.79g and 12.07% of the total waste. The textile portion weighed 43.09g and 21.86% of the total waste. The foam and wood weighed 27.44g and 33.10g and by weight percentage 13.92% and 16.79% of the total waste. Some rubber was present in the waste, weighing 5.08% of the total waste.

Figure 10: FAB cement kiln waste.

3.3 Sample Preparation

A representative fraction of ASR, FAB incinerator waste, and FAB cement kiln waste, is typically separated from inorganics and fines. The separated samples were used for this study. Rubber, textiles, foam, plastics, and other organic materials made up the majority of the used CF 1, CF 2, FAB 1, and FAB 2.

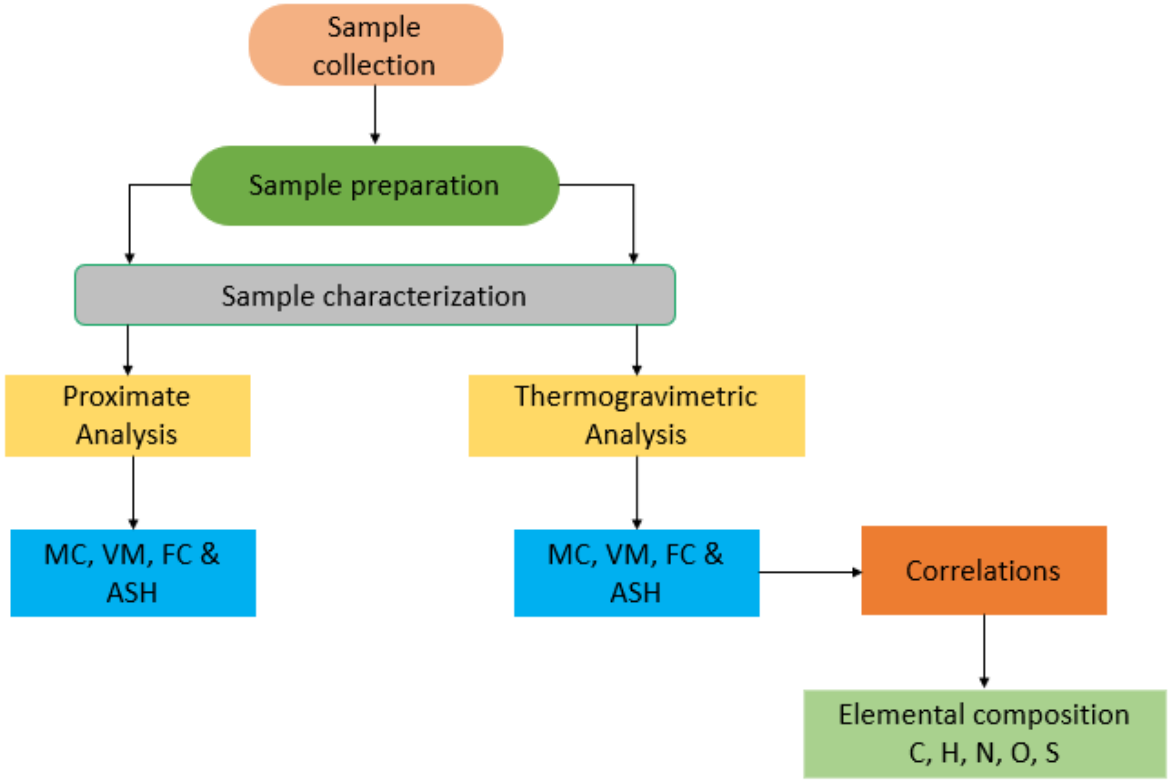

Figure 11: Schematic representation of waste sample preparation & characterization.

The composition of the wastes was calculated by manually separating a representative sample into its constituent parts. Table 6 shows the wastes with their constituents' composition in weight percentage. For CF 1, the compositions of wood, plastics, and foam were considered for sample preparation for waste characterization. Similarly, for CF 2 the compositions of textiles, plastics, tires, and foam, for FAB 1 the compositions of paper, wood, textiles, plastics, and foam, for FAB 2 the compositions of paper, wood, textiles, plastics, foam, and leather were considered for sample for waste characterization.

Table 6: Physical compositions of waste for waste characterization.

Waste constituents (wt%)	Waste category			
	CF 1	CF 2	FAB 1	FAB 2
Paper	0	0	17.025	12.718
Wood	87.91	0	15.874	17.692
Textiles	0	17.674	26.20	23.035
Plastics	5.494	23.292	23.878	26.532
Tire	0	27.033	0	0
Foam	6.593	23.392	17.021	14.668
Rubber	0	0		5.353

After the waste composition was obtained as weight percentage, the samples were manually knifed, and a milling machine for material like wood was used to make a smaller particle size. The sample size varied from 0.5-1mm after manual sieving. The sieve used in the milling machine was 0.5mm. After comminution, the waste constituent's weights were measured and found accordingly in paper, wood, textiles, plastics, tires, foam, and leather.

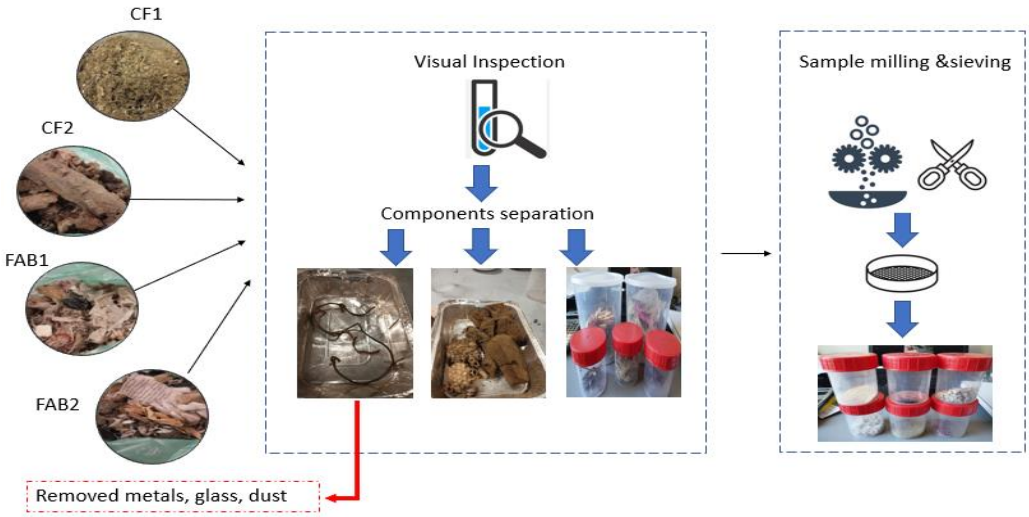

Figure 12:Sample processing and preparation for thermochemical characterization.

After that, the components were mixed according to the weight mentioned in Table 7. The mixed test samples were stirred manually and with a magnetic stirrer to make them homogeneous and representative of the large sample group obtained.

Table 7: Mixture of components in 1g sample.

Waste constituents (g)	Waste category			
	CF 1	CF 2	FAB 1	FAB 2
Paper	_	_	0.170	0.127
Wood	0.879	_	0.158	0.177
Textiles	_	0.176	0.262	0.230
Plastics	0.05494	0.233	0.238	0.265
Tire	-	0.270	_	_
Foam	0.06593	0.234	0.170	0.147
Rubber	_	_		0.054

For the analysis of the individual samples CF 1, CF 2, FAB 1, FAB 2, and their equal weight fraction mixture, we prepared 3 samples for each category in a total of 15 samples.
To investigate the effect of mixing of wastes, the four waste samples were mixed accordingly Table 8-

Table 8: Sample mixing & proportions.

wt fraction / Waste	S-1	S-2	S-3	S-4	S-5
CF 1	1	_	_	_	0.25
CF 2	_	1	_	_	0.25
FAB 1	_	_	1	_	0.25
FAB 2	_	_	_	1	0.25

3.4 Waste Characterization

To determine the moisture content, volatile matter, ash content, and fixed carbon, proximate analysis was employed. The analysis was conducted using a drying oven, furnace, and balance in the laboratory, available at the University of Agder.

3.4.1 Moisture content

The air-dried samples were prepared for weighing before the oven-drying process. Then the samples that were air dried from a particle size category of 1mm were kept in an oven for 24 hours at 105°C until the weight became constant. The time and temperature provided were considered enough to vaporize the moisture within the samples. After drying from the oven, the samples were placed into a glass desiccator to avoid moisture gain from the environment before weighing. The dried samples were then weighed, and the weight difference between the samples before oven-dried and after oven-dried represented the moisture content. The moisture content was determined according to ISO-18134-3 standard using eqn. (1)

3.4.2 Volatile matter

After the samples were dried of moisture the samples were further heated at 900℃ by a closed crucible so that the volatile matter from the samples was driven off. The process is further explained step by step-

A 1 g mixed sample from 1mm particle size was placed in each of three clean dry crucibles. The empty crucibles with a lid were weighed before the samples were put on them. After placing the sample, further weight measurement was done and noted. After that, the samples were put in the furnace and heated for 7 minutes at 900℃. Then the crucibles were removed from the furnace and kept in a decanter for 2 hours to cool down in the lab atmosphere without any weight gain from the atmosphere. The samples were further weighted indicating the weight loss due to thermal decomposition. The volatile matter based on a dry basis was calculated from the weight of the sample before and after the thermal decomposition. The volatile matter was calculated using eqn. (2) as described earlier following ISO 562:1998.

3.4.3 Fixed Carbon and Ash

Ash in biomass is determined using the international standard test ISO 18122, which specifies a method to measure the ash content in all types of solid biofuels. The sample is heated under a controlled temperature of (550± 10)℃ in the presence of air for a specified time and the remaining mass of the residue is calculated to find out the ash content. The apparatus required are a dish, furnace, balance, desiccator, and desiccant. The dish is made of an inert material like porcelain, platinum, or silica and the loading of the test sample should be near 0.1g/cm^2 as a higher mass of sample from this may cause incomplete incineration and absorption of CO2 as calcium carbonate in the calcium-rich sample. The conditioning of the dish is done by heating the empty dish in the furnace to (550± 10)℃ for at least 60 minutes. Then allow the dish to cool on a heat-resistant plate for 5 to 10 minutes and cool the dish at ambient temperature in a desiccator with desiccant. Then, the sample and dish were placed in a cold furnace, and the furnace temperature was evenly raised over 30 minutes to 50 minutes to 250℃ and the heating rate 4.5 ℃/min to 7.5 ℃/min. That temperature is maintained for 60 minutes to allow the volatiles to leave and after that, the temperature increases at a rate of 10℃/min to reach (550±10)℃ over a period of 30 minutes and for 120 minutes the temperature was maintained. Eqn. (3) and eqn. (4) were used to determine the ash and fixed carbon content.

3.4.4 Thermogravimetric Analysis

A thermal analyzer (Mettler Toledo TGA / DSC1) was used at the University of Agder, Termisk Laboratory, and a thermogravimetric analysis was performed on ISW samples. To guarantee the correctness of the experimental data, three duplicates of S-1, S-2, S-3, S-4, and S-5 mentioned in Table 8 weighing roughly 10 mg were used in the experiment. With a particle size of less than 0.5 mm, the ISW sample composition was the same as that utilized in the proximate analysis.

5 samples (CF-1, CF-2, FAB-1, FaB-2, and Total mix) replicating 3 times with a total of 15 samples were used in the TGA experimental procedure that was adapted from ISO 11358. The approach consists of drying the process, pyrolysis (heat decomposition) in the presence of inert gas, and complete

combustion as the last step. The type of process was determined by the medium employed in these inert and oxidation processes. The following is the four-stage TGA program that was adopted:

- Isothermal with an inert gas argon flow rate of 50 milliliters(ml) per minute, 10°C/min from 25°C to 105.0°C.
- At 105°C, Isothermal for 60minutes at argon flow rate 50ml/min.
- From 105°C to 900°C dynamic, at 10°C/min with an argon flow rate of 50ml/min.
- Isothermal for 7minutes at 900°C, with argon flow rate of 50ml/min.
- From 900°C to 850°C, at -10°C/min with argon flow rate of 50ml/min.
- Isothermal combustion at 850°C for 120min in an air atmosphere with an air flow rate 50ml/min.

The four-stage TGA program was first inserted into the linked control computer to begin the experimental operation. The following procedure involved filling fifteen 150µl alumina crucibles with around 10 mg of the well-shaken, well-mixed ISW samples. CF1, CF2, FAB1, and FAB2 were replicated three times to get the mean values for MC, VM, Ash, and FC. The experiment began with blank trials to get baselines to use as corrections. After the placement of one blank, 15 crucibles containing the samples were placed on the TGA analyzer. From the TGA control computer, the MC, VM, and Ash values were obtained from the graph mentioned in Table 16. The TGA control computer exported the text file format including the TG results of the experimental data of the 15 ISW samples. Then data were plotted using Origin Pro software for further analysis.

3.4.5 Ultimate analysis

To determine the elemental compositions of solid wastes, ultimate analysis is performed using a CHN analyzer. However, due to the problem associated with the analyzer, it was not giving the correct values. Due to that, correlation equations are used to calculate the elemental compositions using the moisture content, volatile matter, ash, and fixed carbon value obtained from TGA analysis. The TGA values were used instead of proximate analysis values because the samples were multiplicated during TGA but could not be multiplicated during proximate analysis. Only one representative of each sample was analyzed in proximate analysis whereas in TGA three representatives of each sample were analyzed. The first three equations used to estimate C, H, and N are taken from [63] that are close to the proximate values of this study but no correlations for N (%), and S were provided in that study. For the N and S contents, the correlations were taken from [64], which were for MSW but the proximate values were not as close to this study. The problem is that only one paper was found which concludes MSW elemental compositions prediction using proximate values covering all C, H, N, O, and S contents [64]. The correlations are discussed in eqn. (6),(7),(8),(12), and (13).

3.5 Aspen Simulation Assumption & Plant Design

Aspen plus V11 software is used to simulate all the systems aimed in this study and Gibbs free energy minimizations are followed [15]. The property estimation for the models was done using the Peng-Robinson-Boston Mathias (PR-BM) equation of state. All essential thermodynamic properties were evaluated using the Boston Mathias alpha function [92].

The Dual Fluidized Bed Gasifier (DFB) was considered one Fuel Reactor (FR) and an Air Reactor (AR) [122]. Municipal solid waste, char, and ash are considered non-conventional components, and HCOALGEN and DCOALIGHT are utilized for enthalpy and density calculation. The feedstock MSW or ISW is a non-conventional component that needs to be converted into a conventional component which is done by using the RYIELD block that is widely used to convert non-conventional components like coal, biomass, and MSW into conventional components. CaCO3, CaO, Ca2Fe2O5, Fe2O3, Fe3O4, FeO, and C are considered as solid components. The purity of CaO, Fe2O3 and Ca2FeO5 was considered 100% [97].

The following assumptions are made during ISW sorption enhanced chemical looping gasification and combined pyrolysis with chemical looping gasification-

1. The process is at a steady state condition and reactors are at adiabatic conditions [47].
2. Input parameters for waste are 25^{o}C, and 1 bar [117].
3. No deterioration of OC and sorbent during the process.
4. The carbonator and calciner are considered as isothermal without a temperature gradient.
5. Ash was considered as an inert substance [47].
6. Pb, Cr, and Ni are considered heavy metals, and their weights in char are taken from [123].
7. Tar generation was neglected due to the addition of CaO [122], [90].
8. Liquid yield for the pyrolysis process is neglected due to high-temperature pyrolysis [124].
9. Char is considered a pure solid compound [90].
10. Only CH4 is considered as the hydrocarbon in pyrolysis gas [84].
11. The turbines, compressors, and pumps are considered adiabatic [104].

3.6.1 Model Training & Development

The model training & development part was taken as a case study to develop processes and to compare different OCs interactions with MSW. Three simulation models were developed to conduct the study.

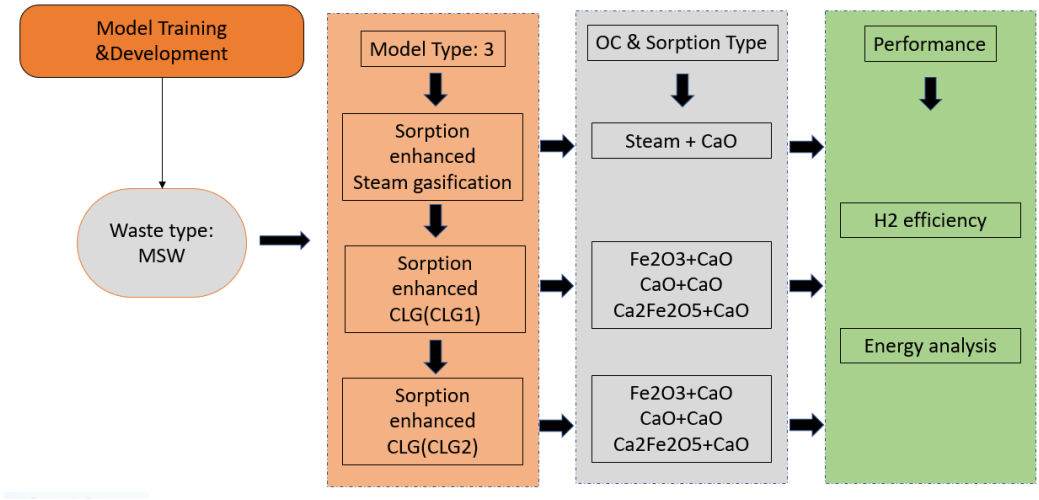

Figure 13: Schematic illustration of model training & development.

The simulation models are described below-

1. Sorption-Enhanced Steam Gasification (SE-SG).
2. Sorption-Enhanced Chemical Looping Gasification (SE-CLG1).
3. Sorption-Enhanced Chemical Looping Gasification (SE-CLG2).

The steam gasification involves steam as a gasifying agent and CaO sorbent looping for CO2 capture which were also used for the other two models. The plant design is presented in Figure 33. For the SE-CLG models, Fe2O3, CaO, and Ca2Fe2O5 were used as OCs. The proximate, ultimate, and sulfanal analysis data of MSW, were taken from the previous study in UiA under the same supervisor. The results obtained from this model training and development were further utilized for a comparative study of the final two developed models (SE-CLG2 &Pyro-CLG) with waste samples ISW and MSW.
These thermochemical waste processing models were compared with previous studies. First, the models were evaluated using the ISW characterization data from existing literature [125].

Table 9: MSW sample characterization data [9].

	MC	VM	FC	Ash		
Proximate values	6.3	78.6	9.0	12.4		
	C(%db)	H(%db)	N(%db)	Ash(%db)	O(%db)	S(%d)
Elemental composition	51.6	6.3	0.8	12.4	28.7	0.2

The model development part also includes development and problem-solving by waste characteristics. From MSW data it is evident that after gasification ash formation will occur. So as previously discussed in section (2.6 Automotive Shredder Residue (ASR)) is about traces of heavy metals and also the formation of ash after thermochemical processes and how it hampers the recyclability of OCs. As discussed in section (2.8.4 Sorption Enhanced Gasification(SEG)) for the solution, a separate combined model Sorption Enhanced Chemical Lopping Gasification with Pyrolysis(Pyro-CLG) with Acid leaching was formed.

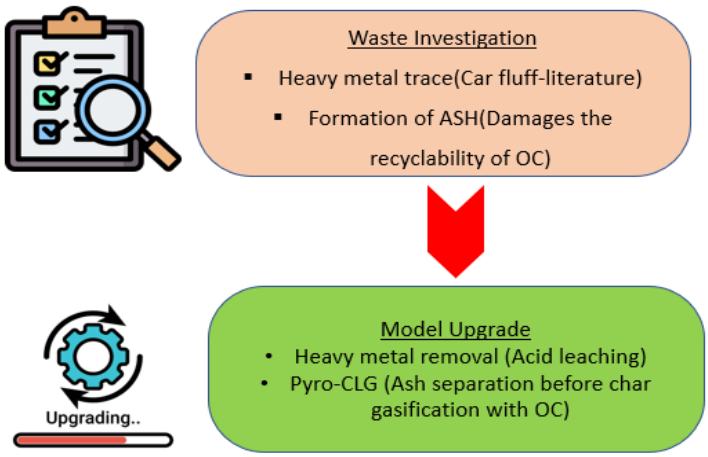

Figure 14: Schematic illustration of model upgrading with waste inspection.

3.6.2 Sorption Enhanced Chemical Looping Gasification(SE-CLG1)

In this process, the waste is first gasified with steam. Then, the gasification product reaches the FR (reducer), where the gas reduces the OC. This generates heat, and then the reduced OC is oxidized in AR (oxidizer) with steam. The model for SE-CLG1 is presented in Figure 34.

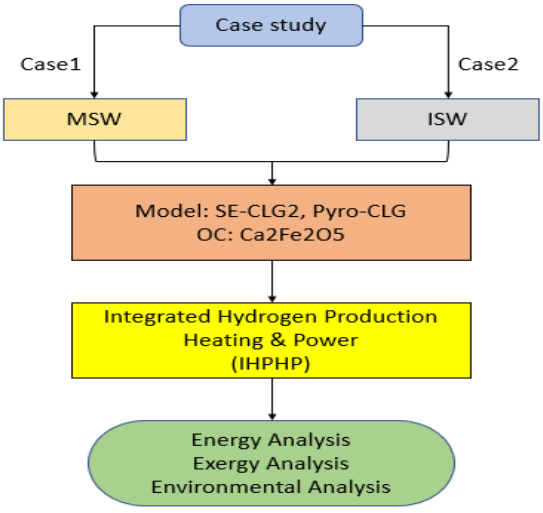

Figure 15: Case study demonstration.

3.6.3 Sorption Enhanced Chemical Looping Gasification (SE-CLG2)

The difference between this process with SE-CLG1 is that in the gasification reactor, the waste is gasified using steam and OC. The OC is reduced in the gasifier then the reduced OC is oxidized in AR with steam. The CaO is used in the WGSR reactor for carbon capture at a flow rate 2000kg/hr, and 1800kg/hr for MSW, and ISW. The OC flow rate was 150kg/hr.
The description of blocks used in the SE-CLG2 model is described in Table 10.

Table 10: Block information.

Model Name SE-CLG2	Name	Aspen model	Operating Conditions
CLG	GASIFIER	RGIBBS	1 bar, 800℃ OC=150 kg/hr Steam=200kg/hr
	OXIDIZER	RGIBBS	1 bar, 800℃ Steam=400kg/hr
WGSR&CO2 capture	WGSR	RGIBBS	1 bar, 700℃ CaO=2000kg/hr Steam=370kg/hr
	CALCINER	RGIBSS	1 bar, 900℃
PSA	H4	HEATER	1 bar, 30℃
	C1	COMPR	Isentropic using ASME method η_{eff}=85%, 10bar
	H5	HEATER	10bar, 40℃
	S8	SEP	H2 purity≈0.9999
HEAT & POWER	P1	PUMP	120bar, η_{pump}=85%
	HPT1	COMPR	40bar, $\eta_{turbine}$=85% $\eta_{mechanical}$=99.99%
	MPT1	COMPR	25bar, $\eta_{turbine}$=85% $\eta_{mechanical}$=99.99%
	LPT1	COMPR	15bar, $\eta_{turbine}$=85% $\eta_{mechanical}$=99.99%
	OT1	COMPR	1bar, $\eta_{turbine}$=85% $\eta_{mechanical}$=99.99%
CO2 STORAGE	COND1	HEATER	73.3bar, 30℃

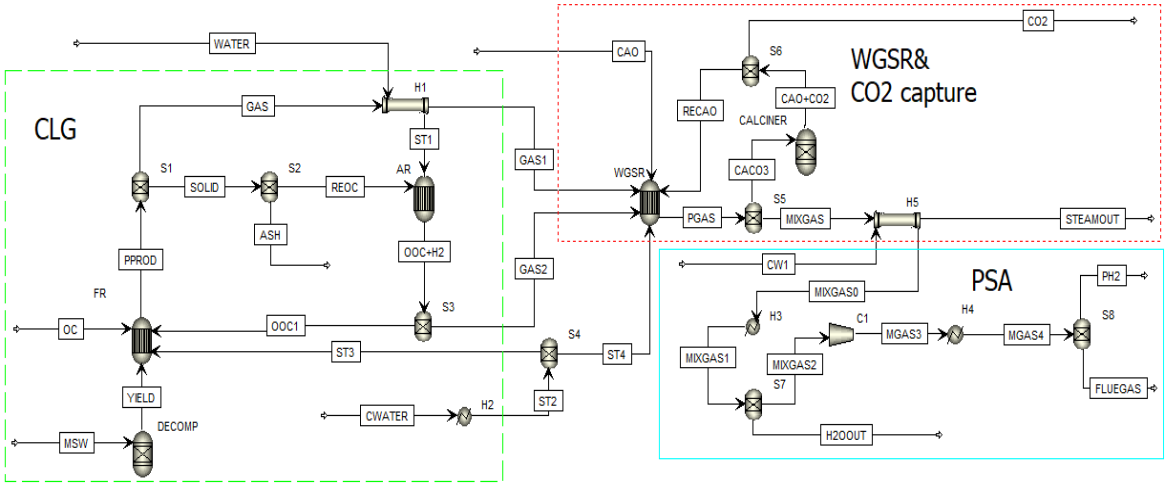

Figure 16: Sorption-Enhanced Chemical Looping Gasification model (SE-CLG2).

In the case of SE-CLG2, while employing different OCs as gasifying agents, when Fe2O3 is used as a gasifying agent an additional block COMBUST was used since after oxidation of Fe & FeO they turn into Fe3O4, which further oxidized with air and Fe2O3 is regenerated according to stoichiometry. For hot water production, all HEATX block hot water outlet temperature was kept at 100°C.

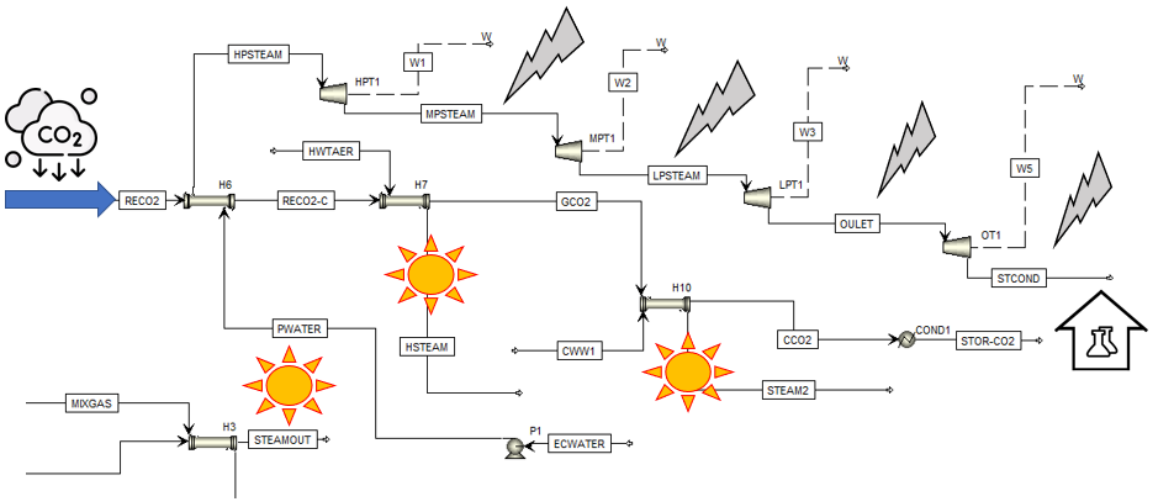

Figure 17: Combined Heat & Power generation (CHP) from captured CO2.

The CHP unit is common for both SE-CLG2 and Pyro-CLG model and it is added with the captured CO2 which is around 900°C and the heat exchanger is used to generate steam with outer water flow rate. The Pyro-CLG model is especially developed for ISW with an addition of acid leaching process of pyrolytic char before chemical looping char gasification with OC. The schematic presentation of the Pyro-CLG model is presented in Figure 18.

3.6.4 Sorption Enhanced Chemical Lopping Gasification with Pyrolysis(Pyro-CLG)

The pyrolysis reactor is simulated using an RGIBBS block with an operating condition of 800°C temperature and 1 bar pressure. All the reactors used in Pyro-CLG are simulated by RGIBBS block except acid leaching. The generated char and ash from the pyrolysis reactor are further separated and the char is sent to an acid-leaching process which is added to remove the heavy metal traces from the char obtained from the pyrolysis of ISW. An RSTOIC and a MIXER block are used to perform the acid leaching with a flow rate of 250kg/hr of 1M HCL at 60°C and 1 bar. The process is discussed in section (2.7 Pretreatment of ASR). The processed char is sent to FR where the char is gasified with OC. The flow rate of OC was 800kg/hr and operating conditions for FR were 800°C and 1 bar for ISW. Reduced OC is oxidized in AR with a steam flow rate of 300 kg/hr, and operating conditions of 900°C, and 1bar. The produced CO from char combustion, H2 produced from OC oxidation by steam, and gas produced from pyrolysis are sent to WGSR. The flow rate of CaO and steam in WGSR is kept at 1000kg/hr, and 370kg/hr for ISW. The flow rate of CaO for MSW was 1000kg/hr. The OC flow rate Ca2FeO5 for MSW and ISW was 1400, and 800 kg/hr. The model is coupled with a PSA unit and also CHP unit for energy recovery.

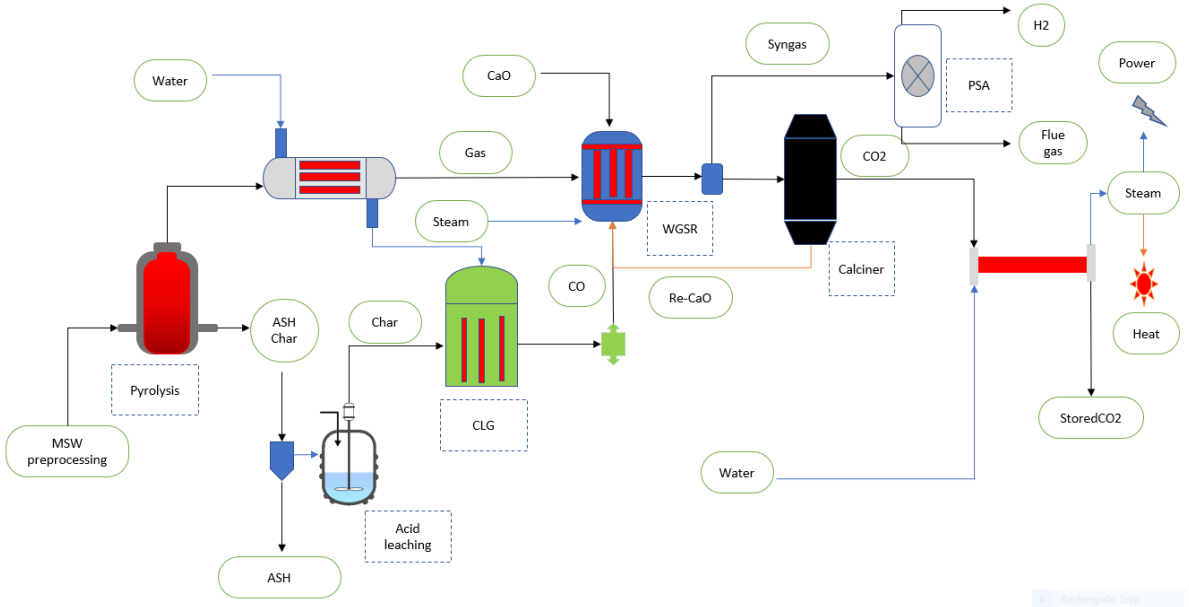

Figure 18: Schematic illustration of Pyro-CLG model with acid leaching heavy metal removal.

4 Results and Discussion

4.1 Introduction

In this chapter, the experimental characterization of waste samples and simulation model analysis results are discussed. In the first part of the chapter, ISW proximate analysis values, results from TGA, and the results of calculated HHV and elemental compositions are discussed. In the latter part of the chapter sensitivity analysis of simulation models, comparison among the models, and H2 efficiency, energy analysis-based selection of OC, and models are discussed. The selected models'(SE-CLG2 & Pyro-CLG2) sensitivity, energy, exergy, environmental analysis, and total output product are also discussed here.

4.2 ISW Characterization

In this chapter, the values obtained from ISW characterization using proximate and TGA analysis are presented. The values obtained are ISW moisture content, volatile matter, fixed carbon, ash, elemental composition, and calorific value. The values are discussed and compared with previous studies.

4.2.1 Proximate Analysis

The proximate analysis result is presented in Table 11 and the calculation and all the related data are presented in Appendix A. The ISW is compared with MSW which are from the same country Norway shows similarity. The variation is due to the more heterogeneity in ISW than MSW as MSW only concluded paper, wood, and plastics were collected from residential areas whereas ISW came from landfills and contains more variety of waste like textiles, leather, tire, and car fluff.

Table 11 Proximate analysis result of ISW

Parameter (wt%) / Sample	Moisture Content (MC)	Volatile Matter (VM)	Fixed Carbon (FC)	Ash
CF1	6.3	71.21	19.71	2.78
CF2	4.4	84.12	8.42	3.06
FAB1	3.1	76.9	14.13	5.87
FAB2	2.4	81.53	13.11	2.96
MSW [9]	6.3	78.6	12.4	9.0

From Table 11, the fixed carbon in CF-1 was found highest as wood constructs the majority portion of the waste we can see from Table 6. The lignin portion of wood increases the fixed carbon content. The ash content and moisture were comparatively lower in ISW than in MSW. The plastic portion was more present in CF-2 and FAB-2, which contributes to the volatile matter portion. The highest moisture content was found in CF-1 as the waste contained some foam and wood which can absorb water and store it for longer periods.

4.2.2 Thermogravimetric Analysis

The thermogravimetric data were further analyzed to obtain the MC, VM, FC, and Ash are presented in Table 12. Every waste category was duplicated three times and the mean values are presented. An additional sample was also analyzed named Total mix which was prepared by taking equal-weight fractions from the four waste categories. The data related to the calculation of individual wastes are presented in Table 16. The TGA results show proximity with proximate analysis values. The moisture content is comparatively lower in TGA value than in proximate analysis, due to the preheating of a sample at 105℃ for 24 hr was the key factor before TGA analysis. Each sample was replicated three times and a total of 15 samples were analyzed. After the experiment, the results were calculated from Analyzing the plots that are presented in
Figure *38*, Figure 39, Figure 40, and Figure 41. From the obtained data mean values are calculated. The value of the total mix ensures that the mixture was prepared correctly. In TGA higher ash content was achieved for CF-2, FAB-1, and FAB-2 than proximate values in Table 11. The volatile matter deviates by 6.23% for CF-1 and shows good similarity for CF-2 and FAB-2. For FAB-1 the fixed carbon deviates by 5.95% and shows good similarity for the rest. The variation in proximate and TGA results can occur due to the lower amounts of samples in TGA analysis.

Table 12: TGA results for MC, VM, Ash, and FC of ISW.

Parameter (wt%) / Sample	Moisture Content (MC)	Volatile Matter (VM)	Fixed carbon	Ash
CF1	3.12	77.44	17.12	2.32
CF2	0.95	84.47	6.53	8.06
FAB1	1.38	81.65	8.18	8.8
FAB2	1.26	81.02	10.59	6.94
Total mixture	2.28	82.29	9.89	5.54

Figure 19 presents the TGA profile of steps like drying, pyrolysis or devolatilization, and combustion. These results are obtained by an average of 3 representatives of the 5 samples as discussed earlier.

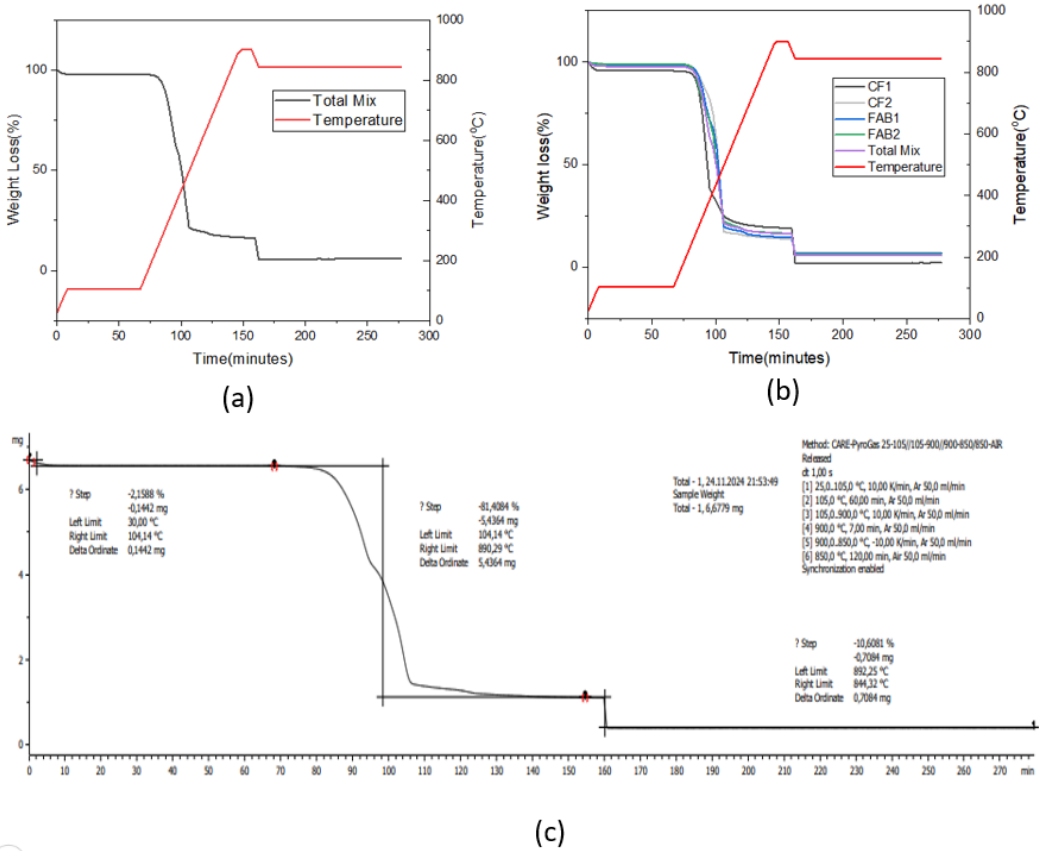

Figure 19:Weight loss of sample as a function of time(a)Weight loss of total mixed (b)Weight loss of individual waste and Total mixed(c) Weight loss of Total mixed sample obtained from TGA software.

Figure 19(a) presents the weight loss of the total mixture of samples prepared by mixing the equal weight fraction of individual waste(CF-1, CF-2, FAB-1, and FAB-2). Figure 19(a) and (c) represent the same Total mixed waste. Figure 19(a), from the temperature profile(TGA program curve) the temperature reaches 105°C from room temperature in 8 minutes and is kept at this temperature for 60 minutes. The first weight loss occurred after 8 minutes which is moisture and inert gas argon flow rate is kept at 50ml/min. The weight loss remains constant up to 60 minutes after the first weight loss is recorded. In this phase weight loss corresponds to moisture which is 2.28%. After that, the temperature increased from 105°C to 900°C. In this stage, devolatilization occurs and from Figure 19(c), we can see the highest weight loss in the devolatilization phase occurred in two steps, the first around 75.6th minute and the second one around 95th minute. This is due to the heterogeneous nature of the waste, consisting of cellulosic and polymer components. In the next stage, the temperature was kept constant at 900°C for 7 minutes with an argon flow rate of 50ml/min to give room for the rest volatile matter to drive out. In this temperature ramp, the weight loss is referred to as volatile matter and the weight loss remains constant after a weight loss of 82.29%. The remaining weight of the sample contains ash and fixed carbon. After that, the temperature drops down to 850°C and at this temperature, the isothermal combustion is done in an air atmosphere with an airflow rate of 50ml/min for 120 minutes. The oxidation of the sample was fast and it started around the 154th minute the weight loss was visible up to the 160th minute and then it remained constant. The weight loss accounts for 9.89% which represents fixed carbon and the remaining is the ash.

4.2.3 Elemental compositions

The ultimate analysis data were obtained from TGA values using the correlations developed to obtain elemental composition values from MC, VM, FC, and Ash. The results of ISW vary by a moderate margin in comparison with MSW. This can occur due to the use of correlations that are not for accurate results like experimental analysis of the CHN-analyzer. Another reason can be the variation of constituents between the wastes. ISW has higher oxygen content and lower carbon content than MSW which is due to the proportion of paper, car fluff, and textiles being higher. The nitrogen and sulfur content are higher in ISW due to the presence of ASR like tires, leather, and foam.

Table 13: Elemental compositions of ISW.

	C	H	O	N	S
CF-1	46.2732	5.67968	42.0868	2.4616	0.54592
CF-2	42.23705	5.53407	41.65125	2.16178	0.49724
FAB-1	41.9173	5.46962	40.87265	2.17382	0.49947
FAB-2	43.33455	5.55541	41.43936	2.26228	0.51429
Total mix	43.60725	5.57631	41.82919	2.25662	0.51154
MSW [9]	51.86	6.3	28.7	0.8	0.2
ASR [52]	51.43	6.4	40.62	1.21	0.34

The H, O, N, and S values of ISW were close to the values presented in ASR as 50% of the Total mix ISW was prepared from Car fluff. However, the presence of FAB-1 and FAB-1 decreased the carbon proportion in ISW.

4.2.4 HHV and LHV results

The HHV and LHV value of ISW was calculated using the following correlations eqn.(14), and (15) discussed in section 2.5 Calorific Value Analysis. The calculated values are presented as –

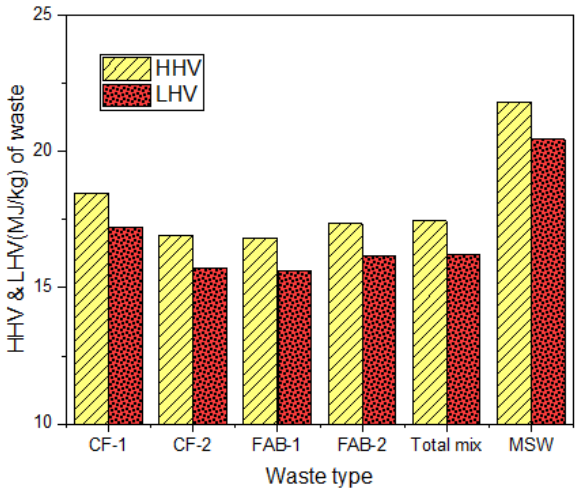

Figure 20: HHV & LHV values of ISW and MSW.

The highest HHV& LHV was obtained for CF-1 among the ISW. Its HHV value is 18.45MJ/kg and LHV is 17.22MJ/kg. CF-1 contains more C and H than the other 3 types of ISW and also from the mixture as

presented in Table 11. HHV & LHV of ISW were comparatively lower than MSW due to lower C and H content, and higher O composition. The C and H content contributes to HHV significantly due to its high energy density during combustion. The effect of H on LHV tends to decrease more than HHV as more energy is required to recover from latent heat and can be explained from the eqn. (15). The difference between HHV and LHV is lower in ISW than in MSW and the values are 1.21 and 1.37 due to higher H content in MSW. The increase in oxygen content lowers the HHV of fuel due to the partial oxidation of fuel internally which decreases the amount of external oxygen needed. The obtained HHVs are 18.46, 16.92, 16.82, 17.35, and 17.43 MJ/kg for CF-1, CF-2, FAB-1, FAB-2, and Total mix. The obtained LHVs are 17.22, 15.72, 15.62, 16.14, and 16.22 MJ/kg for CF-1, CF-2, FAB-1, FAB-2, and Total mix.

4.3 Model Training & Development

In this section, the sensitivity analysis, H2 efficiency, and energy analysis results of the following models Sorption Enhanced Steam Gasification (Steam+CaO), Sorption Enhanced CLG1(OC+CaO), Sorption Enhanced CLG2(OC+CaO), and Pyro-CLG(OC+CaO) are discussed to observe which models and OC should be further analyzed.

4.3.1 Sensitivity Analysis for SE- SG & SE-CLG1

In this section, The sensitivity analysis of two models is presented for the H2, CO, CO2, and H2O outlet flow rate of WGSR.

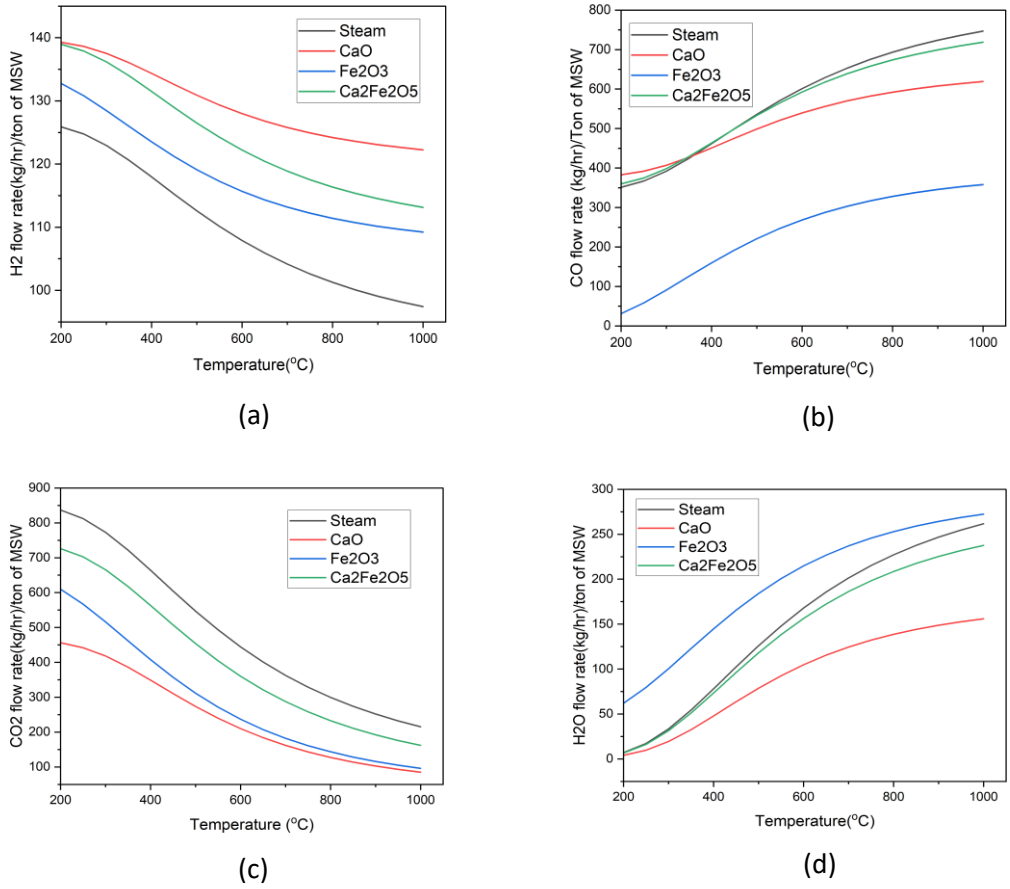

Figure 21: Steam gasification(steam) & CLG1(OC) WGSR outlet flow rate (a)H2 (b)CO (c)CO2(d)H2O

The WGSR was chosen for comparison as this reactor is common for the three models. The reactor parameters are kept common for both the models and in the case of SE-CLG1 OC carrier flow rate for all OCs was 150kg/hr. Three types of OCs were used for SE-CLG1 but the main target was to see the performance of Fe2O3 and CaFe2O5 with steam. In Figure 21 for all cases of SE-CLG1, the hydrogen production rate was higher than steam gasification and with the increase in WGSR reactor temperatures, the production of hydrogen decreased. The favorable temperature for H2 production in WGSR is around 300℃. The production of H2 decreased with the increase of temperature because the exothermic nature of the WGS reaction was discussed in Table 3. The flow rate of CO is highest at

the outlet of Steam gasification. The minimum CO flow rate was observed for Fe2O3 and it can be explained as the easier reduction of Fe2O3 with CO and H2 due to its change of Gibbs free energy is less than in comparison with Ca2Fe2O5 as stated in [126]. From the observation of CO flow rate of Ca2Fe2O5 and CaO, it can be stated that the shift reaction occurred less in the case of Ca2Fe2O5 with an increase of temperature, as at 200℃ both have almost identical flow rates of H2 and from Figure 21(b) CO flow rate was higher in the case of CaO. This higher production of H2 and lower production of CO2 can be explained by CaO as with an increase in reducer temperature the CaO acts as a sorbent for CO2 capture not particularly as a conventional OC [96]. The CO2 production for steam gasification was much higher than SE-CLG. In the case of SE-CLG using Fe2O3 produced the highest amount of CO2 and CaO and Ca2FeO5 almost showed a similar trend for CO2 production after 400℃. With the increase in reactor temperature, CO2 production was reduced due to the low reaction rate of the WGS reaction. For SE-SG the result shows a similar trend with Rudra et al. [9] that with the increase of WGSR temperature, the H2 generation decreases. The reported highest H2 production was at 200℃. The phenomenon is explained as the increase of backward endothermic shift reaction at high temperatures. The highest H2 flow rate in kg/hr for Ca2Fe2O5, CaO, Fe2O3, and steam is 138.96, 139.27, 132.77, and 125.89 at 200℃ of WGSR temperature. And the CO2 flow rate at the same temperature was 726.05, 456.3, 609.93, and 838.08 kg/hr. The generation of H2 from steam gasification showed similarities with Wang et al. [107] as reported 130kg of H2 production from 1ton of MSW.

4.3.2 Sorption Enhanced CLG2 Sensitivity Analysis

The sensitivity analysis of FR is presented below using different OCs. The MSW is gasified by supplying both steam and OCs at a constant flow rate of 200kg/hr and 150kg/hr.

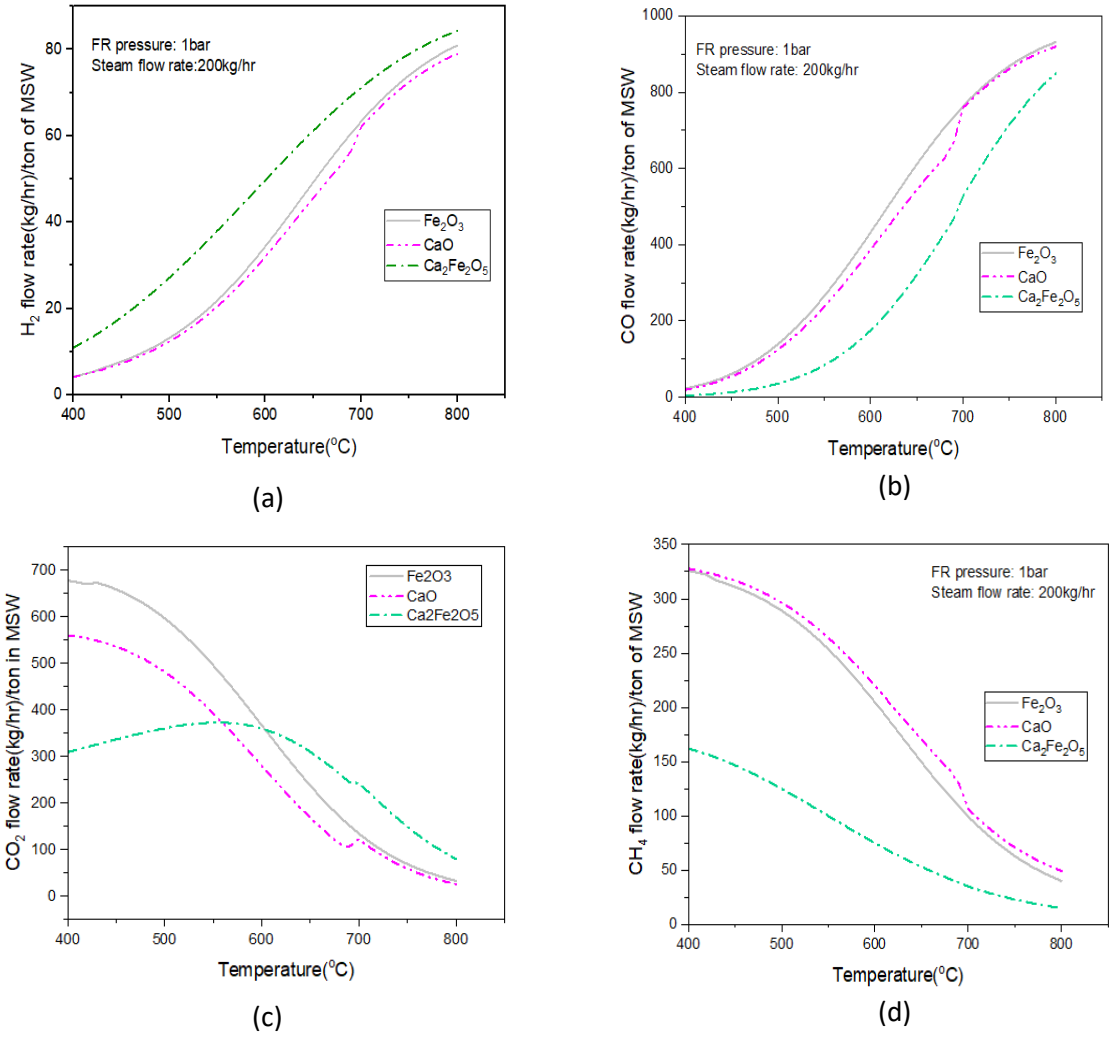

Figure 22: Sorption Enhanced CLG2 FR reactor temperature variation vs outlet gas flow rate using 3 types of OCs (a)H2 (b)CO (c)CO2(d)CH4 flow rate(kg/hr). Feed: MSW

From Figure 22, the highest hydrogen production was achieved at the outlet of FR when Ca2Fe2O5 was used as OCs. The highest hydrogen yield for Ca2Fe2O5, Fe2O3, and CaO at the outlet of FR were 78.982, 84.28, and 80.912 kg/hr. The results show similarity in the case of comparing OCs' performance to produce hydrogen in the case of biomass CLG stated by Hu et al. [96]. The H2 yield was stated in mmol/g of biomass and from CaO, Ca2Fe2O5, and Fe2O3 was 19.94, 23.07, and 20.84. By converting them into Kg/1000kg of biomass to have a better comparison the values are 40.19, 46.53, and 42.01. In the present model, Ca2Fe2O5 produces approximately 4kg and 6 kg more H2 than Fe2O3 and CaO which is similar to the experimental investigation stated by Hu et al. [96]. Higher CO2 production was observed for Fe2O3 and CaO below 600℃ and a higher CO2 flow rate was observed for Ca2Fe2O5

above 600°C. The CO2 generation comparison was stated for CaO>Fe2O3>Ca2Fe2O5 by Hu et al. in vol(%). From this study, the CO2 generation after 600°C in Figure 22(c) shows a similar trend to Hu et al. There is a step increase in the produced gas flow rate in the case of CaO at the temperature range of 690-700°C. This is because, during the temperature range the calcination reaction occurs which causes the release of CO2 and increase in H2 production, and the reaction shifts more towards the product generation. As this situation is discussed in Hu et al. the calcination reaction which is CaCO3 conversion into Cao occurred at 550-670°C and no trace of CaCO3 was found from the XRD results at gasification at 800°C using CaO as OC.

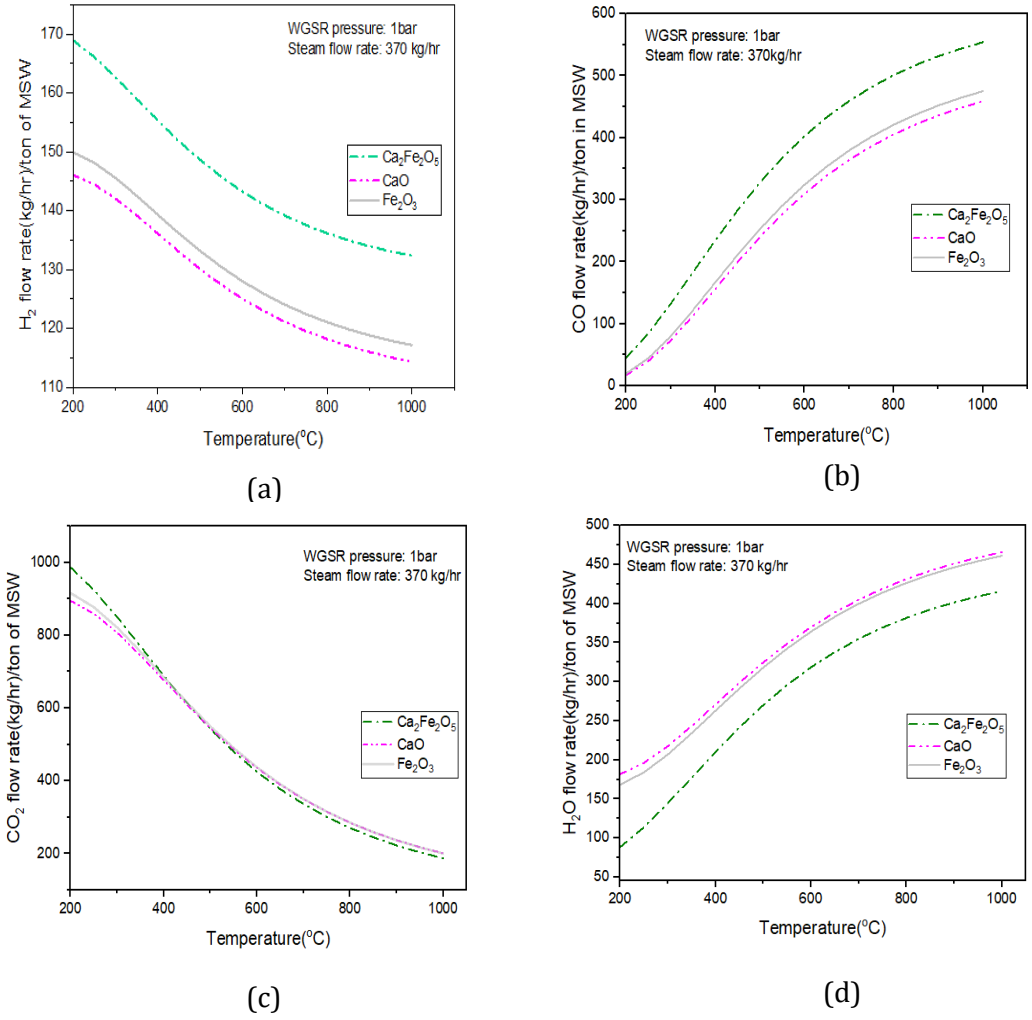

Figure 23: Sorption Enhanced CLG2 WGSR reactor temperature variation vs outlet gas flow rate using 3 types of OCs (a)H2 (b)CO (c)CO2(d)CH4 flow rate kg/hr. Feed: MSW

In Figure 23 the sensitivity analysis for the SE-CLG2 model WGSR is presented. The hydrogen production was higher at lower temperatures but gradually decreased due to the increase in temperature. At higher temperatures, the WGS reaction shifts in the left direction which can be understood from the increase of CO with the increase in temperatures. The production of H2 was highest at 200°C for Ca2Fe2O5 and up to 168.98 kg/hr of hydrogen production can be achieved which is much higher than the other two OCs. The production of CO2 from CA2Fe2O5 was higher than the other two OCs as stated in Figure 23(c) and the CO2 produced at 200°C was nearly 1000kg/hr.

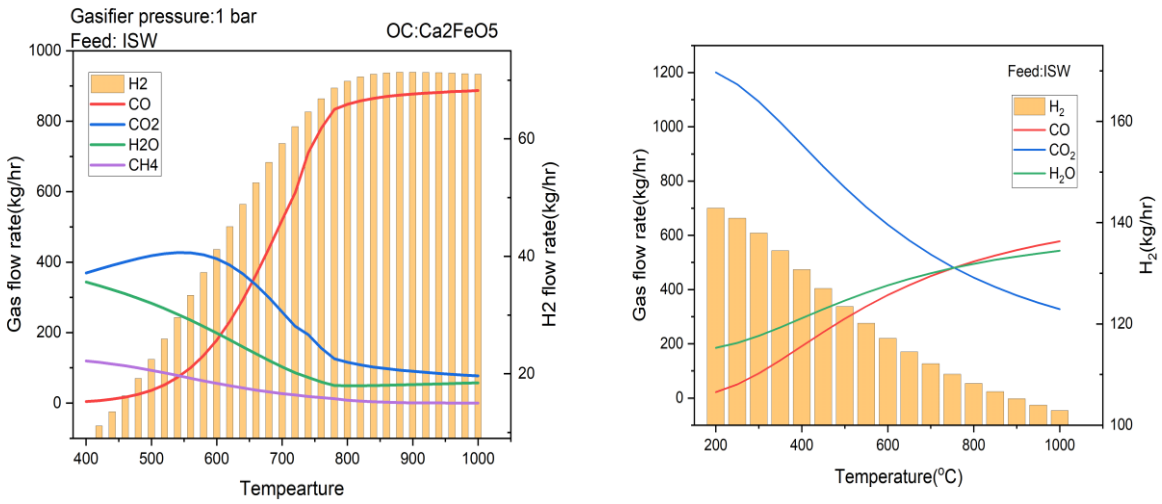

(a) (b)

Figure 24: Sorption Enhanced CLG2 Gasifier & WGSR reactor temperature variation vs outlet gas flow rate(a)Gasifier (b)WGSR Feed: ISW.

In Figure 24 ISW is used as feed for SE-CLG2 using Ca2Fe2O5 as OC. The flow rate of OC is 150kg/hr and as other conditions are kept the same as MSW before. In Figure 24(a) with the increase of gasifier reactor temperature, the hydrogen production gradually increases from 9.015 kg/hr at 400℃ to the highest value of 71.354 kg/hr at 900℃. There is a slight decrease in H2 after 900℃. In Figure 24(b), the highest 143.44 kg/hr hydrogen production was achieved at 200 ℃ of water-gas-shift-reactor temperature. In comparison, with the previous value attained from MSW, it is evident that the H2 production rate from ISW is lower than MSW by 14.458 kg/hr at 800℃ the outlet of FR and Gasifier. This can be explained by the composition of waste that MSW has higher C and H2 composition than ISW. In Figure 24(a) the CO2 flow rate experiences a gradual increase from the temperature 400 to 540℃ and at 540℃ the value of the CO2 flow rate obtains the highest value 427.37 kg/hr. Then with an increase in gasifier temperature, it gradually decreases and at 800 ℃ the value is 115.89kg/hr. The rapid generation of CO can be detected between temperatures 600-780℃. The reason is at this temperature range the reforming of char(17), and Boudouard reactions (19) take place which are highly endothermic. In the case of WGSR, it shows a similar trend with MSW, but CO2 generation is higher for ISW than MSW, and at 200℃ more than 200kg/hr more CO2 is generated.

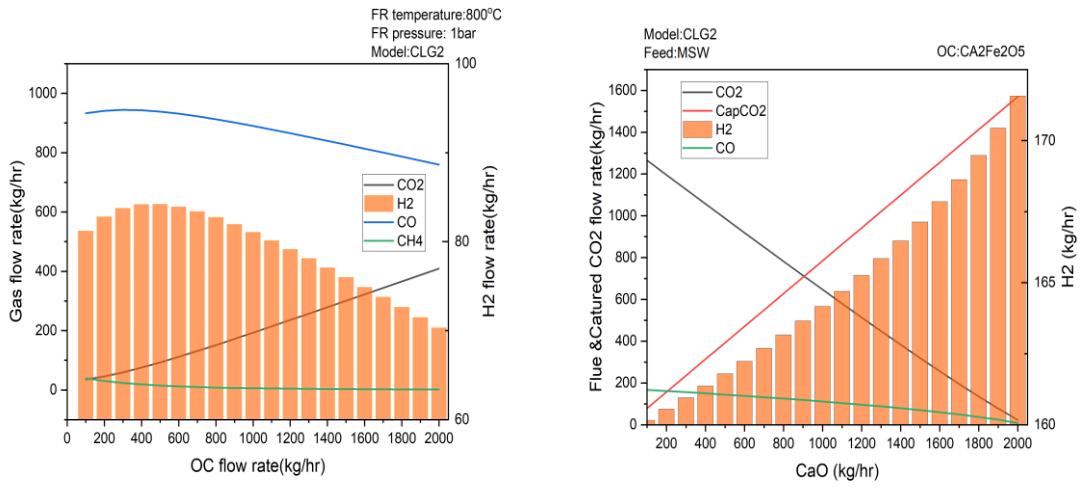

Figure 25: Sorption Enhanced CLG2 (a)FR outlet flow variation w.r. to OC flow rate (b)CaO variation at WGSR.

In Figure 25(a), the Ca2Fe2O5 flow rate is varied from 100 to 2000kg/hr to investigate the outlet gas flow rate of FR. The H2 flow rate gradually increased up to 500kg/hr of OC then gradually decreased after adding OC. The selectivity of H2 reduces from 84.202kg/hr to 70.338kg/hr. The generation of CO shows a similar trend with H2, as it reaches its highest value of 944kg/hr at 300kg/hr flow rate of OC and decreases selectivity of 19.25% at 2000kg/hr of OC flow rate. The CO2 gain the increase of flow rate up to 88.78% with an increase of OC. There is also a reduction in CH4 flow rate and 95.17% of CH4 generation per hour is reduced. Qi et al.[127] for MSW chemical looping gasification varied the flow rate of CuFe2O4 as OC to see the effect on gas composition which supports this study. In Figure 25(b) CaO flow rate is varied to find out the amount of CaO required to completely capture CO2. With CaO mass flow rate of 2000kg/hr complete capture of CO2 can be achieved theoretically. This carbonation reaction helps to shift the WGSR rightward increasing the production of H2.

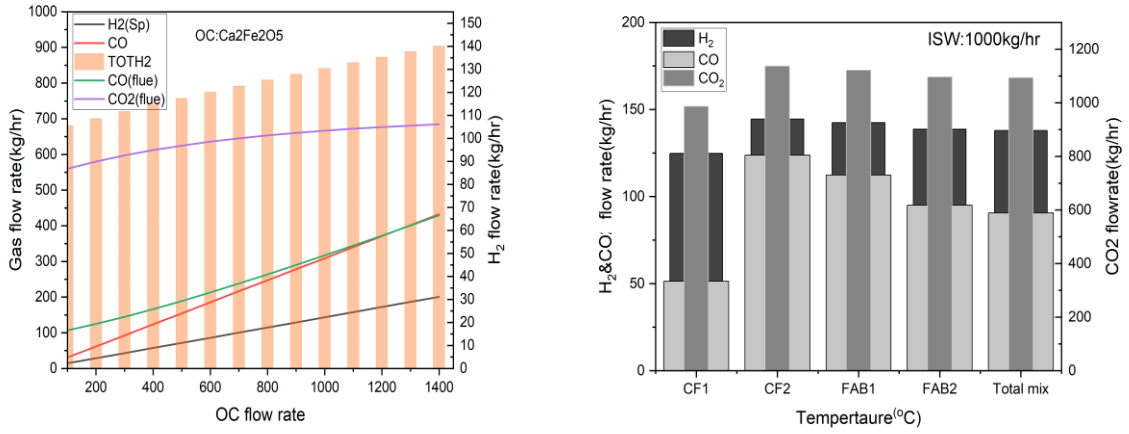

Figure 26: Sorption Enhanced CLG2 (a)OC variation vs Gas flow rate (b) Different ISW as feed vs Gas flow rate.

In Figure 26(a), the variation of the product gas flow rate is shown by changing the input flow rate of OC. The H2(Sp) means the hydrogen generation due to the re-oxidation of OC using steam, discussed in equation (30). The increase in OC flow rate positively impacts the outlet flow rate. Figure 26(b) shows the variation of outlet gas flow rate by changing the type of feed of ISW. The highest H2 production was achieved from CF2 and the lowest was achieved from CF1. It is evident from the elemental composition that CF2 has the highest amount of C and H whereas CF1 has the least. The total mix was simulated by combining 250kg/hr from each waste.

4.3.3 Pyro-CLG model sensitivity analysis

In Figure 27(a) the variation of pyrolysis reactor temperature is shown w.r to the outlet flow rate of H2, CO, CO2, Char, and C. Here C denotes the char flow rate at the outlet of the pyrolysis reactor and Char is the total flow rate of char.

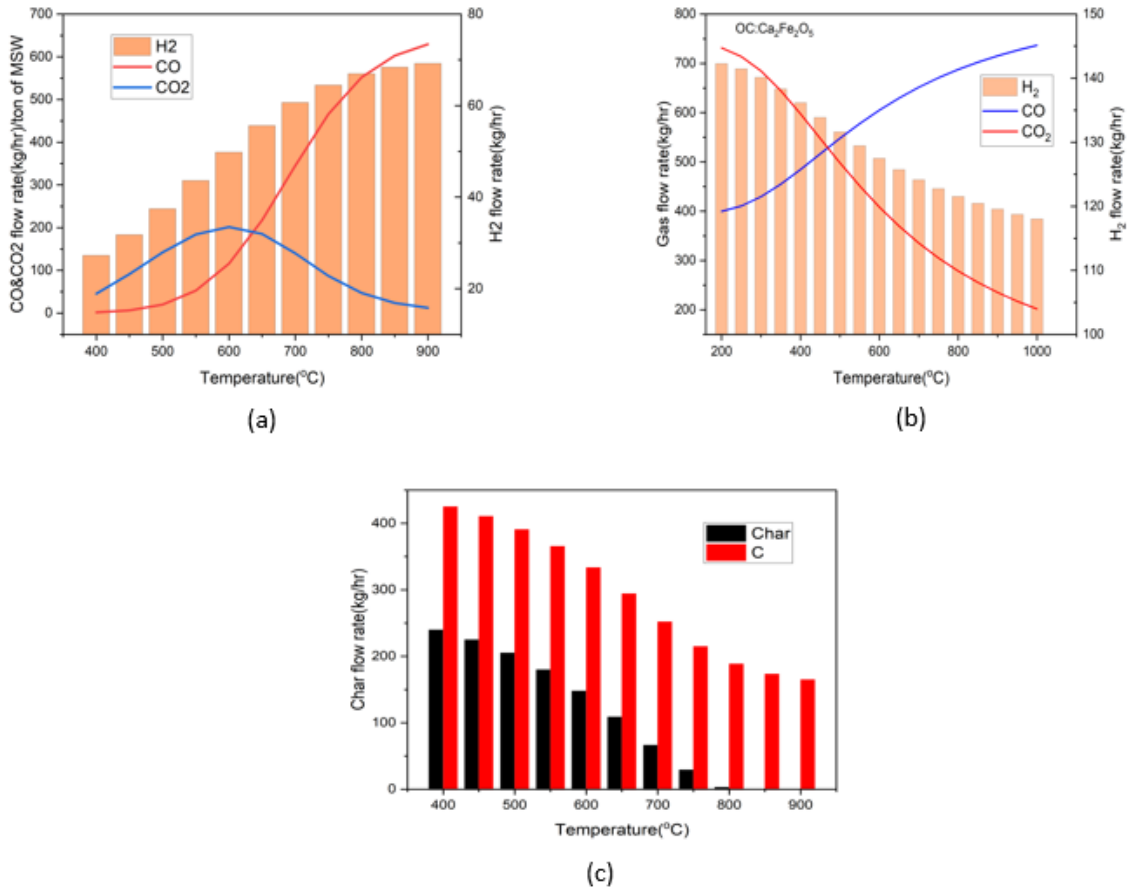

Figure 27:Pyro-CLG sensitivity analysis(a) Gas flow rate variation w.r. to Pyrolysis reactor temperature (b)WGSR temperature variation(c) Char flow rate variation w.r. to Pyrolysis reactor temperature.

The type of waste used is MSW and OC is Ca2fe2O5. The flow rate of OC was kept 1400kg/hr in the FR for pyrolysis at 800°C. With the increase in pyrolysis reactor temperature, in Figure 27(a) the final H2 flow rate increased gradually to the highest flow rate of 69.2191kg/hr at 900°C, and from 400°C to 900°C the flow rate increased 60.62%. The CO2 flow rate gradually increased up to 600°C attaining a maximum value of 201.783 kg/hr and then gradually decreased 24.21% to 94.011% its highest value at 900°C. The flow rate of CO gradually increased from 400°C attaining the highest value of 629.448 kg/hr at 900°C. In Figure 27(c) the generation of char(C) at the outlet of the pyrolysis reactor gradually drops with the increase of pyrolysis reactor temperature by 61.19% from 400°C to 900°C. So, it is evident that with the increase in pyrolysis reactor temperature solid product decreases while gaseous product increases and this statement is supported by Haydary et al. [123]. It was stated that the higher temperature favors the gas yield and decreases the solid yield. From Figure 27(b) the highest H2 production obtained was 142.816 kg/ton of MSW. The increase of CO and decrease of CO2 were observed because the WGS reaction is favorable for the lower temperature. The lowest CO2 generation obtained was 727.53 kg/ton of MSW after the WGS reaction.

4.3.4 H2 Production & Energy Efficiency

For SE-CLG2, the highest hydrogen yield is obtained using steam+Ca2FeO5 as a gasifying agent which is 162.1704 kg/hr at 300℃, and 1 bar for the WGSR reactor. The H2 efficiency was calculated using the following equation discussed in section (2.11)-

$$\eta_{H_2}(\%) = \frac{\dot{m}_{H_2} \times LHV_{H_2}}{\dot{M}_{MSW} \times LHV_{MSW}} \times 100$$

The lower heating values for H2 and MSW are 120MJ/kg [107] and 21.13MJ/kg [9].

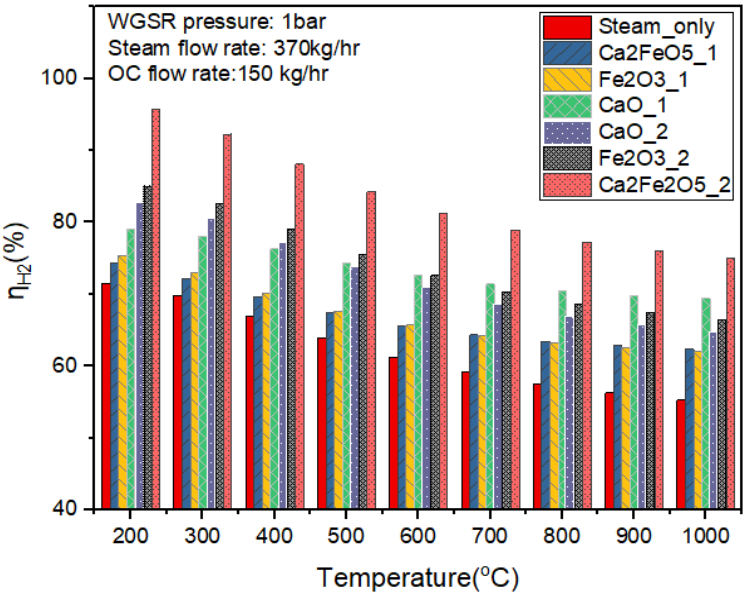

Figure 28: Hydrogen production efficiency w.r. to WSGR temperature for diff OCs (Steam, CLG1, CLG2)

In Figure 28 the hydrogen production efficiency of three different models are represented.
The first model includes only steam (SE-SG) and the other two models include 3 types of OCs with the combined use of steam and OCs. The WGSR was chosen for the sensitivity analysis as it was common for the three reactors. With the increase in temperature, the hydrogen production efficiency decreased for all three reactors, and the lowest H2 efficiency was found for Steam gasification (SE-SG). The highest value obtained for SE-SG was 71.50 and the lowest was 55.33%. The highest efficiency was obtained for SE-CLG2 usingCa2Fe2O5 as OC and steam was 95.97% at 200℃. As the operating condition for WGSR was considered 300℃, so highest efficiency was 92.41% among the models and OCs were for SE-CLG2 using Ca2FeO5.

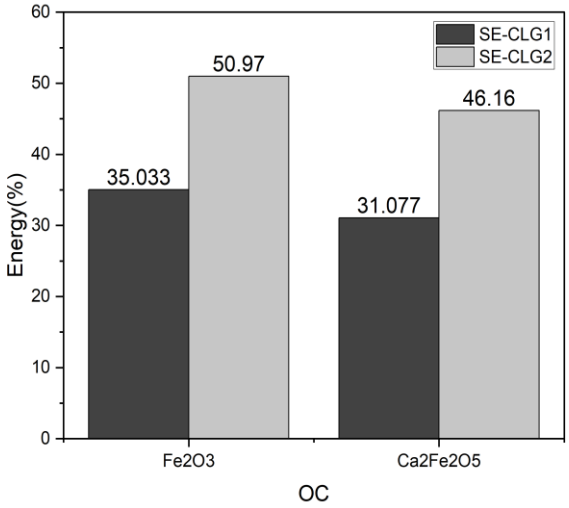

Figure 29: Energy efficiency comparison between SE-CLG1 & SE-CLG2.

Figure 29 presents the energy efficiency of the models SE-CLG1 and SE-CLG2 for two types of OCs Fe2O3 and Ca2Fe2O5. These two models and OCs were chosen for the energy analysis based on their H2 production efficiency. From Figure 4.10 it is evident that for both the models using Fe2O3 as OC the energy efficiency is higher than Ca2Fe2O5. The reason, as earlier discussed in section 2.8.3 is that the oxygen-carrying capacity of Fe2O3 and Ca2fe2O5 is 0.3 and 0.176 respectively. Due to the higher oxygen-carrying capacity of Fe2O3 compared to Ca2fe2O5, Fe2O3 can supply more oxygen for the gasification process, which potentially increases the extent of the reactions and energy release. The model SE-CLG2 has higher efficiency for both types of OC. For, SE-CL2 as presented in Table B.11 and B.12, the FR and GASIFIER reactor heat duty for Fe2O3 and Ca2Fe2O5 are 284.51kW and 348.63kW respectively. And for AR (Air Reactor) heat duty for Fe2O3 and Ca2Fe2O5 are 413.16kW and 507.45kW. So, for Ca2Fe2O5 it requires more power to operate the reaction in those reactors compared to Fe2O3. The energy efficiency estimated is relatable with the findings by Qi et al. [92] reported an overall energy efficiency of 47.76% using NiFe2O4 at 300kg/h for CLG with SMR. Qi represented a comparison between experimental and simulated values where H2 and CO values were relatively higher for simulation than experimental and CO2 and CH4 were lower in simulation than experimental. The major energy loss (200.76kW) reported by Qi et al. is at the FR, due to incomplete combustion and heat loss.

Prioritizing the H2 production efficiency Ca2Fe2O5 and SE-CLG2 are chosen for (3-E) analysis and the Pyro-CLG model is chosen according to properties of waste and the interaction of OC with Ash which damages the recyclability as discussed earlier in section (2.8.3 Oxygen carrier)

4.4 Energy, Exergy, and Environmental (3-E) Analysis

In this section, the energy, exergy efficiency, and environmental analysis of two selected models (SE-CLG2 and Pyro-CLG) using two types of feedstock(MSW and ISW) and using Ca2Fe2O5 as OC is discussed below-

The operating conditions are different for SE-CLG2 and Pyro-CLG2 as both models are different in operations as do the waste properties. For, the Pyro-CLG model using ISW and MSW, the flow rate of CaO was 1000 and 1200 kg/hr respectively. The flow rate of Ca2Fe2O5 was 800kg/hr and 1400kg/hr respectively. This variation is due to the mass balance in the reactor which is discussed in section 2.9. The steam flow rate for AR and WGSR was 500kg/hr and 370kg/hr respectively and kept the same for both wastes in Pyro-CLG. For SE-CLG2 the steam and Ca2Fe2O5 flow rate in the gasification reactor and WGSR was constant for both MSW and ISW and values are 200kg/hr, 370kg/hr, and 150kg/hr. But CaO flow rate varied for MSW and ISW due to reactor mass balance conditions the CaO flow rate for MSW was 2000kg/hr and for ISW it was 1800kg/hr. In Figure 30(a) the energy efficiency of the two models with two different wastes is presented. The energy efficiency using ISW in both models was higher than MSW.

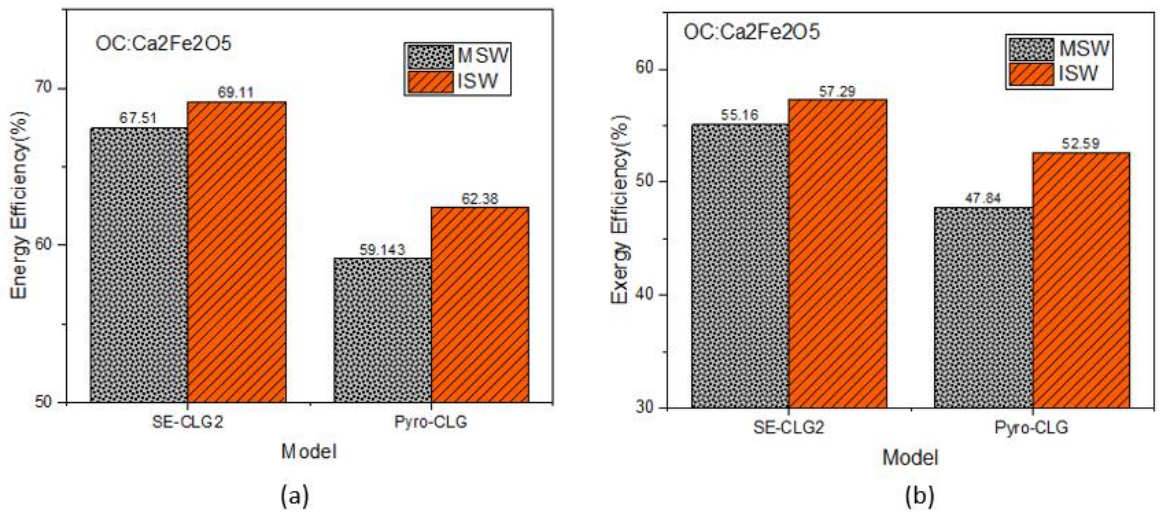

Figure 30: SE-CLG2 & Pyro-CLG using MSW & ISW as feed efficiency analysis(a)Energy(b)Exergy.

The properties of ISW vary one from another. The moisture content discussed in section (4.2.3 Elemental compositions) in MSW is higher than ISW. So, this higher moisture content increases the specific heat load which requires more energy in the gasifier. The presence of oxygen-rich compounds is higher in ISW than in MSW which is obtained from the elemental composition. The presence of a higher portion of oxygen promotes auto-thermal gasification. For MSW gasification the heat demand was greater than the heat generation in SE-CLG2, so resulted in positive heat duty which is presented in Table 17, and for ISW the heat generated due to gasification was greater than heat demand which resulted in negative duty presented in Table 21. The highest energy efficiency 69.11% obtained for SE-CLG2 using ISW for combined heating, power, hydrogen production, and CO2 storage. The energy efficiency in Pyro-CLG is less than 6.73% from SE-CLG2 using ISW. This is because in Pyro-CLG the char generated from pyrolysis reactor goes for char gasification in FR and the reaction with char and OC is

highly endothermic in nature. The required duty for FR in Pyro-CLG is around 1052.63kW, which is a major factor behind the less efficiency of this model than SE-CLG2. The energy efficiency found in SE-CLG2 are comparable with Zare et al. [128] where thermal efficiency was estimated for chemical looping combustion and plastic gasification and the reported value was 77.08%. The variation of efficiency can be for the types of feedstock used was only polyethylene which has higher carbon and hydrogen composition. From the Pyro-CLG model, the highest efficiency obtained using ISW was 62.38% and 59.143% using MSW. Kun et al. [47] presented coal pyrolysis with CLG estimated the overall efficiency of 43.12% and mentioned the drying unit caused the highest energy destruction. The variation of energy with Kun et al. was due to the formation of tar was considered and only electricity generation was mentioned. The drying unit is neglected in the Pyro-CLG model due to less moisture content presence and 13342.83 kW hot water generated which increased the energy efficiency for this model. The exergy efficiency analysis data is presented in Figure 30 and the highest exergy was obtained at 57.29% for model SE-CLG2 using ISW as feed. The electricity generated using the steam turbine, and the heat produced are also included. The exergy efficiency for ISW was higher than MSW for both models. In the Pyro-CLG model, the exergy difference between the two wastes was higher than SE-CLG due to the char gasification process. The higher moisture content in MSW reduces the exergy efficiency due to the need for higher energy and higher oxygen content in ISW leads to auto-thermal gasification. The use of more OC in Pyro-CLG than SE-CLG increases the input exergy. The difference in energy and exergy is relatable to the value obtained by Zare et al. [128] and the reported exergy was 67.62%. For the SE-CLG2 using MSW the exergy value is supported by Sun et al. [93] used the MSW integrated gasification combined cycle and found the MSW to hydrogen production with an exergy efficiency of 46.7%. So, from the energy and exergy analysis, the SE-CLG2 model has better energy and exergy efficiency due to higher H2 and heat production than Pyro-CLG2 and ISW is more dominant in terms of energy and exergy analysis than MSW.

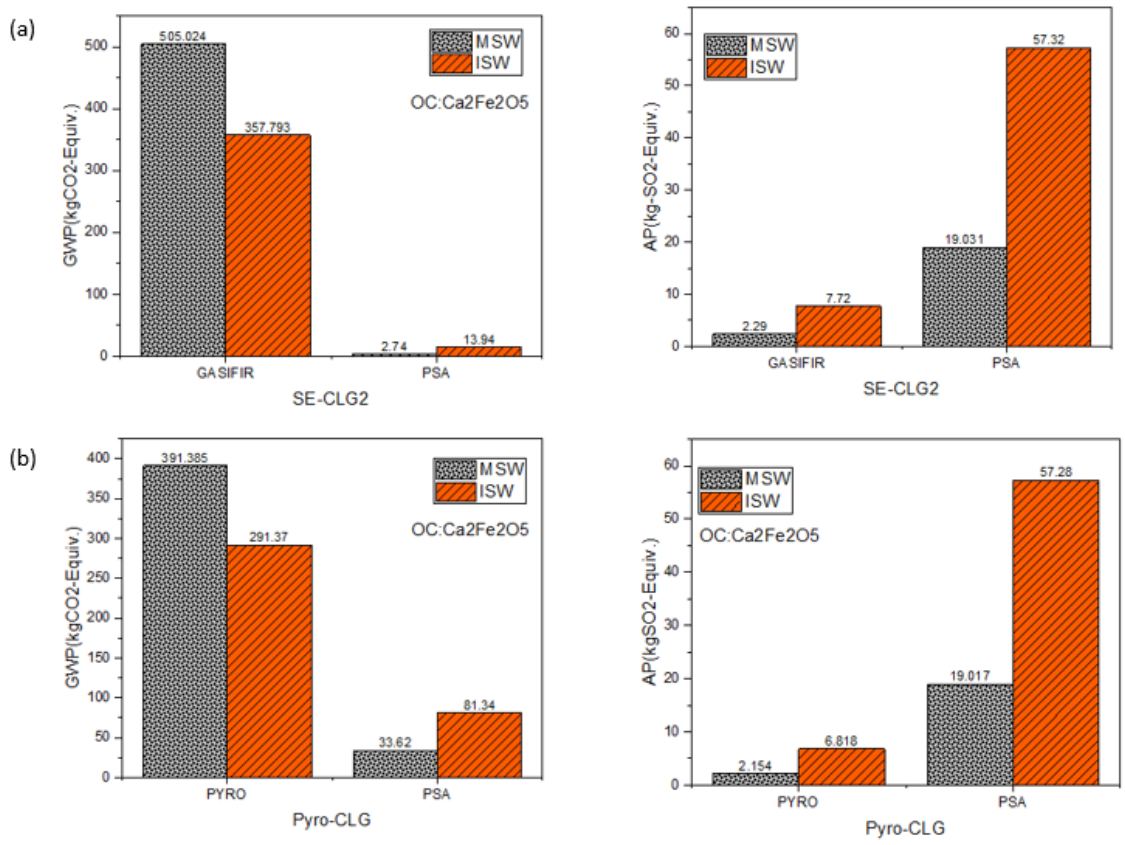

Figure 31:Environmental analysis results (a)SE-CLG2(b)Pyro-CLG.

The environmental analysis for the two models with two types of waste was done as discussed earlier in section 2.13. The analysis includes GWP and AP where, the flow rate of CO2, and CH4 are considered for GWP, and SO2, and NO2 are considered for AP. The flow rates of the components were taken from stream values and GASIFIR, PYRO, and PSA block outlet flow rates were evaluated. In terms of environmental analysis, both models seem close. Regarding waste type, the GWP is higher for MSW than ISW by 25.55% in GASIFIR block which is a gasifier for SE-CLG2. After PSA, the GWP was higher for ISW than MSW by 80.34%. This is due to the amount of CaO used for MSW and ISW being 2000kg/hr and 1800kg/hr respectively due to reactor mass balance and thermodynamic equilibrium. The carbon capture in WGSR was better in action for MSW than ISW, so after the PSA unit the CO2 content was higher for ISW. In the case of AP, MSW has less SO2 and emission in comparison with ISW. The reason for this can be explained from elemental analysis, that MSW contains less S and N content than ISW. After PSA, the AP of MSW was 66.80% less than ISW. So, for SE-CLG2 model using MSW has a lower environmental impact. For the Pyro-CLG model, the pyrolysis reactor has less emission in comparison with SE-CLG2 gasifier for both MSW and ISW dropping in GWP of 22.50% and

18.56%. After PSA, due to a drop of carbon capture in WGSR after PSA, the GWP increased by 91.85% and 82.86% for MSW and ISW in Pyro-CLG2 compared with SE-CLG2. AP value for ISW was 68.41% higher than MSW in the pyrolysis reactor. And it became 66.80% higher after the PSA unit which was the same value for WGSR. So, the SE-CLG2 model performs better than the Pyro-CLG model for GWP using both types of waste. For AP, Pyro-CLG is slightly better than SE-CLG2. The value of AP of SE-CLG2 shows similarity for MSW with Sun et al. [129] reported AP for MSW to hydrogen was 23.9. The GWP for SE-CLG2 is lower than GWP value reported by Qi et al. [130] for CLG. The value reported was 804.75 GWP and from this study of gasifier, it was 505.024. The OC used by Qi et al. was CuFe2O4 which can promote the chemical looping combustion of fuel more than CLG, as Cu and Fe-based OC are at the region of complete oxidation in the Ellingham diagram [99].

4.5 Total product

Table 14 represents the total product obtained from SE-CLG2 and Pyro-CLG using MSW & ISW. The highest H2, heat, and power production was obtained for model SE-CLG2 using MSW. The amount of OC used in the gasifier was 150kg/hr and CaO in WGSR was 2000kg/hr. For the same model, the product decreases using ISW for the same amount of OC and 1500kg/hr of CaO due to reactor mass balance and thermodynamic equilibrium. Similarly, for the Pyro-CLG model, the product declines when ISW is used as feed except for the hot water. The hot water generated using ISW was 14% higher than MSW. The difference in H2 production of SE-CLG2 and Pyro-CLG using ISW is 20.17%. But the problem is in SE-CLG2 the regeneration of OC is limited by the formation of ash which is separated in Pyro-CLG and the char is pretreated to remove heavy metals before the chemical looping char combustion which shows a good regeneration process after several cycles as discussed in section (2.8.3 Oxygen carrier). The use of OC in Pyro-CLG is much higher, 1400kg/hr is used for MSW, and 800 kg/hr is used for ISW as it requires more OC for char combustion eqn.(30).

Table 14: Total product obtained.

Model & Waste type	Total Hydrogen (kg/Ton of waste)	Power (kW/Ton of waste)	Heat (100°C hot water) (kg/Ton of waste)	CO2 stored (KG/Ton of waste)	CO stored (KG/Ton of waste)
SE-CLG2 (MSW)	170.6	23.73	4300	1569.6	-
SE-CLG2 (ISW)	142.8	23.73	4000	1412.65	-
Pyro-CLG (MSW)	131.3	11.87	2480	564.178	740.752
Pyro-CLG (ISW)	114	11.87	2880	784.805	508.8

4.6 Cold Gas Efficiency Using ISW as Feed

The CGE is estimated for the Pyro-CLG model for ISW using eqn. (49) for before and after the water-gas-shift reaction in WGSR. The CGE is determined at WGSR temperature 700℃ and 1 bar pressure. The mass flow rates of H2, CO, CH4, and ISW were taken from stream values from stream results using the simulation. The LHV of ISW was obtained from section (4.2.4 HHV and LHV results). H2 flow before WGSR was 0.014kg/s and after WGSR it was 0.021kg/s. The flow rates of CO and CH4 before WGSR were 0.26kg/s and 0.0023kg/s and after the WGSR were 0.085 and 0.0095kg/s. The flow rate of ISW was 0.28kg/s.

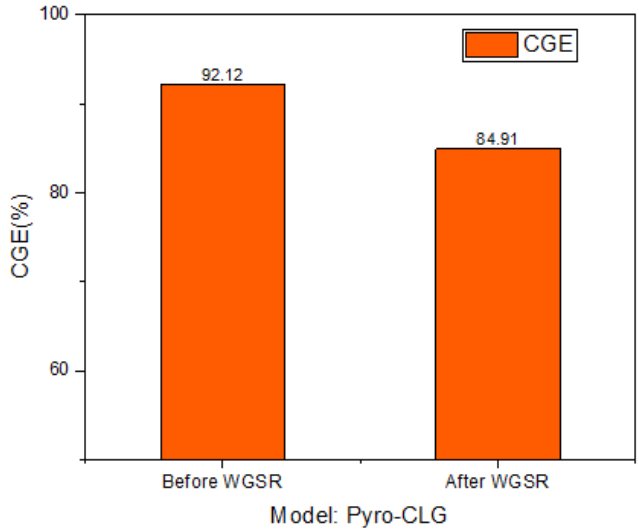

Figure 32: CGE variation before and after the water-gas-shift reaction.

The decrease in CO flow rate after the water gas shift reaction reduced the CGE though the flow rate of H2 and CH4 increased. The CGE decreased by 7.21% after the WGSR. The CGE value obtained in this study shows a similarity with the CGE obtained by Mehdi et al. [131]. Mehdi et al. reported for 800℃ of gasifier temperature, the CGE obtained for metropolitan waste was approximately 91% which is relatively close to CGE before WGSR. He also reported with the increase in temperature of the reactor the CGE decreases.

5 Conclusions

The models designed here are for the effective conversion of ISW and MSW into hydrogen, heat, and power ensuring the minimum emission that can be achieved. For this, the characterization of ISW was done and from that the HHV and LHV were obtained are 17.43 MJ/kg and 16.22 MJ/kg. Most thermochemical properties agreed with other published values and Norway MSW properties. The sensitivity analysis showed a similar trend with existing works. From sensitivity analysis, it was obtained that higher temperatures in the fuel reactor and lower temperatures in the water-gas-shift reactor increase hydrogen production. Ca2Fe2O5 as OC has higher H2 selectivity in comparison with other OCs agreed with previous studies. The H2 efficiency of the SE-CLG2 model using Ca2Fe2O5 flow rate of 150kg/hr can reach up to 92.41% at FR temperature 800^{o}C, and WGSR 300^{o}C. The energy efficiency was higher for ISW when used in both the models than MSW by 1.6% for SE-CLG2 and 3.24% for the Pyro-CLG model. The Pyro-CLG model has less energy efficiency than SE-CLG2 by 8.37% for MSW and 6.73% for ISW. In exergy analysis, the exergy analysis was higher for ISW by 2.13% for SE-CLG2 and 4.75% for Pyro-CLG than MSW. The Pyro-CLG model has less exergy efficiency than SE-CLG2 by 7.32% for MSW and 4.7% for ISW. The product analysis for the SE-CLG2 for the integrated model for MSW waste type was the highest. The highest hydrogen production of 170.6 kg per 1000kg of MSW, with 4300L of hot water was notable. The carbon dioxide captured per 1000kg MSW was around 1570kg. The kgCO2-equiv. emitted to the environment during the process was only 2.72kg per 1000kg of MSW. The ISW sample was dominating in terms of energy and exergy for both SE-CLG and Pyro-CLG. The highest product yield using ISW was in the SE-CLG2 model producing 143kg of hydrogen per 1000kg of ISW and 4000L of hot water for district heating. The carbon dioxide captured was 1413kg per 1000kg of ISW emitting only 13.94 kgCO2-equiv. to the environment. The Pyro-CLG model has the upper hand over the regeneration of OC. The additional carbon monoxide generated can be used to generate hydrogen in two-stage WGSR, which will increase the hydrogen production or this additional CO can be combusted to generate energy to operate the plant. The electricity generated using superheated water for both cases is not sufficient for larger applications. Some generated hydrogen or more steam needed to generate electricity for a larger scale use. SE-CLG2 produces 20.28% more hydrogen which is 29kg hydrogen per 1000kg ISW than Pyro-CLG. The generation of 100^{o}C hot water is 28% more for SE-CLG2 than Pyro-CLG. So, the SE-CLG2 model has higher energy, exergy efficiency, lower environmental impact, and more hydrogen and hot water production. However, the regeneration of OC is a major issue for SE-CLG2 as the formation of CaSiO3 occurs after 3 cycles due to ash formation.

The price of Ca2Fe2O5 varies depending upon purity, quantity, and supplier and is generally quoted at 1900-2350 USD per ton for industrial-grade [132]. So, after 3 cycles formation of CaSiO3 will destroy its regeneration capacity and 150kg OC should be changed after 3 cycles for SE-CLG2 which will cost 288 USD. 29kg H2 will cost around 145 USD. So, if the production of Ca2Fe2O5 is cheaper then SE-CLG2 is suggested. Otherwise, the Pyro-CLG model is recommended. The CGE estimation was done as per Geo4Dynamics recommendation and for the Pyro-CLG model using ISW. The CGE before the WGSR reactor was obtained at 92.12% and after WGSR it was 84.91%. So, if hydrogen is not intended as the major outcome, and syngas is produced for direct power generation, then it is recommended to not to use a water-gas-shift-reactor. With a 200kg/hr flow rate of 1M HCL, total heavy metal removal was achieved.

5.1 Recommendations

The ISW requires proper segregation as it can conclude copper wires, heavy metals, and metals. The pretreatment of ISW is needed as heavy metal or toxic emissions can be exposed to the environment. The heavy metal removal using the acid leaching technique should be experimentally done to get more realistic value, process efficiency, and process handling. Experimental work will provide a closer view of the adopted process to maintain the regeneration of OC. Life cycle analysis of the whole process is an essential tool for the project feasibility and deciding the project. So, performing this analysis will be more helpful for decision-makers for plant implementation.

References

[1] "10513: Waste account for Norway (1 000 tonnes), by treatment, material, contents and year. Statbank Norway." Accessed: Oct. 06, 2024. [Online]. Available: https://www.ssb.no/en/statbank/table/10513/tableViewLayout1/

[2] "13931: Greenhouse gases, by source, energy product and pollutant, GWP-values due to Paris agreement (AR5) 1990 - 2023. Statbank Norway." Accessed: Oct. 07, 2024. [Online]. Available: https://www.ssb.no/en/statbank/table/13931/

[3] R. Rauch, J. Hrbek, and H. Hofbauer, "Biomass Gasification for Synthesis Gas Production and Applications of the Syngas," *Advances in Bioenergy: The Sustainability Challenge*, pp. 73–91, Dec. 2015, doi: 10.1002/9781118957844.CH7.

[4] F. Gharagheizi, P. Ilani-Kashkouli, and R. C. Hedden, "Standard molar chemical exergy: A new accurate model," *Energy*, vol. 158, pp. 924–935, Sep. 2018, doi: 10.1016/j.energy.2018.05.186.

[5] F. Samimi, T. Marzoughi, and M. R. Rahimpour, "Energy and exergy analysis and optimization of biomass gasification process for hydrogen production (based on air, steam and air/steam gasifying agents)," *Int J Hydrogen Energy*, vol. 45, no. 58, pp. 33185–33197, Nov. 2020, doi: 10.1016/j.ijhydene.2020.09.131.

[6] E. Karasavvas, K. D. Panopoulos, S. Papadopoulou, and S. Voutetakis, "Energy and exergy analysis of the integration of concentrated solar power with calcium looping for power production and thermochemical energy storage," *Renew Energy*, vol. 154, pp. 743–753, Jul. 2020, doi: 10.1016/j.renene.2020.03.018.

[7] "Global warming potential | Clean Energy Regulator." Accessed: Nov. 27, 2024. [Online]. Available: https://cer.gov.au/schemes/national-greenhouse-and-energy-reporting-scheme/about-emissions-and-energy-data/global-warming-potential

[8] "Acidification potential - Designing Buildings." Accessed: Dec. 03, 2024. [Online]. Available: https://www.designingbuildings.co.uk/wiki/Acidification_potential

[9] S. Rudra and Y. K. Tesfagaber, "Future district heating plant integrated with municipal solid waste (MSW) gasification for hydrogen production," *Energy*, vol. 180, pp. 881–892, Aug. 2019, doi: 10.1016/j.energy.2019.05.125.

[10] "International Energy Outlook 2014 | Enhanced Reader."

[11] C. Ji *et al.*, "Effect of ammonia addition on combustion and emissions performance of a hydrogen engine at part load and stoichiometric conditions," *Int J Hydrogen Energy*, vol. 46, no. 80, pp. 40143–40153, Nov. 2021, doi: 10.1016/J.IJHYDENE.2021.09.208.

[12] D. Akinyele, E. Olabode, and A. Amole, "Review of Fuel Cell Technologies and Applications for Sustainable Microgrid Systems," *Inventions 2020, Vol. 5, Page 42*, vol. 5, no. 3, p. 42, Aug. 2020, doi: 10.3390/INVENTIONS5030042.

[13] S. Wang *et al.*, "The environmental potential of hydrogen addition as complementation for diesel and biodiesel: A comprehensive review and perspectives," *Fuel*, vol. 342, p. 127794, Jun. 2023, doi: 10.1016/J.FUEL.2023.127794.

[14] "Foundational techniques for catalyst design in the upgrading of biomass-derived multifunctional molecules | Enhanced Reader."

[15] "Hydrogen-rich syngas production from municipal solid waste gasification through the application of central composite design: An optimization study | Enhanced Reader."

[16] J. Hong *et al.*, "Intensification of municipal solid waste disposal in China," *Renewable and Sustainable Energy Reviews*, vol. 69, pp. 168–176, Mar. 2017, doi: 10.1016/J.RSER.2016.11.185.

[17] "Hazardous waste – SSB." Accessed: Nov. 28, 2024. [Online]. Available: https://www.ssb.no/en/natur-og-miljo/avfall/statistikk/farlig-avfall

[18] E. Rada, G. Passamani, M. Ragazzi, V. T.- environment, and undefined 2018, "Dioxin contamination after a hypothetical accidental fire in baled municipal solid waste storage,"

academia.eduEC Rada, G Passamani, M Ragazzi, V Torretta, IA Istrate, G Ciocaenvironment, 2018•academia.edu, Accessed: Nov. 18, 2024. [Online]. Available: https://www.academia.edu/download/90692676/51_20RADA_20C_204_2018.pdf

[19] S. Dhaka City, "People's Republic of Bangladesh Data Collection Survey on Introducing Incineration System JICA in North and."

[20] L. Lombardi, E. Carnevale, and A. Corti, "A review of technologies and performances of thermal treatment systems for energy recovery from waste," *Waste Management*, vol. 37, pp. 26–44, Mar. 2015, doi: 10.1016/J.WASMAN.2014.11.010.

[21] D. Z. Shi *et al.*, "Effect of MSW source-classified collection on the emission of PCDDs/Fs and heavy metals from incineration in China," *J Hazard Mater*, vol. 153, no. 1–2, pp. 685–694, May 2008, doi: 10.1016/J.JHAZMAT.2007.09.026.

[22] "Hydrogen production with an auto-thermal MSW steam gasification and direct melting system: A process modeling | Enhanced Reader."

[23] P. Parthasarathy, K. N.-R. energy, and undefined 2014, "Hydrogen production from steam gasification of biomass: influence of process parameters on hydrogen yield–a review," *ElsevierP Parthasarathy, KS NarayananRenewable energy, 2014•Elsevier*, Accessed: Nov. 19, 2024. [Online]. Available: https://www.sciencedirect.com/science/article/pii/S0960148113007027

[24] V. Belgiorno, G. De Feo, D. Rocca, and R. M. A. Napoli, "Energy from gasification of solid wastes." [Online]. Available: www.elsevier.com/locate/wasman

[25] "Municipal solid waste (MSW) as a source of renewable energy in Bangladesh_ Revisited | Enhanced Reader."

[26] S. Fiore, B. Ruffino, and M. C. Zanetti, "Automobile Shredder Residues in Italy: Characterization and valorization opportunities," *Waste Management*, vol. 32, no. 8, pp. 1548–1559, Aug. 2012, doi: 10.1016/J.WASMAN.2012.03.026.

[27] X. Zhao, H. Zhou, V. Sikarwar, … M. Z.-E. &, and undefined 2017, "Biomass-based chemical looping technologies: the good, the bad and the future," *pubs.rsc.orgX Zhao, H Zhou, VS Sikarwar, M Zhao, AHA Park, PS Fennell, L Shen, LS FanEnergy & Environmental Science, 2017•pubs.rsc.org*, Accessed: Nov. 23, 2024. [Online]. Available: https://pubs.rsc.org/en/content/articlehtml/2017/ee/c6ee03718f

[28] A. Westbye, A. Aranda, G. Grasa, P. D. C. Dietzel, I. Martínez, and L. Di Felice, "Fixed Bed Reactor Validation of a Mayenite Based Combined Calcium-Copper Material for Hydrogen Production through Ca-Cu Looping," *Ind Eng Chem Res*, vol. 58, no. 32, pp. 14664–14677, Aug. 2019, doi: 10.1021/acs.iecr.9b02372.

[29] "Chemical Looping Combustion 150 kW pilot unit at SINTEF - SINTEF." Accessed: Sep. 13, 2024. [Online]. Available: https://www.sintef.no/en/all-laboratories/eccsel-norway-ccs-ri/chemical-looping-combustion-150-kw-pilot-unit-at-sintef/

[30] "Home Page | Data Portal." Accessed: Nov. 19, 2024. [Online]. Available: https://population.un.org/dataportal/home?df=f865e7b8-cf67-4e9e-a7a7-0234a1282089

[31] N. Ministry of Petroleum and N. Ministry of Climate, "Norwegian Ministry of Petroleum and Energy Strategy Norwegian Ministry of Climate and Environment."

[32] M. of Climate, "Priority research needs of the Ministry of Climate and Environment (2016-2021)."

[33] "Waste treatment in waste treatment plants – SSB." Accessed: Nov. 19, 2024. [Online]. Available: https://www.ssb.no/en/natur-og-miljo/avfall/statistikk/avfallshandtering-ved-avfallsanlegg

[34] C. Lausselet *et al.*, "Norwegian Waste-to-Energy: climate change, circular economy and carbon capture and storage."

[35] "Norway waste-to-energy incinerator begins world's first carbon capture experiment | Waste Dive." Accessed: Nov. 19, 2024. [Online]. Available:

https://www.wastedive.com/news/norway-waste-to-energy-incinerator-begins-worlds-first-carbon-capture-expe/413058/

[36] "District heating and district cooling in Norway - SSB." Accessed: Nov. 19, 2024. [Online]. Available: https://www.ssb.no/en/energi-og-industri/artikler-og-publikasjoner/fjernvarme-og-fjernkjoling-i-norge

[37] "Waste accounts – SSB." Accessed: Nov. 19, 2024. [Online]. Available: https://www.ssb.no/en/natur-og-miljo/avfall/statistikk/avfallsregnskapet

[38] A. Mohammadi, A. Anukam, A. Mohammadi, and A. Anukam, "The Technical Challenges of the Gasification Technologies Currently in Use and Ways of Optimizing Them: A Review," *Latest Research on Energy Recovery*, Feb. 2022, doi: 10.5772/INTECHOPEN.102593.

[39] "Teknologi for et bedre samfunn Biomass gasification in Norway."

[40] "SEB invites companies to buy carbon removals from waste incineration | SEB." Accessed: Oct. 07, 2024. [Online]. Available: https://sebgroup.com/press/news/2024/seb-invites-companies-to-buy-carbon-removals-from-waste-incineration

[41] "Turning plastic waste into hydrogen: first commercial plant moves step closer | Recharge." Accessed: Oct. 19, 2024. [Online]. Available: https://www.rechargenews.com/transition/turning-plastic-waste-into-hydrogen-first-commercial-plant-moves-step-closer/2-1-733678?zephr_sso_ott=ROGghZ

[42] S. Damman, E. Sandberg, E. Rosenberg, P. Pisciella, and U. Johansen, *Largescale hydrogen production in Norway-possible transition pathways towards 2050*.

[43] "Hydrogen will be a key contributor to the energy transition - Equinor." Accessed: Nov. 19, 2024. [Online]. Available: https://www.equinor.com/energy/hydrogen

[44] S. Damman, E. Sandberg, E. Rosenberg, P. Pisciella, and U. Johansen, *Largescale hydrogen production in Norway-possible transition pathways towards 2050*.

[45] C. Siew and W. Cheng, "THE PROSPECTS OF GREEN AND BLUE HYDROGEN PRODUCTION IN NORWAY FOR ENERGY EXPORT."

[46] "CORPORATE OVERVIEW JUNE 2024."

[47] Z. Kun, D. He, J. Guan, and Q. Zhang, "Thermodynamic analysis of chemical looping gasification coupled with lignite pyrolysis," *Energy*, vol. 166, pp. 807–818, Jan. 2019, doi: 10.1016/j.energy.2018.10.027.

[48] M. Niu, Y. Huang, B. Jin, and X. Wang, "Simulation of Syngas Production from Municipal Solid Waste Gasification in a Bubbling Fluidized Bed Using Aspen Plus," *Ind Eng Chem Res*, vol. 52, no. 42, pp. 14768–14775, Oct. 2013, doi: 10.1021/IE400026B.

[49] N. Soobhany *et al.*, "Spectroscopic, thermogravimetric and structural characterization analyses for comparing Municipal Solid Waste composts and vermicomposts stability and maturity," *Bioresour Technol*, vol. 236, pp. 11–19, 2017, doi: 10.1016/j.biortech.2017.03.161.

[50] S. Lotfi, O. K. Itimi-Elo, J. C. Morais, M. Jankovic, W. Ma, and G. Robertson, "Experimental study of catalyst performance on hydrothermal gasification of automotive fluff as a complex plastic containing waste," *Fuel*, vol. 371, Sep. 2024, doi: 10.1016/j.fuel.2024.130897.

[51] K. S. Williams and A. Khodier, "Meeting EU ELV targets: Pilot-scale pyrolysis automotive shredder residue investigation of PAHs, PCBs and environmental contaminants in the solid residue products," in *Waste Management*, Elsevier Ltd, Mar. 2020, pp. 233–239. doi: 10.1016/j.wasman.2020.02.005.

[52] S. Y. Cheng, N. T. Ngoc Lan Thao, and K. Y. Chiang, "Hydrogen gas yield and trace pollutant emission evaluation in automotive shredder residue (ASR) gasification using prepared oyster shell catalyst," *Int J Hydrogen Energy*, vol. 45, no. 42, pp. 22232–22245, Aug. 2020, doi: 10.1016/j.ijhydene.2020.01.005.

[53] "Biomass Gasification and Pyrolysis: Practical Design and Theory - Prabir Basu - Google Books." Accessed: Nov. 07, 2024. [Online]. Available: https://books.google.no/books?hl=en&lr=&id=QSypbUSdkikC&oi=fnd&pg=PP1&dq=P.+Basu,+Biomass+gasification+and+pyrolysis:+practical+design+and+theory.+Amsterdam:+Elsevier,++2

010.&ots=ViYn-2Dvl7&sig=8Q9Hy0j9OSg41-l6srGYmsuPypU&redir_esc=y#v=onepage&q=P.%20Basu%2C%20Biomass%20gasification%20and%20pyrolysis%3A%20practical%20design%20and%20theory.%20Amsterdam%3A%20Elsevier%2C%20%202010.&f=false

[54] A. K. Majumder, R. Jain, P. Banerjee, and J. P. Barnwal, "Development of a new proximate analysis based correlation to predict calorific value of coal," *Fuel*, vol. 87, no. 13–14, pp. 3077–3081, Oct. 2008, doi: 10.1016/j.fuel.2008.04.008.

[55] A. ÖzyuğUran and S. Yaman, "Prediction of Calorific Value of Biomass from Proximate Analysis," in *Energy Procedia*, Elsevier Ltd, Feb. 2017, pp. 130–136. doi: 10.1016/j.egypro.2016.12.149.

[56] "Introduction to Biomass Energy Conversions - Sergio Capareda - Google Books." Accessed: Nov. 07, 2024. [Online]. Available: https://books.google.no/books?hl=en&lr=&id=5ZXXEAAAQBAJ&oi=fnd&pg=PP1&dq=+Sergio+C.+Capareda,+Introduction+to+biomass+energy+conversions:+Sergio+C.+Capareda.+Boca++Raton:+CRC+Press,+2014.&ots=qT-lR9arB_&sig=7WfRMa2yi1AavuOpM9wG0KgQHgI&redir_esc=y#v=onepage&q&f=false

[57] "Municipal Solid Waste Characterization according to Different Income Levels: A Case Study | Enhanced Reader."

[58] "Solid biofuels-Determination of moisture content-Oven dry method-Part 3: Moisture in general analysis sample," 2015. [Online]. Available: www.iso.org

[59] D. Mboowa, S. Quereshi, C. Bhattacharjee, K. Tonny, and S. Dutta, "Qualitative determination of energy potential and methane generation from municipal solid waste (MSW) in Dhanbad (India)," *Energy*, vol. 123, pp. 386–391, 2017, doi: 10.1016/j.energy.2017.02.009.

[60] "ISO 18122 Solid Biofuels Determination of Ash Content".

[61] "ISO-562-1998".

[62] K. A. Motghare, A. P. Rathod, K. L. Wasewar, and N. K. Labhsetwar, "Comparative study of different waste biomass for energy application," *Waste Management*, vol. 47, pp. 40–45, Jan. 2016, doi: 10.1016/J.WASMAN.2015.07.032.

[63] J. Shen, S. Zhu, X. Liu, H. Zhang, and J. Tan, "The prediction of elemental composition of biomass based on proximate analysis," *Energy Convers Manag*, vol. 51, no. 5, pp. 983–987, May 2010, doi: 10.1016/j.enconman.2009.11.039.

[64] S. Chakma and R. Chandra Vaishya, "MODELING ELEMENTAL COMPOSITIONS OF MUNICIPAL SOLID WASTE FROM PROXIMATE ANALYSIS."

[65] S. Patel, B. Kumar, Y. Badhe, B. Sharma, S. S.- Fuel, and undefined 2007, "Estimation of gross calorific value of coals using artificial neural networks," *ElsevierSU Patel, BJ Kumar, YP Badhe, BK Sharma, S Saha, S Biswas, A Chaudhury, SS TambeFuel, 2007•Elsevier*, Accessed: Nov. 09, 2024. [Online]. Available: https://www.sciencedirect.com/science/article/pii/S0016236106002961

[66] S. S. Hla and D. Roberts, "Characterisation of chemical composition and energy content of green waste and municipal solid waste from Greater Brisbane, Australia," *Waste Management*, vol. 41, pp. 12–19, Jul. 2015, doi: 10.1016/J.WASMAN.2015.03.039.

[67] H. A. Arafat and K. Jijakli, "Modeling and comparative assessment of municipal solid waste gasification for energy production," *Waste Management*, vol. 33, no. 8, pp. 1704–1713, Aug. 2013, doi: 10.1016/j.wasman.2013.04.008.

[68] S. Lotfi, O. K. Itimi-Elo, J. C. Morais, M. Jankovic, W. Ma, and G. Robertson, "Experimental study of catalyst performance on hydrothermal gasification of automotive fluff as a complex plastic containing waste," *Fuel*, vol. 371, p. 130897, Sep. 2024, doi: 10.1016/J.FUEL.2024.130897.

[69] V. J. Inglezakis and A. A. Zorpas, "Automotive shredder residue (ASR): a rapidly increasing waste stream waiting for a sustainable response," *WIT Transactions on Ecology and the Environment*, vol. 120, p. 835, 2009, doi: 10.2495/SDP090782.

[70] S. Y. Cheng, N. T. Ngoc Lan Thao, and K. Y. Chiang, "Hydrogen gas yield and trace pollutant emission evaluation in automotive shredder residue (ASR) gasification using prepared oyster shell catalyst," *Int J Hydrogen Energy*, vol. 45, no. 42, pp. 22232–22245, Aug. 2020, doi: 10.1016/j.ijhydene.2020.01.005.

[71] J. Yu *et al.*, "Study on the behavior of heavy metals during thermal treatment of municipal solid waste (MSW) components," *Environmental Science and Pollution Research*, vol. 23, no. 1, pp. 253–265, Jan. 2016, doi: 10.1007/s11356-015-5644-7.

[72] G. Trouveâ, A. Kau€mann, and L. Delfosse, "Comparative thermodynamic and experimental study of some heavy metal behaviours during automotive shredder residues incineration."

[73] S. Galvagno, F. Fortuna, G. Cornacchia, S. Casu, T. Coppola, and V. K. Sharma, "Pyrolysis process for treatment of automobile shredder residue: preliminary experimental results," *Energy Convers Manag*, vol. 42, no. 5, pp. 573–586, Mar. 2001, doi: 10.1016/S0196-8904(00)00089-3.

[74] R. Taylor, R. Ray, and C. Chapman, "Advanced thermal treatment of auto shredder residue and refuse derived fuel," *Fuel*, vol. 106, pp. 401–409, Apr. 2013, doi: 10.1016/J.FUEL.2012.11.071.

[75] M. Edo, I. Aracil, R. Font, M. Anzano, A. Fullana, and E. Collina, "Viability study of automobile shredder residue as fuel," *J Hazard Mater*, vol. 260, pp. 819–824, Sep. 2013, doi: 10.1016/J.JHAZMAT.2013.06.039.

[76] A. Santini, F. Passarini, I. Vassura, D. Serrano, J. Dufour, and L. Morselli, "Auto shredder residue recycling: Mechanical separation and pyrolysis," *Waste Management*, vol. 32, no. 5, pp. 852–858, May 2012, doi: 10.1016/J.WASMAN.2011.10.030.

[77] N. Meng *et al.*, "Sulfur transformation in coal during supercritical water gasification," *Fuel*, vol. 186, pp. 394–404, Dec. 2016, doi: 10.1016/J.FUEL.2016.08.097.

[78] M. Bernardo, N. Lapa, M. Gonçalves, B. Mendes, and F. Pinto, "Study of the organic extraction and acidic leaching of chars obtained in the pyrolysis of plastics, tire rubber and forestry biomass wastes," in *Procedia Engineering*, Elsevier Ltd, 2012, pp. 1739–1746. doi: 10.1016/j.proeng.2012.07.567.

[79] Z. Kun, D. He, J. Guan, and Q. Zhang, "Thermodynamic analysis of chemical looping gasification coupled with lignite pyrolysis," *Energy*, vol. 166, pp. 807–818, Jan. 2019, doi: 10.1016/j.energy.2018.10.027.

[80] X. Zhu, Q. Imtiaz, F. Donat, C. R. Müller, and F. Li, "Chemical looping beyond combustion-a perspective," Mar. 01, 2020, *Royal Society of Chemistry*. doi: 10.1039/c9ee03793d.

[81] K. Anaya, A. Olufemi Oni, and A. Kumar, "Investigating the techno-economic and environmental performance of chemical looping technology for hydrogen production," *Sustainable Energy Technologies and Assessments*, vol. 56, Mar. 2023, doi: 10.1016/j.seta.2022.103008.

[82] L. Zeng, Z. Cheng, J. A. Fan, L. S. Fan, and J. Gong, "Metal oxide redox chemistry for chemical looping processes," *Nature Reviews Chemistry 2018 2:11*, vol. 2, no. 11, pp. 349–364, Oct. 2018, doi: 10.1038/s41570-018-0046-2.

[83] M. Ismail, W. Liu, M. S. C. Chan, M. T. Dunstan, and S. A. Scott, "Synthesis, Application, and Carbonation Behavior of Ca2Fe2O5 for Chemical Looping H2 Production," *Energy and Fuels*, vol. 30, no. 8, pp. 6220–6232, Aug. 2016, doi: 10.1021/ACS.ENERGYFUELS.6B00631/SUPPL_FILE/EF6B00631_SI_001.PDF.

[84] J. Haydary, D. Susa, V. Gelinger, and F. Čacho, "Pyrolysis of automobile shredder residue in a laboratory scale screw type reactor," *J Environ Chem Eng*, vol. 4, no. 1, pp. 965–972, Mar. 2016, doi: 10.1016/j.jece.2015.12.038.

[85] A. Santini, F. Passarini, I. Vassura, D. Serrano, J. Dufour, and L. Morselli, "Auto shredder residue recycling: Mechanical separation and pyrolysis," *Waste Management*, vol. 32, no. 5, pp. 852–858, May 2012, doi: 10.1016/j.wasman.2011.10.030.

[86] J. Tan, W. Li, L. Tang, X. Chen, H. Liu, and F. Wang, "Study on the pyrolysis characteristics and char gasification kinetics of pre-separated automobile shredder residues," *J Environ Chem Eng*, vol. 12, no. 2, Apr. 2024, doi: 10.1016/j.jece.2024.112520.

[87] K. Anaya, A. Olufemi Oni, and A. Kumar, "Investigating the techno-economic and environmental performance of chemical looping technology for hydrogen production," *Sustainable Energy Technologies and Assessments*, vol. 56, Mar. 2023, doi: 10.1016/j.seta.2022.103008.

[88] Z. Kun, D. He, J. Guan, and Q. Zhang, "Thermodynamic analysis of chemical looping gasification coupled with lignite pyrolysis," *Energy*, vol. 166, pp. 807–818, Jan. 2019, doi: 10.1016/j.energy.2018.10.027.

[89] P. Li *et al.*, "Biomass pyrolysis-gasification-hydrogen generation cycle system coupled with tar chemical looping reforming process," *Int J Hydrogen Energy*, vol. 72, pp. 367–379, Jun. 2024, doi: 10.1016/j.ijhydene.2024.05.263.

[90] M. P. S. Santos and D. P. Hanak, "Techno-economic feasibility assessment of sorption enhanced gasification of municipal solid waste for hydrogen production," *Int J Hydrogen Energy*, vol. 47, no. 10, pp. 6586–6604, Feb. 2022, doi: 10.1016/j.ijhydene.2021.12.037.

[91] Y. Zhao *et al.*, "Energy, efficiency, and environmental analysis of hydrogen generation via plasma co-gasification of biomass and plastics based on parameter simulation using Aspen plus," *Energy Convers Manag*, vol. 295, Nov. 2023, doi: 10.1016/j.enconman.2023.117623.

[92] J. Qi, H. Li, G. Chen, B. Yan, and J. Yao, "Thermodynamic modeling and performance analysis of chemical looping gasification combined with steam reforming for municipal solid waste: An Aspen Plus approach," *Energy Convers Manag*, vol. 314, Aug. 2024, doi: 10.1016/j.enconman.2024.118655.

[93] Y. Sun, Z. Qin, Y. Tang, T. Huang, S. Ding, and X. Ma, "Techno-environmental-economic evaluation on municipal solid waste (MSW) to power/fuel by gasification-based and incineration-based routes," *J Environ Chem Eng*, vol. 9, no. 5, Oct. 2021, doi: 10.1016/j.jece.2021.106108.

[94] V. Shah, P. Mohapatra, and L. S. Fan, "Thermodynamic and Process Analyses of Syngas Production Using Chemical Looping Reforming Assisted by Flexible Dicalcium Ferrite-Based Oxygen Carrier Regeneration," *Energy and Fuels*, vol. 34, no. 5, pp. 6490–6500, May 2020, doi: 10.1021/acs.energyfuels.0c00479.

[95] S. G. Gopaul, A. Dutta, and R. Clemmer, "Chemical looping gasification for hydrogen production: A comparison of two unique processes simulated using ASPEN Plus," in *International Journal of Hydrogen Energy*, Elsevier Ltd, Apr. 2014, pp. 5804–5817. doi: 10.1016/j.ijhydene.2014.01.178.

[96] Q. Hu, Y. Shen, J. W. Chew, T. Ge, and C. H. Wang, "Chemical looping gasification of biomass with Fe2O3/CaO as the oxygen carrier for hydrogen-enriched syngas production," *Chemical Engineering Journal*, vol. 379, Jan. 2020, doi: 10.1016/j.cej.2019.122346.

[97] Q. Hu, Y. Shen, J. W. Chew, T. Ge, and C. H. Wang, "Chemical looping gasification of biomass with Fe2O3/CaO as the oxygen carrier for hydrogen-enriched syngas production," *Chemical Engineering Journal*, vol. 379, Jan. 2020, doi: 10.1016/j.cej.2019.122346.

[98] J. Zhang *et al.*, "The search of proper oxygen carriers for chemical looping partial oxidation of carbon," *Appl Energy*, vol. 190, pp. 1119–1125, 2017, doi: 10.1016/j.apenergy.2017.01.024.

[99] U. Mohamed, "Biomass Chemical Looping Gasification for Power Generation," 2021.

[100] R. Habibi and M. Mehrpooya, "A novel integrated Ca-Cu cycle with coal/biomass gasification unit for clean hydrogen production," *Energy Convers Manag*, vol. 228, Jan. 2021, doi: 10.1016/j.enconman.2020.113682.

[101] W. Wu, L. Zheng, B. Shi, and P. C. Kuo, "Energy and exergy analysis of MSW-based IGCC power/polygeneration systems," *Energy Convers Manag*, vol. 238, Jun. 2021, doi: 10.1016/j.enconman.2021.114119.

[102] Z. Kun, D. He, J. Guan, and Q. Zhang, "Thermodynamic analysis of chemical looping gasification coupled with lignite pyrolysis," *Energy*, vol. 166, pp. 807–818, Jan. 2019, doi: 10.1016/J.ENERGY.2018.10.027.

[103] P. C. Kuo, W. Wu, and W. H. Chen, "Gasification performances of raw and torrefied biomass in a downdraft fixed bed gasifier using thermodynamic analysis," *Fuel*, vol. 117, no. PARTB, pp. 1231–1241, Jan. 2014, doi: 10.1016/j.fuel.2013.07.125.

[104] S. S. Seyitoglu, I. Dincer, and A. Kilicarslan, "Energy and exergy analyses of hydrogen production by coal gasification," *Int J Hydrogen Energy*, vol. 42, no. 4, pp. 2592–2600, Jan. 2017, doi: 10.1016/j.ijhydene.2016.08.228.

[105] L. Yan, G. Yue, and B. He, "Thermodynamic analyses of a biomass–coal co-gasification power generation system," *Bioresour Technol*, vol. 205, pp. 133–141, Apr. 2016, doi: 10.1016/J.BIORTECH.2016.01.049.

[106] M. P. S. Santos and D. P. Hanak, "Techno-economic feasibility assessment of sorption enhanced gasification of municipal solid waste for hydrogen production," *Int J Hydrogen Energy*, vol. 47, no. 10, pp. 6586–6604, Feb. 2022, doi: 10.1016/j.ijhydene.2021.12.037.

[107] H. Wang, R. Ren, B. Liu, and C. You, "Hydrogen production with an auto-thermal MSW steam gasification and direct melting system: A process modeling," *Int J Hydrogen Energy*, vol. 47, no. 10, pp. 6508–6518, Feb. 2022, doi: 10.1016/j.ijhydene.2021.12.009.

[108] T. Li *et al.*, "Performance analysis of an integrated biomass-to-energy system based on gasification and pyrolysis," *Energy Convers Manag*, vol. 287, p. 117085, Jul. 2023, doi: 10.1016/J.ENCONMAN.2023.117085.

[109] S. Wang and S. Wang, "Exergy analysis and optimization of methanol generating hydrogen system for PEMFC," *Int J Hydrogen Energy*, vol. 31, no. 12, pp. 1747–1755, Sep. 2006, doi: 10.1016/j.ijhydene.2005.12.005.

[110] I. Dincer and M. A. Rosen, "Exergy as a Driver for Achieving Sustainability," *Int J Green Energy*, vol. 1, no. 1, pp. 1–19, Dec. 2004, doi: 10.1081/ge-120027881.

[111] F. Gharagheizi and M. Mehrpooya, "Prediction of standard chemical exergy by a three descriptors QSPR model," *Energy Convers Manag*, vol. 48, no. 9, pp. 2453–2460, Sep. 2007, doi: 10.1016/j.enconman.2007.04.005.

[112] F. Samimi, T. Marzoughi, and M. R. Rahimpour, "Energy and exergy analysis and optimization of biomass gasification process for hydrogen production (based on air, steam and air/steam gasifying agents)," *Int J Hydrogen Energy*, vol. 45, no. 58, pp. 33185–33197, Nov. 2020, doi: 10.1016/j.ijhydene.2020.09.131.

[113] Y. Sun, Z. Qin, Y. Tang, T. Huang, S. Ding, and X. Ma, "Techno-environmental-economic evaluation on municipal solid waste (MSW) to power/fuel by gasification-based and incineration-based routes," *J Environ Chem Eng*, vol. 9, no. 5, Oct. 2021, doi: 10.1016/j.jece.2021.106108.

[114] R. Rivero and M. Garfias, "Standard chemical exergy of elements updated," *Energy*, vol. 31, no. 15, pp. 3310–3326, 2006, doi: 10.1016/j.energy.2006.03.020.

[115] "all enthalpy entropy for ca2fe2o5".

[116] Z. Xu *et al.*, "Exergy, techno-economic and environment analysis of food waste plasma gasification and syngas chemical looping processes," *J Clean Prod*, vol. 386, Feb. 2023, doi: 10.1016/j.jclepro.2022.135835.

[117] S. A. Zaman and S. Ghosh, "A generic input–output approach in developing and optimizing an Aspen plus steam-gasification model for biomass," *Bioresour Technol*, vol. 337, Oct. 2021, doi: 10.1016/j.biortech.2021.125412.

[118] "Norsk Gjenvinning: Løsninger for bedriftskunder." Accessed: Oct. 19, 2024. [Online]. Available: https://www.norskgjenvinning.no/

[119] V. J. Inglezakis and A. A. Zorpas, "Automotive shredder residue (ASR): a rapidly increasing waste stream waiting for a sustainable response," *WIT Transactions on Ecology and the Environment*, vol. 120, p. 835, 2009, doi: 10.2495/SDP090782.

[120] R. Sasso *et al.*, "Valorization of Biomass and Industrial Wastes as Alternative Fuels for Sustainable Cement Production," *Clean Technologies 2024, Vol. 6, Pages 814-825*, vol. 6, no. 2, pp. 814–825, Jun. 2024, doi: 10.3390/CLEANTECHNOL6020042.

[121] "Norcem to spend up to Euro8m on alternative fuels upgrades at Kjøpsvik plant." Accessed: Oct. 20, 2024. [Online]. Available: https://cemfuels.com/news/item/3306-norcem-to-spend-up-to-euro8m-on-alternative-fuels-upgrades-at-kjopsvik-plant

[122] I. Martínez, G. Grasa, M. S. Callén, J. M. López, and R. Murillo, "Optimised production of tailored syngas from municipal solid waste (MSW) by sorption-enhanced gasification," *Chemical Engineering Journal*, vol. 401, Dec. 2020, doi: 10.1016/j.cej.2020.126067.

[123] J. Haydary, D. Susa, V. Gelinger, and F. Čacho, "Pyrolysis of automobile shredder residue in a laboratory scale screw type reactor," *J Environ Chem Eng*, vol. 4, no. 1, pp. 965–972, Mar. 2016, doi: 10.1016/j.jece.2015.12.038.

[124] J. Haydary, D. Susa, V. Gelinger, and F. Čacho, "Pyrolysis of automobile shredder residue in a laboratory scale screw type reactor," *J Environ Chem Eng*, vol. 4, no. 1, pp. 965–972, Mar. 2016, doi: 10.1016/j.jece.2015.12.038.

[125] S. Rudra and Y. K. Tesfagaber, "Future district heating plant integrated with municipal solid waste (MSW) gasification for hydrogen production," *Energy*, vol. 180, pp. 881–892, Aug. 2019, doi: 10.1016/j.energy.2019.05.125.

[126] G. Liu, Y. Liao, Y. Wu, and X. Ma, "Application of calcium ferrites as oxygen carriers for microalgae chemical looping gasification," *Energy Convers Manag*, vol. 160, pp. 262–272, Mar. 2018, doi: 10.1016/j.enconman.2018.01.041.

[127] J. Qi *et al.*, "Hydrogen production from municipal solid waste via chemical looping gasification using CuFe2O4 spinel as oxygen carrier: An Aspen Plus modeling," *Energy Convers Manag*, vol. 294, Oct. 2023, doi: 10.1016/j.enconman.2023.117562.

[128] A. A. D. Zare and M. Yari, "Comprehensive examination and analysis of thermodynamics in a multi-generation hydrogen, heat, and power system based on plastic waste gasification integrated biogas -fueled chemical looping combustion," *Process Safety and Environmental Protection*, vol. 183, pp. 976–991, Mar. 2024, doi: 10.1016/j.psep.2024.01.060.

[129] Y. Sun, Z. Qin, Y. Tang, T. Huang, S. Ding, and X. Ma, "Techno-environmental-economic evaluation on municipal solid waste (MSW) to power/fuel by gasification-based and incineration-based routes," *J Environ Chem Eng*, vol. 9, no. 5, Oct. 2021, doi: 10.1016/j.jece.2021.106108.

[130] J. Qi *et al.*, "Hydrogen production from municipal solid waste via chemical looping gasification using CuFe2O4 spinel as oxygen carrier: An Aspen Plus modeling," *Energy Convers Manag*, vol. 294, Oct. 2023, doi: 10.1016/j.enconman.2023.117562.

[131] M. Mehdi *et al.*, "Aspen plus simulation model of municipal solid waste gasification of metropolitan city for syngas production," *Fuel*, vol. 344, Jul. 2023, doi: 10.1016/j.fuel.2023.128128.

[132] "China Calcium Ferrite, Calcium Ferrite Wholesale, Manufacturers, Price | Made-in-China.com." Accessed: Dec. 05, 2024. [Online]. Available: https://www.made-in-china.com/products-search/hot-china-products/Calcium_Ferrite.html

Appendix A

This chapter includes the proximate analysis and thermogravimetric analysis calculation.

Table 15: Volatile matter in ISW.

	M1	M2	M3	$\frac{M2-M3}{M2-M1}$=m	m× 100	(m× 100) − MC Volatile (%)
CF1	91.4297	91.5004	91.4456	0.775106	77.51061	71.21061
CF2	81.6308	81.6953	81.6382	0.885271	88.52713	84.12713
FAB1	92.9376	93.0051	92.9511	0.8	80	76.9
FAB2	93.3948	93.4807	93.4086	0.839348	83.93481	81.53481

Table 16: Moisture, volatile, ash, and fixed carbon values obtained from TGA.

	Moisture	Volatile matter	Fixed carbon	Ash
CF1-2	3.6756	76.8335	16.7167	2.7742
CF1-3	2.5631	78.0458	17.5165	1.8746
Mean	3.11935	77.43965	17.1166	2.3244
CF2-1	0.8893	85.0912	6.9432	7.0763
CF2-2	1.0177	86.8311	5.2678	6.8834
CF2-3	0.928	81.4741	7.3722	10.2257
Mean	0.945	84.46547	6.527733	8.0618
FAB1-1	1.3747	83.9062	7.787	6.9321
FAB1-2	1.3714	81.623	8.3612	8.6444
FAB1-3	1.3727	79.4247	8.3814	10.8212
Mean	1.372933	81.6513	8.176533	8.799233
FAB2-1	0.9421	82.5998	9.997	6.4611
FAB2-2	1.9218	80.9789	10.2561	6.8432
FAB2-3	0.9174	80.0488	11.5263	7.5075
Mean	1.260433	81.20917	10.59313	6.937267
Total-1	2.1585	81.4084	10.6081	5.825
Total-2	2.5324	81.8539	10.1325	5.4812
Total-3	2.1566	83.5959	8.9452	5.3023
Mean	2.2825	82.28607	9.895267	5.536167

Appendix B

1. Plant design

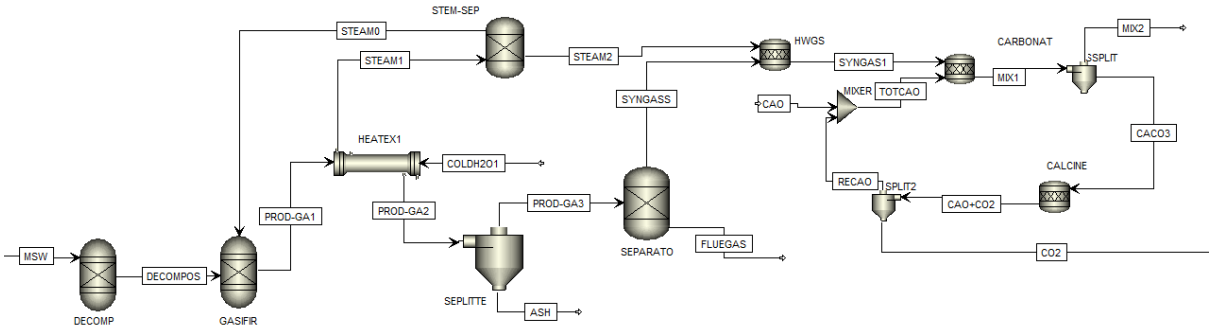

Figure 33. SE-Steam gasification (SE-SG).

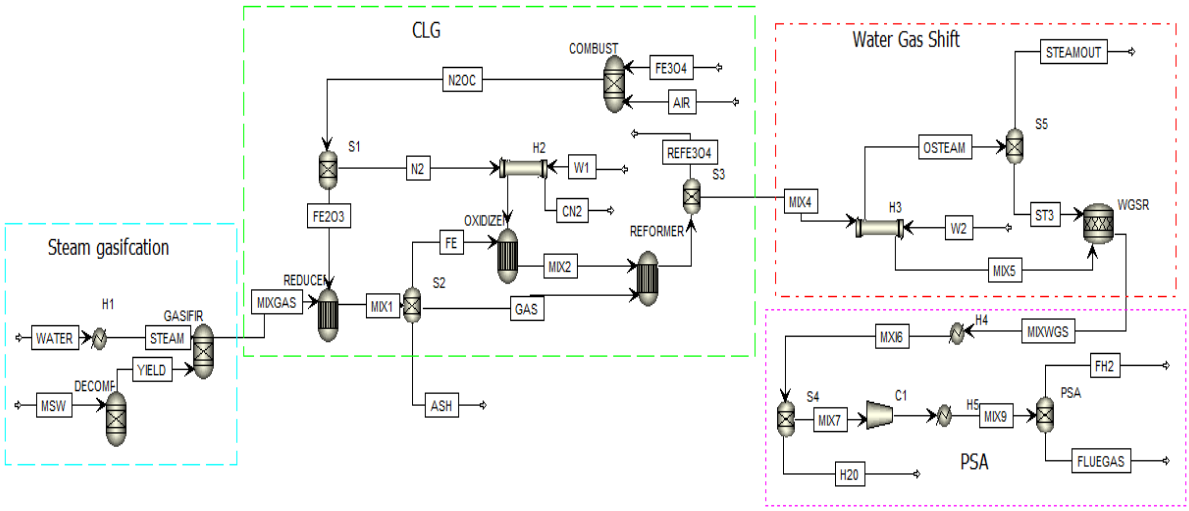

Figure 34 Sorption-Enhanced Chemical looping gasification model (SE-CLG 1).

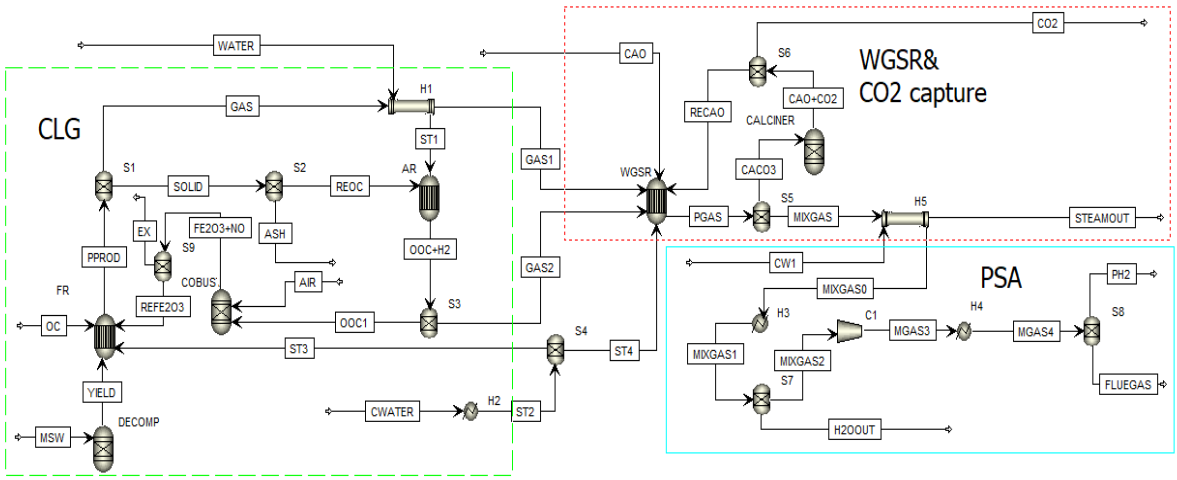

Figure 35: SE-CLG2 model when Fe2O3 is used as an oxygen carrier.

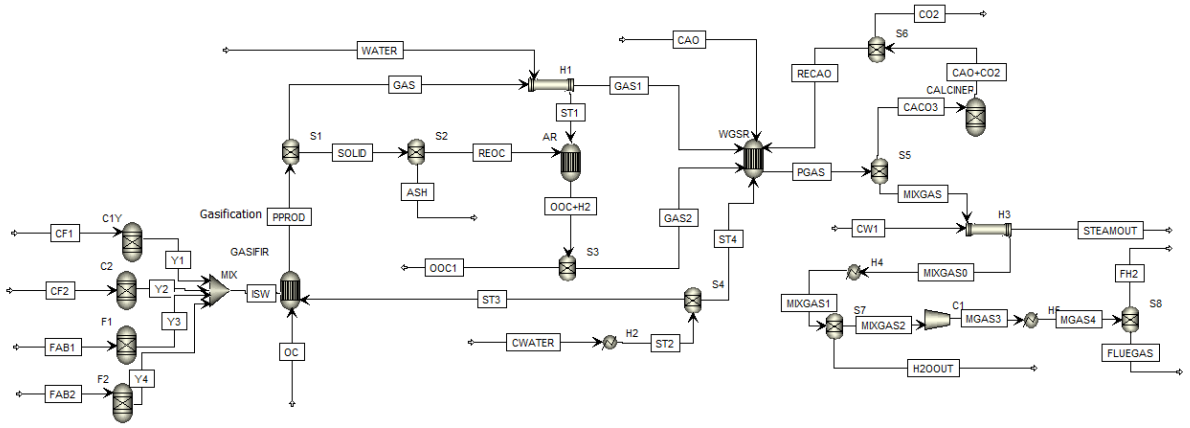

Figure 36: SE-CLG2 model for individual & combined variation of ISW.

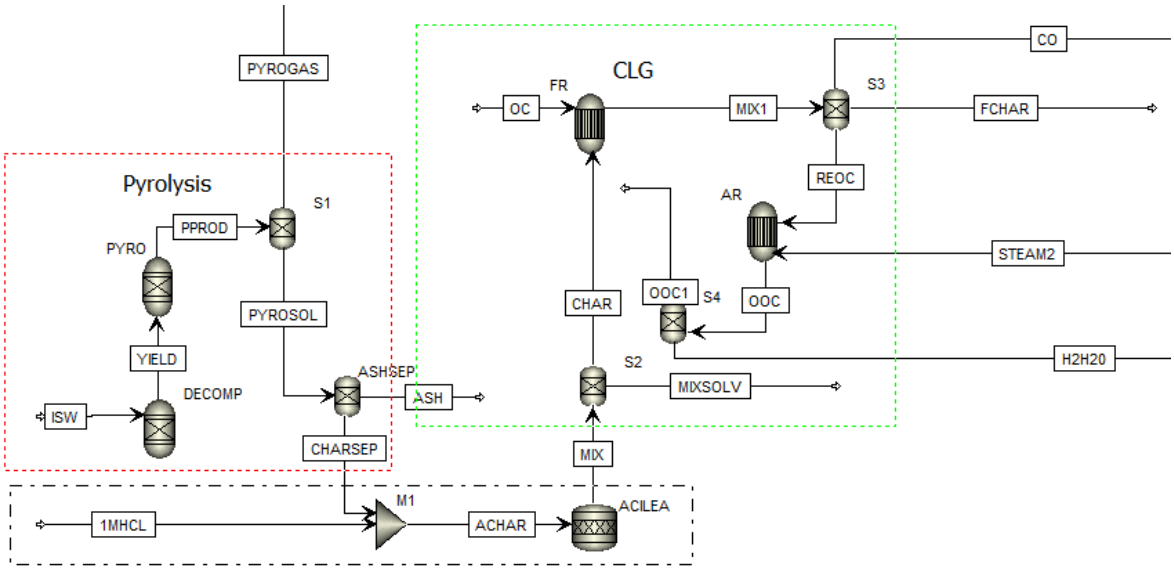

Figure 37: Pyro-CLG model Pyrolysis and char gasification portion.

2. Energy & Exergy calculations

Table 17: Final energy analysis for SE-CLG2.

Waste type: MSW OC: Ca2Fe2O5							
Hin	KW	Qadded	KW	Houtput	KW	Qgen	KW
CAO	-6291.8	GASIFIR	348.6265	ASH	-0.9425	WGSR	-2001.3
CW1	-6655.03	AR	507.4524	FH2	10.37622	H4	-63.7249
CWATER	-2528.91	H1	37.87783	FLUEGAS	-70.2349	H5	-224.951
MSW	-1600.85	CALCINER	2383.758	H2OOUT	-288.613	S7	-40.052
OC	-327.893	H2	53.9759	OOC1	-304.936	S8	-1.73005
WATER	-1774.68	H3	142.0419	RECAO	-5841.77	W1	-7.17706
ECWATER	-443.669	C1	232.041	STEAMOUT	-6512.99	W2	-2.68008
HSTEAM	-4436.69	H6	92.24833	CO2-STOR	-3981.28	W3	-2.65381
WATER1	-8873.38	H7	9.47E+01	HSTEAMOU	-4341.99		
		H10	160.9808	STCOND	-374.991	W5	-11.2117
		P1	0.391253	STEAM2	-7381.39	CON1	-160.016
		H8	189.3891				
Total	-32932.9		4243.478		-29088.8		-2515.5

The equation used for energy analysis-

$$EN_{in} + Q_{supply} = EN_{out} + Q_{gen} + EN_{loss}$$

Input energy=32932.9+4243.48= 37176.4 kW

Output energy=-10.37622+6512.99+3981.28+4341.99+374.991+7381.39= 25097.8 kW

So, the energy efficiency

$$\eta_{EN} = \frac{25097.8}{37176.4} \times 100 = 67.51\%$$

2.1 Exergy analysis

The MSW chemical exergy is determined using the following equation-

$$EX_{MSW} = (2442 \times mc + LHV_{MSW}) \times (0.1882 \times \frac{H}{C} + 0.0404 \times \frac{N}{C} - 0.0610 \times \frac{O}{C} + 1.0437)$$

The standard chemical exergy for the oxygen carrier Ca2Fe2O5 is determined using the following equation equal-

$$EX_{ch}^{O} = \Delta G_f^o + \sum n_i EX_{ch,i}^o$$

The Standard Gibbs free energy of formation ΔG_f^o of Ca2Fe2O5 is calculated using the following equation-

$$\Delta G_f^o(Ca2Fe2O5) = \Delta H_0 - T_o \Delta S_o$$

Where T_o=298.15K

Where ΔH_0=-55kJ/mol; $\Delta S_o = 0.5755 kJ/mol$

Table 18: Exergy analysis for CLG2 using Ca2Fe2O5 as OC Ca2FeO5 and Feed: MSW.

Physical exergy		Chemical exergy					Total exergy
Feed							
	kW	n_i	$EX_{ch,i}^o$				
			kJ/mol	mol/hr	kJ/hr	kW	
OC	0	1	2217.525	551.781	1223588	339.8856	339.8856
CaO	0	1	119.62	35664.99	4266246	1185.068	1185.068
ST1	4.100956	1	9.5	22203.37	210932.1	58.59224	62.69319
ST2	5.843862	1	9.5	31639.81	300578.2	83.49394	89.3378
HPSTEAM	39.85561	1	9.5	5550.844	52733.01	14.64806	54.50367
WATER1	-0.00087	1	0.9	111016.9	99915.18	27.75422	27.75335
MSW	0	1	439.63	50220.8	22078570	6132.936	6132.936
CW1	-0.00065	1	0.9	83262.65	74936.39	20.81566	20.81501
CWW1	-0.00074	1	0.9	94364.3	84927.9	23.5911	23.5903
							7936.584

Physical exergy		Chemical exergy					Total exergy	P_{gen}	
Product	kW	n_i	$EX_{ch,i}^o$						
			kJ/mol	mol/hr	kJ/hr	Kw	kW		
CO2-STOR	92.91	1	19.87	35664.9	708663.4	196.85	289.766	W1	-7.17
FH2	134.6	1	236.1	85109.02	20094239	5581.73	5716.41	W2	-2.68
HSTEAM	10.25	1	9.5	55508.4	527330.1	146.480	156.73	W3	-2.65
STEAMOUT	15.37	1	9.5	83262.6	790995.2	219.72	235.099		
STCOND	13.12	1	9.5	5550.84	52733.01	14.648	27.77	W5	-11.2
STEAM2	20.50	1	9.5	94363.3	896461	294.017	269.522		
							6695.3		-23.72

For total input exergy, the Qadded mentioned in *Table 17* is also added with input stream exergy.

$$\sum EX_{in} = 7936.58 + 4243.48 = 12180.1\ kW$$

For total output exergy, the power generated Pgen is added with output stream exergy.

$$\sum EX_{out} = 6695.3 + 23.72 = 6719.02\ kW$$

$$\eta_{EX} = \frac{6719.02}{12180.1} \times 100 = 55.16\%$$

Table 19: Energy analysis data for Pyro-CLG with Ca2Fe2O5 , Feed: MSW.

Hin	KW	Qadded	KW	Houtput	KW	Qgen	KW
1MHCL	-860.56	H1	94.69	ST-CO2	-2482.2	PYRO	-294.75
CAO	-4718.9	FR	1052.63	CSTEAM	-434.20	ACILEA	-83.4
CW1	-4436.7	AR	388.11	FCHAR	1.173	WGSR	-1043.7
CWATER	-4436.7	CALCINER	1377.75	FH2	8.637	H5	-371.73
CWATER1	-3549.4	H2	47.345	STOR-CO	-430.24	S8	-39.52
CWATAER1	-443.67	H3	94.69	H2OOUT	-982.07	H6	-222.28
CWW1	-221.83	H7	28.41	MIXSOLV	-875.22	S9	-0.228
MSW	-1600.8			OOC1	-2818.4		
OC	-3060.3	H8	46.12	RECAO	-4461.4	COND	-88.91
CWW2	-4436.7	P1	0.196	STCOND	-187.49	HP	-3.588
				STEAM3	-2735.4	MP	-1.34
		H10	113.63	STEAM4	-4341.9	LP	-1.33
		C2	5.29	STEAMOUT	-1302.6	OT	-5.6
		H9	113.63	STEAM5	-4341.9	H12	-7.323
Total	-27765.5		3362.53		-16246.3		-2163.7

The equation used for energy analysis-

$$EN_{in} + Q_{supply} = EN_{out} + Q_{gen} + EN_{loss}$$

Input energy=23328.8+348.75= 26814.5 kW

Output energy=14936.4kW

So, the energy efficiency

$$\eta_{EN} = \frac{18410}{31128} \times 100 = 59.143\%$$

Table 20: Exergy analysis of Pyro-CLG with OC: Ca2Fe2O5 and Feed: MSW.

Input							
Physical exergy		Chemical exergy					Total
Feed	kw	xi	Exch				
			kJ/mol	mol/hr		kW	
1MHCL	-0.0018	1	84.2	10900.79	917846.4	254.9573	254.9555
CAO	0	1	119.62	26748.74	3199685	888.8013	888.8013
STEAM1	3.793	1	9.5	20538.12	195112.1	54.19782	57.99082
CWATER	-0.0004	1	0.9	27754.22	24978.8	6.938554	6.938122
CWATER1	-0.0003	1	0.9	44406.75	39966.07	11.10169	11.10134
CWW1	-2.16E-05	1	0.9	2775.422	2497.88	0.693855	6.94E-01
MSW	0	1	439.63	50220.8	22078570	6132.936	6132.936
OC	0	1	2217.525	5149.956	11420155	3172.265	3172.265
STEAM2	5.126	1	9.5	27754.22	263665.1	73.2403	78.3663
							10604.05

Output									
Physical exergy		Chemical exergy					Total	Pgen	
Feed	kw	xi	Exch						
			kJ/mol	mol/hr		kW			
STEAM3	6.46	1	9.5	34970.3	332218	92.28	98.741	W1	-3.59
FCHAR	3.35	1	410.3	257.32	105568.3	29.32	32.6745	W2	-1.34
STEAM4	10.25	1	9.5	66610.12	632796.2	175.78	186.026	W3	-1.33
STEAMOUT	3.07	1	9.5	16652.53	158199	43.94	47.019	W4	-5.62
FH2	112.07	1	236.1	70845.71	1672667 2	4646.298	4758.376		
STOR-CO	6.71	1	275.1	14541.9	4000477	1111.244	1117.954		
CSTEAM	1.025	1	9.5	5550.844	52733.01	14.64806	15.67306		
STCO2	57.81	1	19.87	22235.76	441824.6	122.7291	180.5421		
STEAM5	12.3	1	9.5	79932.14	759355.3	210.932	223.232		
STCOND	0.512	1	9.5	3330.504	31639.79	8.78883	9.30133		
							6669.54		-11.86

$$\sum EX_{in} = 10604.5 + 3362.53 = 13966.6kW$$

$$\sum EX_{out} = 6669.54 + 11.86 = 6681.4\ kW$$

$$\eta_{EX} = \frac{6407.711}{13966.6} \times 100 = 47.84\%$$

Table 21: Energy analysis of SE-CLG2 with OC: Ca2Fe2O5 and Feed: ISW.

Hin	KW	Qadded	KW	Houtput	KW	Qgen	KW
CAO	-5662.6	AR	403.26	ASH	-0.88653	WGSR	-1671.5
CW1	-6655.03			FH2	8.77	H4	-195.03
CWATER	-2528.9	H1	37.878	FLUEGAS	-166.92	H5	-223.04
ISW	-1519.7	CALCINER	2145.382	H2OOUT	-888.28	S7	-40.51
OC	-327.89	H2	53.98	OOC1	-304.94	S8	-1.17
WATER	-1774.7	H3	142.042	RECAO	-2920.88	W1	-7.18
ECWATER	-443.67	C1	229.92	STEAMOUT	-6512.99	W2	-2.68
HWATER	-4436.7	H6	46.124	CO2-STOR	-1990.64	W3	-2.65
WATER1	-8873.4	H7	9.47E+01	HSTEAM	-4341.99	GASIFIR	-298.91
CWW1	-6211.4	H10	160.98	STCOND	-187.50	W5	-11.21
		P1	0.196	STEAM2	-7381.39	CON1	-137.63
		H8	189.39	STEAM3	-6078.79		
		HCO2	132.57				
Total	-38434		3636.41		-30766.4		-2591.5

Input energy=38434+3636.41= 42070.4 kW

Output energy=26484.5+2591.53=29076.1kW

So, the energy efficiency

$$\eta_{EN} = \frac{29076.1}{42070.4} \times 100 = 69.11\%$$

Table 22: Exergy analysis data for SE-CLG2 with OC: Ca2fe2O5 and Feed: ISW

Input							
Physical exergy		Chemical exergy					
Feed	kw	xi	Exch				
			kJ/mol	mol/hr	kJ/hr	kW	
OC	0	1	2217.525	551.781	1223588	339.8856	339.8856
CaO	0	1	119.62	32098.5	3839623	1066.562	1066.562
ST1	4.100956	1	9.5	22203.37	210932.1	58.59224	62.69319
ST2	5.843862	1	9.5	31639.81	300578.2	83.49394	89.3378
HPSTEAM	39.85561	1	9.5	5550.844	52733.01	14.64806	54.50367
WATER1	-0.00087	1	0.9	111016.9	99915.18	27.75422	27.75335
ISW	0	1	430.82	39181.88	16880338	4688.983	4688.983
CW1	-0.00065		0.9	83262.65	74936.39	20.81566	20.81501
CWW1	-0.00074		0.9	77711.78	69940.6	19.42795	19.42721
							6369.96

Output									
Physical exergy		Chemical exergy					Total	P(gen)	
Product	kW	xi	Exch						
			kJ/mol	mol/hr	kJ/hr	kW	KW		
CO2-STOR	83.62	1	19.87	32097.9	637785.3	177.16	260.78	W1	-7.18
FH2	114.43	1	236.1	72325.3	17076013	4743.33	4857.77	W2	-2.68
HSTEAM	10.25	1	9.5	55508.4	527330.1	146.48	156.73	W3	-2.65
STEAMOUT	14.53	1	9.5	77711.8	738262.6	205.07	219.60		
STCOND	13.12	1	9.5	5550.84	52733.01	14.65	27.77	W5	-11.21
STEAM3	16.89	1	9.5	63997.9	607980.5	168.88	185.77		
							5708.43		

$$\sum EX_{in} = 6369.96 + 3636.41 = 10000.4kW$$

$$\sum EX_{out} = 5708.43 + 23.73 = 5732.15\ kW$$

$$\eta_{EX} = \frac{5732.15}{10006.4} \times 100 = 57.29\%$$

Table 23: Energy analysis data for Pyro-CLG with OC: CA2Fe2O5 and Feed: ISW

Hin	KW	Qadded	KW	Houtput	KW	Qgen	KW
1MHCL	-860.56	H1	94.69	ST-CO2	-2275.9	PYRO	-912.14
CAO	-4718.8	FR	715.45			ACILEA	-60.70
CW1	-4436.7	AR	444.52	FCHAR	1.983	WGSR	-744.79
CWATER	-4436.7	CALCINER	1276.14	FH2	7.115	H5	-371.73
CWATER1	-3549.4	H2	47.35	STOR-CO	-396.75	S8	-33.53
		H3	94.69	H2OOUT	-1378.4	H6	-189.37
CWW1	-221.8	H7	28.41	MIXSOLV	-873.88	S9	-0.313
ISW	-1519.7	C1	195.71	OOC1	-1912.5		
OC	-2076.6	H8	46.12	RECAO	-4461.4	COND	-68.25
CWW2	-5324.03	P1	0.195	STCOND	-187.50	HP	-3.59
				STEAM3	-2735.5	MP	-1.34
				OTSTEAM	-5210.4	LP	-1.33
		C2	5.26	STEAMOUT	-1302.6	OT	-5.60
		H9	113.63	STEAM4	-4341.99	H12	-8.68
	-27144.4		3062.19		-25067.7		-2401.4

Input energy=27144.4+3062.19= 30206.6 kW

Output energy=18842.8 kW

So, the energy efficiency

$$\eta_{EN} = \frac{18842.8}{30206.6} \times 100 = 62.38\%$$

Table 24 Exergy analysis data for Pyro-CLG with OC: Ca2Fe2O5 and Feed: ISW

Input							
Physical exergy		Chemical exergy					Total exergy
Feed	kw	xi	Exch				
			kJ/mol	mol/hr	kJ/hr	kW	
1MHCL	-0.00187	1	84.2	10900.79	917846.4	254.9573	254.9555
CAO	0	1	119.62	26748.74	3199685	888.8013	888.8013
STEAM1	3.793	1	9.5	20538.12	195112.1	54.19782	57.99082
CWATER	-0.00043	1	0.9	27754.22	24978.8	6.938554	6.938122
CWATER1	-0.00035	1	0.9	44406.75	39966.07	11.10169	11.10134
CWW1	-2.16E-05	1	0.9	2775.422	2497.88	0.693855	0.693834
STEAM2	5.126	1	9.5	27754.22	263665.1	73.2403	78.3663
ISW	0	1	430.82	39181.88	16880338	4688.983	4688.983
OC	0	1	2217.525	3494.613	7749392	2152.609	2152.609

							8140.439

Output									
Physical exergy		Chemical exergy					Total exergy		
Feed	kw	xi	Exch						
			kJ/mol	mol/hr		kW			
FCHAR	5.66	1	410.3	434.69	178335.9	49.54	55.20	W1	-3.59
FH2	92.32	1	236.1	58358.7	13778480	3827.36	3919.7	W2	-1.34
OTSTEAM	12.3	1	9.5	79932.14	759355.3	210.93	223.23	W3	-1.33
STCO2	53.01	1	19.87	20387.9	405108.2	112.53	165.54	W4	-5.60
STCOND	0.5125	1	9.5	3330.50	31639.79	8.79	9.30		
STEAM3	6.459	1	9.5	34970.3	332218	92.28	98.74		
STEAM4	10.25	1	9.5	66610.12	632796.2	175.78	186.03		
STEAMOUT	3.075	1	9.5	16652.5	158199	43.94	47.02		
STOR-CO	7.05	1	275.1	15277.7	4202884	1167.5	1174.52		
							5879.2		11.86

$$\sum EX_{in} = 8140.39 + 3062.19 = 11202.6kW$$

$$\sum EX_{out} = 5879.25 + 11.86 = 5891.11\ kW$$

$$\eta_{EX} = \frac{5891.11}{11202.6} \times 100 = 52.59\%$$

Table 25: Energy analysis data for SE-CLG1 with Fe2O3 OC.

Feedstock type: MSW							
Hinput	kW	Qsuppy	kW	Houtput	kW	Qgen	kW
Air	-0.0115	H1	150.27	ASH	49.098	REDUCER	-557.456
CAO	-786.47	GASIFIR	818.607	CN2	22.534	S2	-1.54E-11
FE3O4	-63.679	S1	3.30E-10	CO2	-434.16	COMBUST	-103.919
MSW	-1600.8	OXIDIZER	43.45561	FH2	8.0542	WGSR	-396.465
W1	-310.56	H2	6.62862	FLUEGAS	-2509.9	S7	-5.83E-10
W2	-3105.6	S3	7.30E-08	H2O	-186.099	S6	-8.83E-09
WATER	-887.33	REFORMER	346.0743	RECAO	-730.221	H4	-228.062
		H3	66.2862	REFE3O4	-179.487	S4	-29.5644
		S5	0	STEAMOUT	-1519.7	H5	-227.259
		CALCINER	297.9698			PSA	-0.14273
		C1	235.0997				
Total	-6754.6		1964.391		-5479.88		-1542.8

The equation used for energy analysis-

$$EN_{in} + Q_{supply} = EN_{out} + Q_{gen} + EN_{loss}$$

Input energy=6745.61+1964.391= 8719 kW

For the Output streams, STEAMOUT and PH2 are considered for energy efficiency calculation.

Output energy=1519.7-8.054+1542.8=3054.51 kW

So, the energy efficiency

$$\eta_{EN} = \frac{3054.51}{8719} \times 100 = 35.033\%$$

Table 26: Energy analysis data for CLG1 with Ca2Fe2O5 OC.

Feedstock type: MSW							
Hinput	kW	Qadded	kW	Houtput	kW	Qgen	kW
Air	-0.0115	H1	150.272	ASH	-288.43	REDUCER	-673.41
CAO	-943.77	GASIFIR	818.607	CN2	33.21513	S1	-1.92E-06
CA2FE2O5	-327.8	OXIDIZER	52.57	CO2	-2091.93	WGSR	-375.22
MSW	-1600.8	H2	6.628	FH2	7.588888	S7	-3.17E-11
W1	-310.56	REFORMER	363.323	FLUEGAS	-1222.56	S8	-2.47E-08
W2	-3105.6	H3	66.286	H2O	-494.945	H4	-238.41
WATER	-887.33	S5	0	RECAO	-876.265	S4	-35.552
		CALCINER	834.315	REFE3O4	-114.319	H5	-195.65
		C1	202.082	STEAMOU	-1519.7	PSA	-0.07474
		COMBUST	81.1325			S2	-1.56E-11
						S3	-2.38E-07
	-7176.1		2575.2		-6567.35		-1518.34

The equation used for energy analysis-

$$EN_{in} + Q_{supply} = EN_{out} + Q_{gen} + EN_{loss}$$

Input energy= 7176.11+ 2575.219= 9751.33 kW

For the Output streams, STEAMOUT and PH2 are considered for energy efficiency calculation.

Output energy=1519.7-7.58+1518.34=3030.45 kW

So, the energy efficiency

$$\eta_{EN} = \frac{3030.45}{9751.33} \times 100 = 31.077\%$$

Table 27 Energy analysis data for SE-CLG2 with Fe2O3 OC.

Feedstock type: MSW							
Hinput	kW	Qadded	kW	Houtput	kW	Qgen	kW
AIR	-0.0019	FR	284.509	ASH	-0.9424	WGSR	-888.51
CAO	-943.77	S1	2.07E-05	CO2	-521.00	COMBUST	-24.607
CW1	-6655.03	S2	0	PH2	8.88598	S9	-2.46E-11
CWATER	-2528.91	AR	413.156	FLUEGAS	-2926.5	S3	-3.78E-08

MSW	-1600.85	H1	37.877	H2OOUT	-940.71	S5	-3.66E-05
OC	-215.388	H2	426.76	RECAO	-876.26	S6	-1.06E-08
WATER	-1774.68	S4	0	STEAMOUT	-6512.9	H3	-247.01
		CALCINER	357.563	EX	-166.66	S7	-48.539
		H5	142.041			H4	-263.56
		C1	271.527			S8	-1.5422
	-13718.6		1933.44		-11936.2		-1473.7

The equation used for energy analysis-

$$EN_{in} + Q_{supply} = EN_{out} + Q_{gen} + EN_{loss}$$

Input energy=13718.6+1933.44= 15652.1 kW

For the Output streams, STEAMOUT and PH2 are considered for energy efficiency calculation.

Output energy=6512.99-8.886+1473.7=7977.88 kW

So, the energy efficiency

$$\eta_{EN} = \frac{7977.88}{15652.1} \times 100 = 50.97\%$$

Similarly, for Ca2Fe2O5 in CLG2-

Table 28: Energy analysis data for SE-CLG2 with Ca2FeO5 OC.

Feedstock type: MSW							
Hinput	kW	Qadded	kW	Houtput	kW	Qgen	kW
CAO	-943.77	GASIFIR	348.6265	ASH	-0.9425	WGSR	-563.382
CW1	-6655.03	AR	507.4524	CO2	-521.001	S6	-1.06E-08
CWATER	-2528.91	H1	37.87783	FH2	9.602856	S5	-4.38E-05
MSW	-1600.85	CALCINER	357.5637	FLUEGAS	-2963.94	H4	212.8332
OC	-327.893	S1	-2.49E-06	H2OOUT	-708.935	S7	-51.7729
WATER	-1774.68	S2	0	OOC1	-304.936	H5	-281.026
		S3	-6.12E-10	RECAO	-876.265	S8	-0.14892
		H2	53.9759	STEAMOUT	-6512.99		
		S4	0				
		H3	142.0419				
		C1	290.6236				
	-13831.1		1738.162		-11879.4		-683.496

Input energy=13831.1+1738.12=15569.3kW

Output energy=6512.99-9.603+683.496=7186.88kW

The energy efficiency

$$\eta_{EN} = \frac{7186.88}{15569.3} \times 100 = 46.16\%$$

Similarly, for Ca2Fe2O5 in Pyro-CLG-

Table 29: Energy analysis data for Pyro-CLG with Ca2FeO5 OC.

Hinput	kW	Qadded	kW	Houtput	kW	Qgen	kW
1MHCL	-860.56	S1	3.53E-11	CO2	-537.36	PYRO	-294.75
CAO	-943.77	S2	0	FCHAR	1.17313	ACILEA	-83.398
CW1	-4436.6	FR	1052.639	FH2	8.37075	S3	-2.35E-09
CWATER	-4436.6	AR	2.87E+02	FLUEGAS	-2168.3	S4	-1.33E-07
CWATER1	-3549.3	H1	9.47E+01	H2OOUT	-713.53	S5	-9.31E-13
MSW	-1600.8	CALCINER	3.25E+02	MIXSOLV	-875.21	WGSR	-286.88
OC	-3060.3	H3	94.69457	OOC1	-2751.5	S7	-1.50E-09
		H2	37.87782	RECAO	-892.28	S6	-3.12E-07
		S10	0.00E+00	STEAM3	-2735.4	H5	-316.56
		H7	37.87783	STEAM4	-4341.9	S8	-46.43
		C1	263.0369	STEAMOUT	-1736.8	H6	-255.31
						S9	-0.936
	-18888.2		2190		-16743		-1284.2

Input energy=18888.2+2190=21078.2kW

Output energy=1736.8+4341.9+2735.4-8.37075-1.17313+1284.2=10089kW

The energy efficiency

$$\eta_{EN} = \frac{10089}{21078.2} \times 100 = 47.858\%$$

3. Environmental analysis

GWP and AP is calculated using the following equation as described in section (2.13 Environmental Analysis)

$$GWP = \sum (EF_{GWP,i} \times AMT_{GG,i})$$

$$AP = \sum (EF_{AP,i} \times AMT_{AP,i})$$

Table 30: Environmental analysis of Pyro-CLG using Ca2Fe2O5 and Feed: ISW.

GWP				AP		
Flow rate	kg/hr	kg/hr	kg CO2 equivalent per hour	kg/hr	kg/hr	kg SO2 equivalent per hour
	CO2	CH4		SO2	NO2	
PYRO	61.393	8.72	291.37	6.818	5.13E-24	6.818
PSA	81.234	0	81.234	9.61	68.105	57.28

Table 31: Environmental analysis of SE-CLG2(ISW).

GWP				AP		
Flow rate	kg/hr	kg/hr	kg CO2 equivalent per hour	kg/hr	kg/hr	kg SO2 equivalent per hour
	CO2	CH4		SO2	NO2	
GASIFIR	113.47	8.72	357.793	7.72	1.149E-23	7.72
PSA	13.94	0	13.94	9.61	68.16	57.32

Table 32: Environmental analysis of Pyro-CLG (MSW).

GWP				AP		
Flow rate	kg/hr	kg/hr	kg CO2 equivalent per hour	kg/hr	kg/hr	kg SO2 equivalent per hour
	CO2	CH4		SO2	NO2	
PYRO	47.657	12.276	391.385	2.154	2.43E-24	2.154
PSA	33.62	0	33.62	3.393	22.318	19.017

Table 33: Environmental analysis of SE-CLG2(MSW).

GWP				AP		
Flow rate	kg/hr	kg/hr	kg CO2 equivalent per hour	kg/hr	kg/hr	kg SO2 equivalent per hour
	CO2	CH4		SO2	NO2	
GASIFIR	80.18	15.173	505.024	2.29	3.46E-24	

						2.29
PSA	2.74		2.74	3.40	22.33	19.031

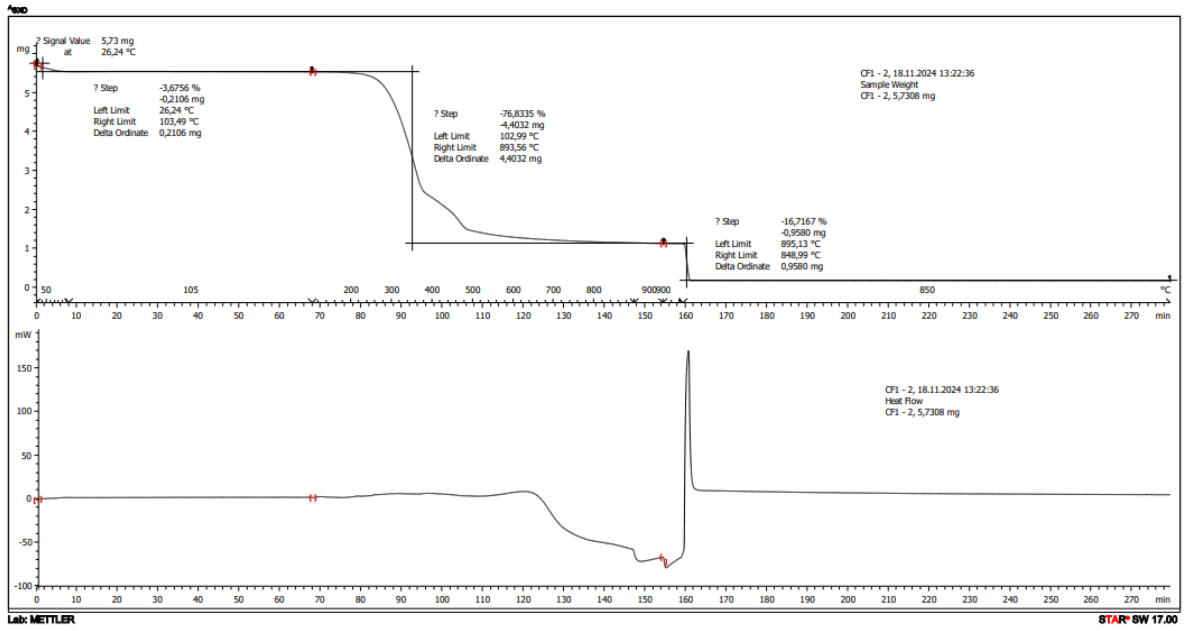

Figure 38: TGA curve for CF1.

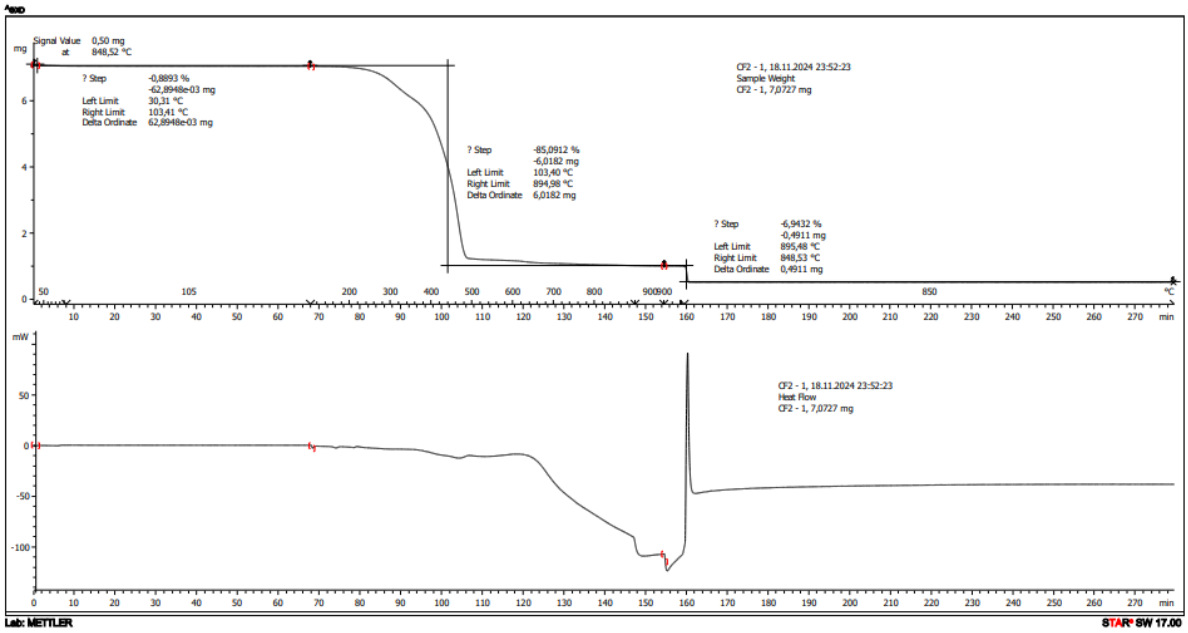

Figure 39: TGA curve of CF2.

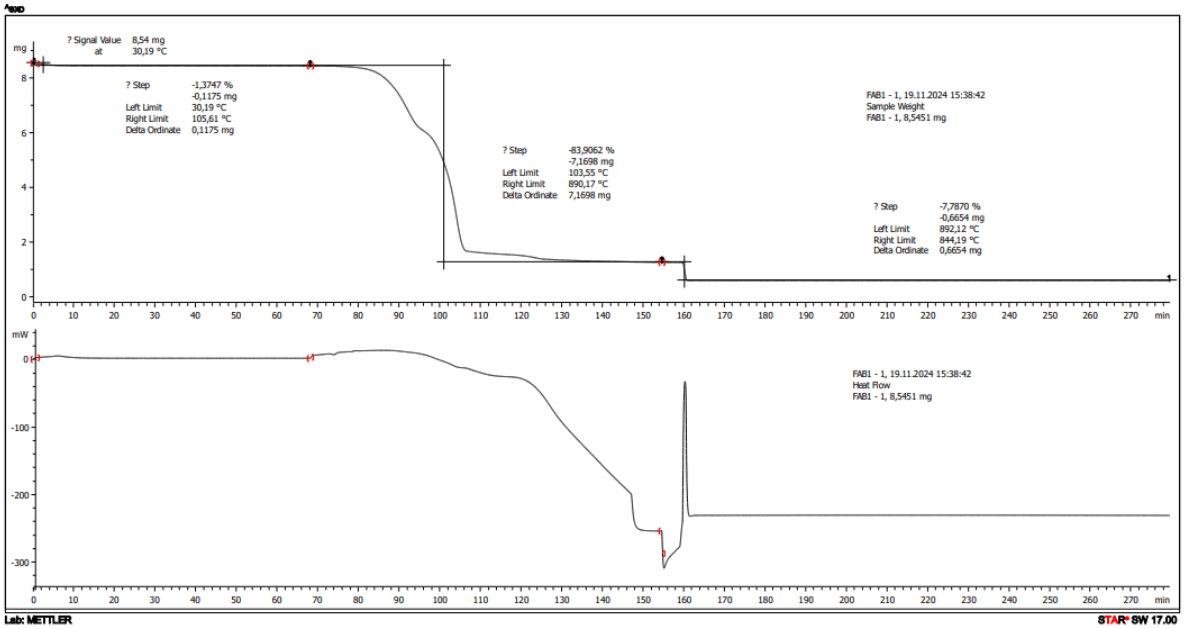

Figure 40: TGA curve of FAB1.

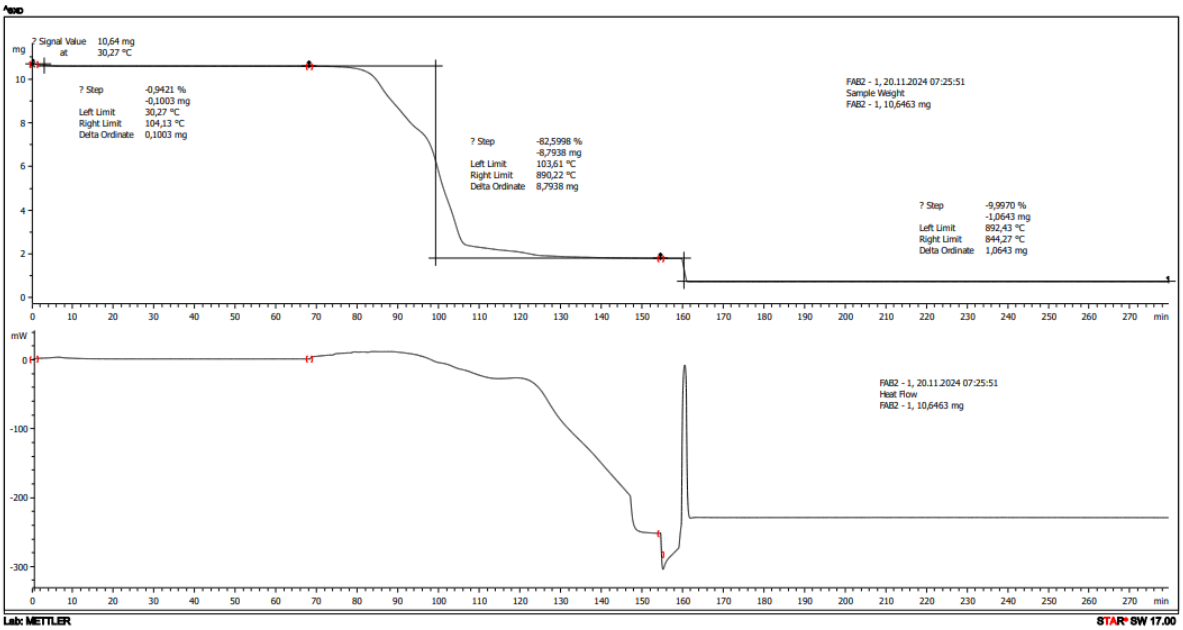

Figure 41: TGA curve of FAB2

Thermogravimetric analysis was performed by using a Mettler Toledo TGA / DSC1 thermal analyzer.

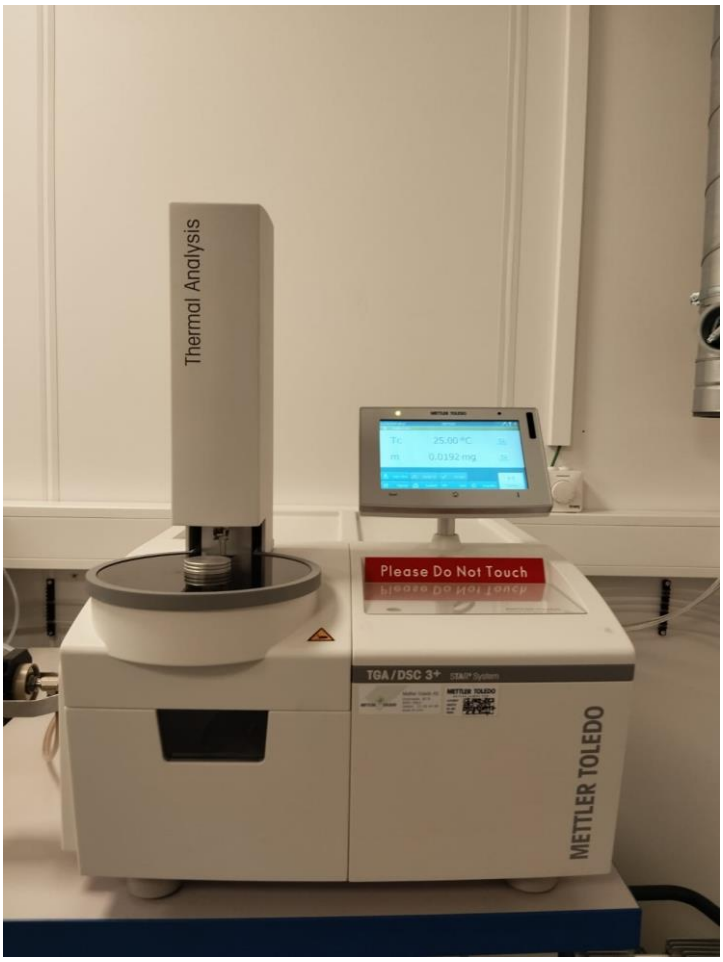

Figure 42: Mettler Toledo TGA / DSC1 thermal analyzer.